NUMERICAL MODEL STUDIES TO PREDICT THE WIND-WAVE CLIMATE CONSIDERING CLIMATE CHANGE EFFECTS

Thesis
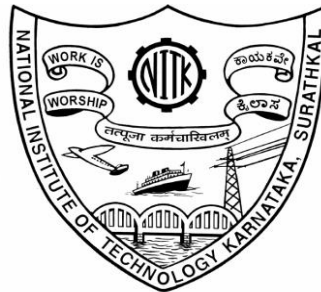Submitted in partial fulfilment of the requirements for the degree of

DOCTOR OF PHILOSOPHY

by

SANDESH UPADHYAYA K.

(177114AM008)

**DEPARTMENT OF WATER RESOURCES AND OCEAN ENGINEERING
NATIONAL INSTITUTE OF TECHNOLOGY KARNATAKA
SURATHKAL, P.O. SRINIVASNAGAR-575 025
MANGALURU, INDIA**

MAY 2021

NUMERICAL MODEL STUDIES TO PREDICT THE WIND-WAVE CLIMATE CONSIDERING CLIMATE CHANGE EFFECTS

Thesis
Submitted in partial fulfilment of the requirements for the degree of
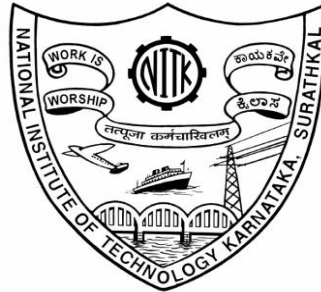
DOCTOR OF PHILOSOPHY

by

SANDESH UPADHYAYA K.
(177114AM008)

Under the guidance of

Prof. SUBBA RAO AND Dr. MANU

**DEPARTMENT OF WATER RESOURCES AND OCEAN ENGINEERING
NATIONAL INSTITUTE OF TECHNOLOGY KARNATAKA
SURATHKAL, P.O. SRINIVASNAGAR-575 025
MANGALURU, INDIA**

MAY 2021

D E C L A R A T I O N

By the Ph.D. Research Scholar

I hereby *declare* that the Research Thesis entitled "**Numerical model studies to predict the wind-wave climate considering climate change effects,**" which is being submitted to the **National Institute of Technology Karnataka, Surathkal** in partial fulfilment of the requirements for the award of the Degree of **Doctor of Philosophy** in **Department of Water Resources and Ocean Engineering** is a *bonafide report of the research work* carried out by me. The material contained in this Research Thesis has not been submitted to any University or Institution for the award of any degree.

177114AM008, SANDESH UPADHYAYA K.

(Register Number, Name & Signature of the Research Scholar)

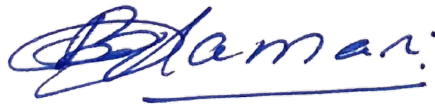Department of Water Resources and Ocean Engineering

Place: NITK-Surathkal

Date: 14.05.2021

C E R T I F I C A T E

This is to *certify* that the Research Thesis entitled **"Numerical model studies to predict the wind-wave climate considering climate change effects,"** submitted by Sandesh Upadhyaya K. (Register Number: 177114AM008) as the record of the research work carried out by him is *accepted as the Research Thesis submission in* partial fulfilment of the requirements for the award of the degree of **Doctor of Philosophy.**

14/05/21

Prof. SUBBA RAO

(Research Guide)

14-05-2021

Dr. MANU

(Research Guide)

Prof B M Dodamani

Chairman - DRPC

Department of Water Resources and Ocean Engineering

National Institute of Technology Karnataka, Surathkal

ACKNOWLEDGEMENT

Sandesh Upadhyaya K.

ABSTRACT

The waves propagating over an area under the action of the wind is termed as wind waves. The disturbances on the ocean surface by the wind are restored to a calm equilibrium position by the action of gravity. The fundamental element in the wind-wave generation is the interaction between air and ocean. During this interaction, there is an energy and momentum transfer between the atmosphere and ocean. The climate change affects the atmospheric temperature which in turn alters the wind patterns. The wave conditions change according to the wind pattern.

Studies on global climate changes and extreme weather events have fascinated researches all over the world. Climate change, a global phenomenon, is a consequence of ever-increasing greenhouse gas concentration and is considered a serious threat to mankind. Climate change is a phenomenon triggered by natural and anthropogenic activities, which is one of the most discussed topics in the research community today. An increase in global sea level, changes in wind pattern and an increase in the frequency of extreme wave events which is caused by climate change have critical impacts on the coastal population around the world.

Indian coast measures about 7500 km along with the nine coastal states which host marine and coastal biodiversity. Thirteen major ports and associated activities play a prominent role in coastal population concentration of about 14% along the Indian coast. The coastal and offshore structures are typically designed for the significant wave height (H_S) corresponding to a specific return period and it is, therefore, necessary to know possible changes in their magnitudes at different locations of interest. Structures built in the sea are traditionally designed according to historical climate observations or hindcasted data. For structural safety, consideration of such climate change effects is highly desirable.

Computational advancements in recent times have resulted in various General Circulation Models being developed and effectively used for assessing the atmospheric and ocean circulation. The performance of these modelled result can be compared with the in-situ measurements of shorter duration. Forecast of the climate parameters incorporating climate change effects are developed. These data products can be used to develop numerical wave models for long term analysis of wind and wave patterns which will aid in the design of coastal and offshore structures.

In the present study, hindcasting from 1980 for the Indian domain is performed from reanalysed gridded global wind speed dataset called ERA-Interim. The performance of this global dataset is assessed by comparing it with in-situ measurements recorded at the east and west coast of India. As the ERA-Interim dataset showed a good match with the in-situ records these long-term wind speeds are used as an input to the numerical wave model. MIKE 21 SW numerical wave model is developed for the Indian domain with coordinates - 4º to 30º N 40º to 95ºE. Significant wave heights from this wave model driven by ERA-Interim wind speeds are extracted at locations nearshore to Karwar and offshore OB03 location for validation. After validation, the numerical model is used to perform long-term wave analysis, shoreline analysis, assessment of wind-wave climate along the Indian coast and wave climate predictions along Karnataka coast for the near future.

The numerical model output depends on the input which is global wind speed dataset. Wind speed analysis is initially performed before using it in the numerical model. As ERA-Interim dataset does not provide forecasts, global wind speeds provided by the CMIP5 database is considered in this study. Wind speed projections from 38 different CMIP5 global models are compared against ERA-Interim global wind speeds for the Indian domain. The performance of datasets is graphically evaluated based on Taylor plots. Initially, statistical analysis of monthly wind speeds from 1980 to 2005 is performed to arrive at four best performing datasets for the Indian domain. Further, a nowcast study on daily wind speeds from 2006 to 2018 considering the four climate change scenarios termed as Representative Concentration Pathways (RCPs) is carried out. From the nowcast analysis, an Italian CMIP5 dataset called CMCC-CM for RCP 4.5 matched well with the real-time reanalysed wind speeds provided by ERA-Interim. Hence in the present study, wave climate predictions for the Indian domain is based on wind speeds driven by CMCC-CM RCP 4.5.

The long-term analysis is performed based on the five probability distributions such as Log-normal distribution, Gumbel distribution, Fretchet distribution, Exponential distribution, and Weibull distributions to arrive at significant wave height with 10 and 50 year return period for New Mangaluru port location. Initially, long-term analysis is performed on in-situ records measured for 5 years near New Mangaluru Port. From this analysis, Weibull distribution with α=1.3 showed good performance and is used to arrive at significant wave heights with 10 and 50 year return period. The same approach is extended on the MIKE 21 simulated significant wave heights from 38-year ERA-Interim hindcast. The results showed 2.6% and 5.44% increase in significant wave height with 10 year and 50 year return period at the location studied.

A shoreline analysis is performed using LITPACK tool along the coast adjacent to the New Mangaluru Port. The volume of sediment transport is analysed and the shoreline changes from 1980 to 2015 is studied to understand the erosion and accretion patterns. The performance of the numerical model matched well with the satellite measurements.

In an attempt to explore the renewable energy potential along the Indian coast the numerical wave model is also used to assess the wind-wave climate based on ERA-Interim wind speed data of 38 years. The results showed amongst the locations studied off Goa, Karnataka, Kerala, Tamil Nadu, and Andhra Pradesh had good potential to extract offshore wind energy from offshore wind turbines.

MIKE numerical model driven by wind speeds from CMCC-CM RCP 4.5 up to the year 2070 is used to simulate the wave climate along the Karnataka coast. The monsoon wave climate is studied to arrive at wave parameters with 10 and 50 year return period at six locations along the Karnataka coast.

Keywords: *MIKE 21 SW, Global wind speeds, ERA-Interim, CMIP5, Climate Change, wave climate, Long-term analysis, Shoreline changes, Indian domain, Karnataka coast.*

TABLE OF CONTENTS

LIST OF FIGURES

LIST OF TABLES

NOMENCLATURE

H_s	Significant wave height
T	Wave period
U_{10}	Zonal component wind speeds at 10 m from mean sea level
V_{10}	Meridional component wind speed at 10 m from mean sea level
V	Wind speed
C_{dis} and δ_{dis}	White capping dissipation coefficients
α	Shape parameter
T_R	Return period
$H_{S(T_R)}$	Design wave height
H_t	Threshold wave height
R	Correlation Coefficient
$RMSE$	Root Mean Square Error

ABBREVIATIONS

IPCC	Intergovernmental Panel on Climate Change
AR5	Assessment Report 5
GCM	General Circulation Model
RCP	Representative Concentration Pathway
ECMWF	European Centre for Medium-Range Weather Forecasts
ERA	ECMWF Re-Analysis
CMIP5	Coupled Model Intercomparison Project Phase 5
SW	Spectral Wave
DHI	Danish Hydraulic Institute
WWIII	WAVEWATCH III
SWAN	Simulating Waves Nearshore
WAM	Wave Modelling
POT	Peaks over Threshold
GEV	Generalized Extreme Values
GPD	Generalized Pareto Distribution
AS	Arabian Sea
BoB	Bay of Bengal
JONSWAP	Joint North Sea Wave Project
GEBCO	General Bathymetric Chart of the Oceans
ORE	Offshore Renewable Energy
WEC	Wave Energy Converters
NMP	New Mangalore Port
BW	Breakwater
JJAS	Monsoon months from June to September

1.1 GENERAL

Ocean waves are generated by air-sea interaction where the wind plays a vital role in wave generation. Characteristics of wind over the ocean surface are one of the important factors in the design of marine structures. The fundamental element in wind waves generation is the interaction between air and sea which helps in momentum exchange between atmosphere and ocean. Wind waves are generated under the action of wind stress acting over the ocean surface. The wave parameters are the function of wind speed, fetch and duration of wind. The numerical approach is best suited for predictions over a wider area whereas data-driven techniques are more applicable for location-specific studies (Sarkar et al., 2020). Wave hindcast using a numerical model is an effective method to assess the wave climate due to discontinuous in-situ measurements (Amrutha et al., 2016). Numerical wave models provide economically viable solutions for evaluating global Ocean wave data (Sreelakshmi and Bhaskaran, 2020). Extreme value analysis on wave heights can be performed on these long-term data which is a necessity for the design of marine structures. Analysis of wind-wave climate has profound importance to the oceanographers and coastal zone management authorities in context to ocean energy research.

1.2 CLIMATE CHANGE

The variability of average weather over a period of time is referred to as 'Climate'. World Meteorological Organization (WMO) suggests the period of time in the above definition can ideally be of 30 years. Changes to this state of climate due to natural and anthropogenic activities result in altering the atmospheric composition and this phenomenon is popularly known as 'Climate Change' as per Intergovernmental Panel on Climate Change (IPCC). United Nations Framework Convention on Climate Change (UNFCCC) defines climate change as "A change of climate which is attributed directly or indirectly to human activity that alters the composition of the global atmosphere and which is in addition to natural climate variability observed over comparable time

periods". The trends observed in Antarctica ice sheet depletion and Arctic sea ice decline validates the effects of global warming. The above two effects of global warming have resulted in sea level rise, with the former contributing in terms of expansion of sea waters and the latter increasing water as a result of the melting of ice. IPCC has shown its concern over the rising sea level on a global scale in its fifth assessment report (Pachauri et al., 2014). An increase in global sea level, changes in wind pattern and increase in the frequency of extreme wave events which is caused by climate change have critical impacts on the coastal population around the world. Hence, the prediction of wave climate based on a long-term period is vital for the analysis and design of marine structures. Climate change will result in sea level increase, geomorphology changes, indentation, changes in surface waves, tides, currents and extreme events (Rani et al., 2015). The constant increase in population also increases the emission of greenhouse gases which adds to the severity of climate change effects. Shipping activities and other existing marine structures will also be affected.

1.2.1 Indian domain

India has a coastline of about 7500 km passing through nine states. Indian coast has 13 major ports and more than 1500 fish landing centres contributing to the blue economy of the country. As a result of infrastructural development in 66 coastal districts and port-led industrialization, Indian coastal districts hosts a population of about 171 million (Census report, 2014). Compared to the Inland regions, nearshore coastal zones have a higher average population density (Patra and Bhaskaran, 2016; Umesh et al., 2017). The climate change effects are one of the decisive factors along the Indian Ocean as it is densely populated (Kumar et al., 2013). The low lying areas are at serious threats from flooding and erosion. The changes in wave climate will affect the operations in offshore platforms as it increases the risks of damage (Reistad, 2001 and Ruggiero et al., 2010). Several technical reports and articles have shed light upon the alarming rate of anthropogenic activity contributing to climate change, which in turn increases the risks of seawater inundation, changes in wave climate and frequency of storm events along the Indian coast (Figure 1.1).

The monsoons attract severe winds in the north Indian Ocean domain. The surface

winds blowing from June to November from the west coast of the Indian peninsula are named as the southwest monsoon (Vethamony et al., 2006). These winds might also create cyclones events in the Arabian Sea portion. The region also experiences winds from the northeast direction from December to May and this phase is termed as the northeast monsoon. During this period the Bay of Bengal region experiences frequent cyclones (Kumar and Philip, 2010)
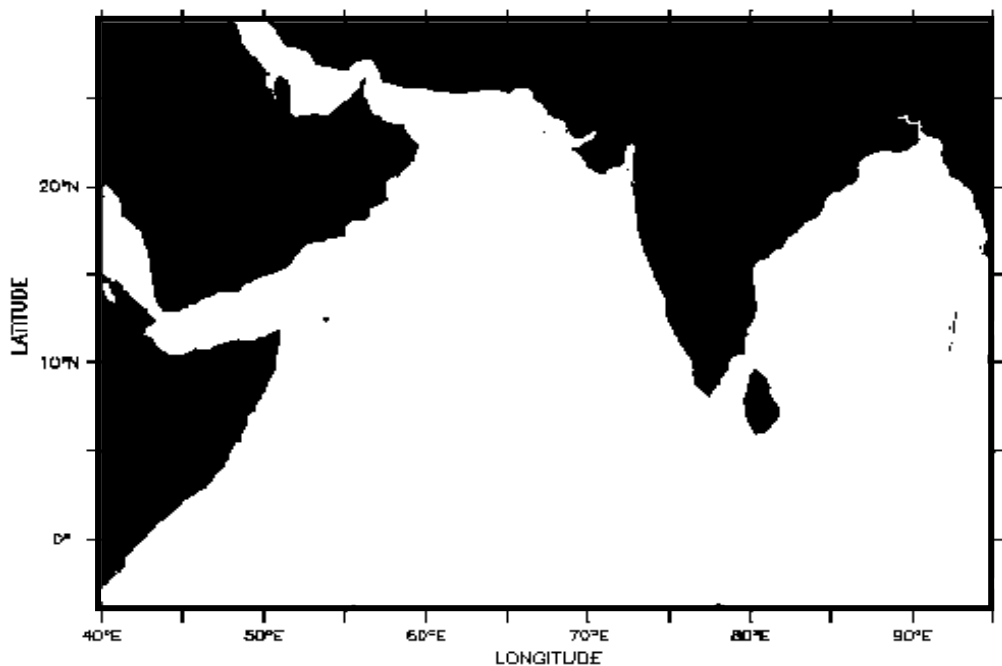
Fig. 1.1 Study domain

1.3 DATASETS

The computational advancements have helped in capturing air-sea interaction in a mathematical form. This has resulted in global climate models which can be further enhanced by some additional in-situ measurements along with satellite datasets. Global climate models contain downscaled data of future variables at larger spatial grids. The void which was bothering the coastal engineers to study the long-term behaviour of waves has been filled with these atmospheric and ocean models. General Circulation Models (GCMs) are used in two types of studies, one where the model is run in past to see how climate has varied over the historical past. Secondly, to predict the future climate in terms of scenarios suggested in IPCC AR5 called Representative

Concentration Pathways (RCPs). The amount of greenhouse gases, aerosols and land use are the key variables contributing to climate change which will be accounted for by RCPs. As the available measured data about wave climate is minimal, relaying of GCMs becomes essential. These GCMs give wind speeds from which the wave characteristics can be assessed by numerical wave models (Krishnan and Bhaskaran, 2019).

The General Circulation Model (GCM) is earth models which is a mathematical representation of the physical processes that happen in the atmosphere, ocean, land surface and cryosphere as mentioned in the fifth assessment report of IPCC (IPCC AR5, 2014). These mathematical equations are solved using a computer or supercomputers depending on their complexity. GCM uses a three-dimensional grid over the globe to represent the climate. GCMs corresponds to coarser grids, as they have a horizontal resolution between 250 to 600 km and vertical layers range from 10 to 30 depending on whether it is atmosphere or ocean. The climate system simulates responses based on concepts of mass, momentum and energy balance making it a popular model which is being used worldwide (Kulkarni et al., 2014).

1.3.1   European Centre for Medium-range Weather Forecasts

The European Centre for Medium-Range Weather Forecasts (ECMWF) is an independent intergovernmental organization that came into existence in 1975. ECMWF is based in the United Kingdom and is supported by 34 member states. ECMWF is a research institute, which also provides operational service round the clock. This Centre provides medium-range forecasts and aims to accurately predict climate data. Amongst the various products offered by ECMWF, ERA-Interim is one such latest reanalyzed dataset that spans the entire twentieth century. Reanalysis is a method of reprocessing observations using state of the art system so that the resulting climate dataset will be improved continuously (Bindoff et al., 2010). Dee et al., (2011) mentions ERA-interim as a gridded data product with 3 hourly surface parameters which describes ocean waves, land surface and weather conditions.

The data is updated every month, which works on the data assimilation technique. Data assimilation technique is used to initialize numerical forecast model which is obtained

4

by the combination of meteorological observations of variables like atmospheric pressure and temperature. ERA-Interim is based on the Integrated Forecast System (IFS) for data assimilation which includes 4-Dimensional Variational analysis (4D-Var). 4D-Var is a sophisticated assimilation technique with an operational configuration named Cy31r2, where the assimilation window is 12-hour long. The data is accessible from the public web interface (https://www.ecmwf.int/).

Through ERA-Interim data, details of zonal and meridional wind data for a particular latitude and longitude, at a definite time interval can be obtained. The wind speed data (m/s) is available from January 1979 and is updated in real-time with a delay of two months. As these datasets are reanalyzed several times, it adds great value in the field of atmospheric research. Reanalysis of data is a record of global atmospheric circulation which is spatially complete, multivariate and coherent. The reanalysis has always supplemented in developing a homogeneous record of past atmospheric evolution that is free from shifts. The reanalyzed versions of such climate variables contribute to removing errors and bias from the climate output (Deepthi and Deo, 2010). These datasets are highly regarded in the scientific community and many researchers have found them to be closer to the observed measurements (Alexandru and Sushama, 2015; Umesh et al., 2017).

1.3.2 Coupled Model Intercomparison Project Phase 5

Coupled Model Intercomparison Project (CMIP) is a standard experimental protocol meant to study the output of Atmosphere-Ocean General Circulation Models (AOGCMs) established under the World Climate Research Program (WCRP). CMIP5 was developed in 2005 involving 20 model developing groups around the world. CMIP in coordination with climate model experiments from multiple international modelling teams worldwide defines common experiment protocols, forcings and output (Eyring et al., 2016). CMIP5 is a set of coordinated climate model experiments that was framed to address the scientific questions raised in the IPCC fourth assessment report. CMIP5 provides a model simulation of the recent past, projections for the short term (till 2035) and long-term (till 2100). CMIP5 includes a comprehensive representation of the carbon cycle to the models referred to as Earth System Models (ESMs). Some cases

such as dynamic vegetation component, interactive prognostic aerosol and chemistry may also be included in ESMs (Emori et al., 2016). CMIP5 has provided information for IPCC working groups and has been mentioned in the fifth assessment report of IPCC published in 2014. CMIP5 supports climate model diagnosis, validation, intercomparison, documentation along with data access. Datasets can also be downloaded from the Asia Pacific Research Data Center (APRDC) http://apdrc.soest.hawaii.edu/. The contribution of various institutes has made the model better as the quality of input data and assimilation has been enhanced.

Taylor, et al. (2009) mentions that individual modelling groups of CMIP5 may perform near-term experiments (decadal), long-term experiments (century) or both. The different modelling groups may perform experiments with AOGCMs or ESMs in different time-slices with varying spatial resolution. The modelling groups may consider parameters such as Sea Surface Temperature (SST), Air pressure, wind speeds etc. while performing the experiments. The model errors like systematic model biases, scientific gaps and shortcomings observed in CMIP5 has influenced the design of CMIP6 (Stouffer et al., 2017). Krishnan and Bhaskaran, (2020) have assessed the capabilities of CMIP5 and CMIP6 models simulated wind speeds dataset for Bay of Bengal region. The wind speed data (m/s) will be essential for the present study to assess the wave climate. Hence, CMIP5 global wind speed dataset is used.

Representative Concentration Pathways (RCPs) are scenarios that help in predicting trajectories of the future climate, majorly as a consequence of anthropogenic activities. The amount of greenhouse gases, aerosols and land use are the key variables contributing to climate change which will be accounted for by RCPs. RCP 2.6, RCP 4.5, RCP 6 and RCP 8.5 are four RCP scenarios used in climate modelling and research which is also been adopted by IPCC AR5, (2014). RCP is an indicator of concentration pathway that approximately results in that targeting radioactive forcing (W/m^2) at the year 2100 relative to pre-industrial conditions (Eg: RCP 6 identifies a concentration pathway that approximately results in a radioactive forcing of 6 W/m^2 at the year 2100). Vuuren et al. (2011) based on works of literature, mentions that the RCPs can also be expressed in terms of concentrations of CO_2 equivalent: reaching ~ 490 ppm for RCP

2.6; ~ 650 ppm for RCP 4.5; ~ 850 ppm for RCP 6 and ~ 1370 ppm for RCP 8.5 by the year 2100. An RCP provides atmospheric concentration for the period 2005- 2100, whereas some specific models give Extended Concentration Pathways (ECPs) where the period is extended up to the year 2300. Figure 1.2 shows the global mean temperature change averaged from all CMIP5 models relative to 1980-2005 data for all four RCP scenarios. The ranges of global temperatures at the end of the 21st century in a broader range can also be observed from Figure 1.2 (Collins et al., 2013). Climate change scenarios on future climate as mentioned in IPCC AR5 depends on physical, ecological and socio-economical processes. The scenario's goal is not only to predict the future but also to understand the uncertainties involved in future climate studies. The criteria for the selection of a particular scenario is based on its consistency with global projection, physical plausibility, applicability in impact assessments, representability and accessibility. RCPs consider global greenhouse gases and aerosol concentrations at the initial point, rather than using socio-economic scenarios based on greenhouse gas emissions as the starting point. The present study considers RCP scenarios for wave climate prediction.
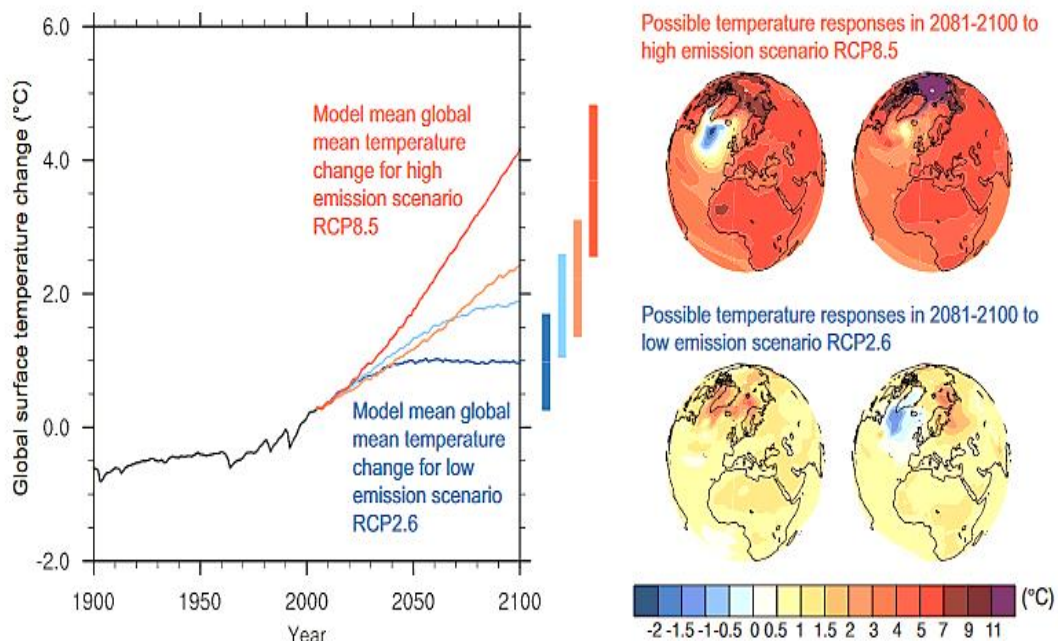
Fig. 1.2 Changes in the global mean temperature from the average of CMIP5 models predictions for the different RCPs (Collins et al., 2013)**.**

7

1.3.3 In-situ Measured Data

Initially, historical data was obtained from ship observations which were confined to calm weather season and along particular routes only. Nowadays, in-situ measurements recorded with the help of different instruments is considered reliable. In-situ buoy measurements are spatially fixed with high time scale density (Kumar et al., 2013). Young (1999) expresses his concern over the significant cost involved for in-situ measurements and relative short measurements recorded. There is a possibility of data gaps as buoys might have to be taken out for maintenance or buoys might even get displaced during a storm event (Aboobacker et al., 2009). Hence, these short measured data are feasible for validation of the numerically run models.

Location-specific measured data of ocean parameters are sparse. Compared to the Atlantic and Pacific region, the Indian Ocean region has limited in-situ observations (Thomas and Dwarakish, 2015; Patra and Bhaskaran, 2016). As there are several potential areas for development along the Indian coast and offshore, good quality wave measurements through wave buoys are very much essential (Kumar et al., 2012). Realizing the importance of ocean observations along the Indian coast, the Earth System Science Organization (ESSO) which is governed by the Ministry of Earth Sciences, India formed organizations such as the National Institute of Ocean Technology (NIOT), Indian National Centre for Ocean Information Services (INCOIS) and National Institute of Oceanography (NIO). Real-time oceanographic and meteorological data are made available from 1997 by these organizations. Air-sea interactions are studied based on vital parameters like Sea Surface Temperature and wind speeds. NIOT has carried out limited duration experiments such as the Arabian Sea Monsoon Experiment (ARMEX), Bay of Bengal Monsoon Experiment (BOBMEX) and Ocean Moored Buoy Network for the Northern Indian Ocean (OMNI) which provides ocean observations (Venkatesan et al., 2016). The information obtained is vital to the coastal population, fisherfolk, in particular, to carry out fishing activities safely. ESSO-INCOIS monitors the ocean climate and also provides warning services during tsunami, storms and extreme wave climate.

Table 1.1 Details of the In-situ measurements

| Station ID | Location (in degrees) | | Year | Time interval | Location details |
	Latitude	Longitude			
Karwar	14.82	74.08	2011	30 minutes	Nearshore Karwar
OB03	12.50	72.01	2005	180 minutes	Offshore Mangaluru
AD02	15.02	69.01	2011	24-hours	Offshore Goa
BD11	13.50	84.00	2013	24-hours	Offshore Chennai

1.4 NUMERICAL MODELLING

The improvements in the field of numerical modelling and computational techniques have resulted in third-generation models where parameterization of nonlinear wave-wave interaction is represented with more detail (Moeini and Shahidi, 2007). One such third-generation model is MIKE 21 which is a computer programed tool for 2-dimensional wave modelling and simulation developed by the Danish Hydraulic Institute (DHI), Denmark. An unstructured flexible mesh that works under the cell-centred finite volume solution technique is adopted in MIKE 21 (Pentapati et al., 2015). The method used for representing and solving partial differential equations is termed the Finite Volume Method (FVM). Cell centred finite volume solution is based on linear triangular elements, which performs spatial discretization of differential equations of wave action (Kumaran et al., 2015). A small volume near the node on the mesh is taken into consideration. The area with extensive detail can be represented by small elements in the mesh and the area with lesser details can be large elements (Patra et al., 2015). The unstructured mesh is used for the horizontal plane and a structured mesh is used for vertical 3D models. 2D models comprise triangular or quadrilateral elements and 3D models with prism or brick elements (DHI, 2015).

MIKE 21 is a versatile tool for modelling coastal zones, physical, chemical and biological processes. The two modules attached with MIKE 21 are the Flow Model module (FM) and Spectral Wave module (SW). MIKE 21 FM module helps in realistic visualization of nature. Hence, used for complex oceanographic and estuary conditions. Flow Model module supports both spherical and Cartesian coordinates.

MIKE 21 SW module is a numerical modelling tool used for the prediction and simulation of the spectral wind-wave model. The transformation of wind-generated waves and swells in the offshore region can be simulated by solving energy and mass balance equations (Pentapati et al., 2015). DHI, (2015) specifies two formulations involved in MIKE 21 SW which are - i) Fully spectral formulation (based on wave action conservation equation) ii) Direction decoupled parametric formulation (based on a parameterization of wave action conservation equation). Remya et al., (2012) mentions that the first formulation is suitable for nearshore and offshore studies while the second is only for nearshore applications. The numerical model for the Indian domain is modelled and validated in MIKE 21 SW. In the present study, the numerical model is used for

i)   Wave hindcasting studies
ii)   Wave forecasting and simulation
iii)   Assessing the shoreline changes of Mangaluru coast
iv)   Wave climate assessment and prediction for the nearshore locations along the Indian coast
v)   Wave climate prediction along Karnataka coast

The predictions for the future on a temporal scale can be termed as forecasting, the present estimates can be termed as nowcasting and, the historical or past estimates are popularly termed as hindcasting.

1.5 ORGANISATION OF THE THESIS

The thesis titled "**Numerical model studies to predict the wind-wave climate considering climate change effects**," consists of the following chapters:

Chapter 1 introduces wind waves and their variability due to climate change. Also, the chapter discusses the available datasets for long-term studies. An introduction to MIKE numerical model is also mentioned here.

Chapter 2 provides a detailed review of the literature on long-term analysis. The chapter also has an overview of the numerical models used for wave climate studies. The objectives of the present study are mentioned in this chapter.

In **Chapter 3** methodology adopted is explained in this chapter and the flow chart indicating the sequence of work is shown. Details of wind data and the numerical model is mentioned

Chapter 4 is on long-term analysis of waves performed on in-situ measurements and numerically simulated wave heights. The results obtained from the shoreline studies along the Mangaluru coast is also mentioned in this chapter.

Chapter 5 illustrates the wind-wave climate analysis performed along nine different locations along the Indian coast and discusses the renewable energy potential along the Indian coast.

Chapter 6 illustrates the forecast of wave climate along the Karnataka coast based on CMCC-CM RCP 4.5 projected wind speeds. The wave parameters for the 10 and 50 year return period is evaluated here.

The study concludes with a brief on MIKE numerical models performance to forecast the wind-wave climate for the Indian domain and this is presented in **Chapter 7**

Studies on global climate changes and extreme weather events have fascinated researches all over the world. The coastal regions are most venerable to climate change effects. The focus of this chapter is to critically review the research carried on forecasting the wave climate.

2.1 LITERATURE ON LONG-TERM ANALYSIS

The studies on wave climate were initially performed based on hindcast obtained from in-situ measured parameters (Dattatri et al., 1979). Long-term statistical analysis based on various distributions contributed to arrive at an expected wave height at a given return period. With recent advancements in modelling and computational techniques, it is now possible to present high-quality data for wind-wave climate studies. The global wind data inputs in the form of GCM data developed from different agencies like ECMWF, CMIP5, National Oceanic and Atmospheric Administration (NOAA), Climate Forecast System Reanalysis (CFSR) etc. provide reasonably good estimates of wave climate. Wind speeds that are reliable generally from international agencies like ECMWF, NCEP, and CMIP are used by several researchers for ocean modelling (Boudia and Santos 2019).

An understanding of long-term variation in wave climate is a necessity when an engineer has to design an offshore or a coastal structure. Kumar and Deo (2004) mention that the long-term distributions like Generalized Pareto Distribution (GPD), Generalized Extreme Value (GEV), Gumbel distribution and Weibull distributions can be used to obtain design wave height with different return period for short-term measurements. These variations inclusive of the climate change effect should be taken into account when the structure is designed for a particular return period.

Kumar and Deo (2004) in their technical note discuss the estimation of design wave considering the directional distribution of waves. The analysis was based on one-year

buoy measurement collected from Goa and Nagapattinam stations where buoy at a water depth of 23 m and 15 m respectively were installed. Ship measurements along the site route were also considered for the study. From the datasets used month-wise wave directions were monitored at the buoy locations. Weibull distribution was used to fit these data to obtain design wave height with 100 years return period. The obtained direction design wave heights were compared with omnidirectional wave heights. The authors found a reduction factor of 4.6% at Goa and 0.5% at Nagapattinam considering wave direction effects. The ship observations gave a reduction factor which varied between 1.7% to 3.7%. Hence they conclude that wave direction should be taken in to account for design wave height calculation at water depths greater than 15m.

Caires and Sterl (2005) estimated wind speeds and wave heights for 100 years return period globally. The data from ERA-40 is used which is 6 hourly wind and wave data with 1.5°x 1.5° resolution. This data was corrected based on buoy data measured at 20 stations obtained from the NDBC database and altimeter data from the TOPEX satellite mission. Return period values of wind and waves are based on the Peaks over Threshold (POT) method. Buoy data from 1990 to 1999 was used for validation of ERA-40 values using the POT method which revealed ERA-40 underestimates the values of significant wave heights. The relation between all three datasets was developed for the records of 1993 to 2000. The scatter plot showed more variation in ERA-40 when the TOPEX dataset was also compared with buoy data. Hence, the corrected wind speed and wave height with 100 years return period estimates were obtained for three different 10 year periods of ERA-40 data. The authors conclude that in some locations establishing exponential distribution may be useful. The selection of thresholds has to be addressed and reliable ways to obtain estimates from satellite data has to be worked on.

Subba Rao et al., (2008) have undertaken a study that deals with the long-term analysis of the wave record off Mangalore coast on the west coast of India. This analysis was done as a part of the project Integrated Coastal and Marine Area Management (ICMAM). The wave height data was collected from New Mangalore Port, Panambur for 5 year period (1999-2004). Data was obtained from wave rider buoy and wave tide

gauge which was used for the spectral analysis and subsequently long-term analysis. The energy spectrums were obtained based on the in-situ measurements. The spectrum had multiple peaks, the primary peak was because of the sea and the secondary was due to swell. Wave spectrum for pre and post-monsoon seasons were smoothened using the Parzen lag window of MATLAB. The measured spectrum was compared with theoretical spectra like Bretschneider, Neumann and Scott spectrum. The results show Scott spectrum fitted well to the measured data along Mangalore Coast. The Secondary peak was about 1.5 times the peak frequency that signifies the region is dominant with swell wave field. The wave energy was dominating during the pre-monsoon period compared to the post-monsoon period.

Ruggiero et al., (2010) in their paper studied the changes in the significant wave height of the US Pacific North West (PNW) offshore region. The study was extended to examine extreme value assessment employed to assess the coastal hazard using buoy data from Oregon and Washington. The analysis was based on two offshore buoy measured hourly wave heights which were obtained from the National Data Buoy Center (NDBC). Inconsistency in the Oregon buoy measured data is observed for durations when the buoy was taken out of commission, hence combined time series were obtained from the two buoys to achieve good data. Linear least square regression analysis was performed to identify extreme waves in a long trend. Various methods were used for estimating extreme significant wave height for return periods. Methods like annual maximum from Generalized Extreme Values (GEV), r-largest-order statistics model and Peak over threshold values were used. It was observed that a gradual change in the mean climate environment will significantly increase the frequency of extreme events. Results obtained from statistical analysis indicates a progressive increase in 25 years and 100-year projections. The findings indicated an annual average of deepwater significant wave height has increased at a rate of 0.015 m/yr.

Kumar et al., (2012) studied the variations of nearshore waves along the Karnataka coast. Three shallow water buoy measurements were recorded at Malpe, Honnavar and

Karwar with water depths 9 m, 9 m and 7m respectively. Wave spectra record for pre-monsoon (April-May), summer monsoon (June-July) and post-monsoon (October) seasons were recorded for the year 2009. Wave spectrum was obtained based on Fast Fourier Transforms (FFT) and was studied as normalized energy densities. The dominance of swell along Honnavar was further studied for 2008 and 2010. The maximum wave heights at locations Karwar, Honnavar and Malpe were 1.2, 1.3 and 1.3 m at pre-monsoon 2.4, 2.9 and 3 m at monsoons; 1.1, 1.3 and 1.2 m during post-monsoon respectively.

Deepthi and Deo (2010) considered climate change effects for estimating wind speed at Indian offshore locations along the Arabian Sea and Bay of Bengal. Statistical downsizing method of Artificial Neural Network (ANN) was used with wind inputs in the form of historical wind speeds (NCEP/NCAR) along with model projected (GCM) wind speeds which considers climate change effects. The ANN model was designed initially for which it was trained with NCEP reanalyzed data for the period of 1998-2005. The next stage was the ANN model application where the regional climate variable was based on the GCM-CGCM3 model corresponding to the A2 scenario. This GCM model helped in predicting the wind speeds for the next century. As the two datasets correspond to different resolution re-gridding of data was done.

Before performing statistical analysis using Gumbel and Weibull distributions for different return periods, the ANN predicted winds speeds were compared with buoy observed data. The observed data which was in the form of buoy data from NIOT buoys at the two locations with measurements from 1998-2005 was used as this dataset was independent of climate change effects.

Further correlation between predictions based on NCEP/NCAR data and CGCM3 data was performed to check the relevance of GCM used. After obtaining a good correlation for both the locations, long-term analysis based on Gumbel and Weibull distributions were performed on ANN outputs and observed buoy data. From the results, the increase in wind speeds for 100 years return period varied from 44 % to 74%. The increase in

16

the location corresponding to east coast India was higher than the west coast. Gumbel distribution showed less variation when compared to the Weibull distribution.

Radhika et al., (2013) estimated significant wave heights on three different locations along the Indian coast considering the climate change effect for a return period of 100 years. The locations were offshore Chennai and Goa and the shallow region of Mangalore coast. Wind data is taken from NCEP/NCAR reanalyzed data which was used to create a downscaled model of the study region. The downscaled model was conveniently modelled using ANN where 80 % of the wind data was used for training. The climate change scenario considered was based on 20C3M data and for validation observed values were considered. GCMs are run for various climate change scenarios.

For hindcast, principal components of significant wave height obtained from NCEP/NCAR wind data for the period 1981 to 2010 was used. The wave heights obtained was input for future prediction (2011 to 2040) which was based on A2, B1 and A1B daily wind data scenarios for the same domain. The data collected were based on the Total Sample and Peak over Threshold approach. Gumbel and Weibull distributions are used to predict 100-year values. The obtained results were expressed as time history and a linear trend was observed for the increasing wave heights. The results reveal an increase of about 8-42% at offshore of Bay of Bengal location, 27-44% at offshore of the Arabian Sea and 22-32% the nearshore of Arabian Sea considering climate change effects based on Weibull distribution adopting POT approach for a return period of 100 years.

Kulkarni et al., (2014) studied the climate change effects on design and operational wind on the two offshore locations along the west coast of India. Initially, re-girding of the datasets used was performed for the GCM of the past (CGCM-20C3M) and the future (CGCM-RCP 4.5) along with ERA-40 and NCEP/NCAR datasets. Standardization of datasets was achieved by the principal component analysis technique. Bias removal was based on buoy measurements for NCEP and GCM data, which were represented as scatter plots. Future wind speeds for 30 years were obtained from ANN which worked on downscaling of GCM. Later a comparison between past

and future 30 years wind speeds was performed by fitting Generalized Pareto and Weibull distributions to extract long-term winds with different return periods. A statistical comparison of training and testing data was done and were comparable to each other. The results indicate an increase due to climate change in wind by 11%-14% when no downscaling of GCMs were done and 14% -17% when downscaling was performed.

Kulkarni et al., (2016) work are based on the long-term analysis of wind necessary for the structural design of offshore structures. Extreme winds of 10 GCMs from the CMIP5 project were extracted for 27 years Climate Forecast System Reanalysis (CFSR) data were used as a standard reference which is obtained from NOAA. Kanyakumari, Rameshwaram and Jakhau are the locations identified based on the wind potential as per the Government of India. Bias correction for the past and future period is performed using CFSR data as a reference. The average of 10 GCM was defined as Multi-Model Ensemble (MME) which helps in capturing spatial variability. Design wind speed with 100 years return period is evaluated by fitting GEV distribution for both past (1979-2005) as well as future (2006-2032) using the POT approach. MATLAB was the tool used by the authors to perform these statistical analyses. Probability Distribution Functions (PDFs) of wind speed were plotted for 10 GCMs results and compared with CFSR values. Substantial variation of GCM PDFs when compared with CFSR values was observed.

It was concluded that wind turbines along the Indian coast were not effected by extreme winds. Compared to individual GCM extremes MME extremes show closer results to CFSR reanalysis data. Bias was low for most of the regions. Based on MME data the high wind potential days might increase from 5-7% on the west coast and 2% along the east coast. A significant change in 100 year return period was not observed along the Indian coast.

Takbash et al., (2019) performed a long-term analysis based on 30 years altimeter and radiometer datasets. POT method is adopted for extreme value analysis. A comparison of estimates with NDBC buoy measurements of shorter duration was also performed.

18

The altimeter measurements of wave heights and 10 m wind speeds were corresponding to measurements from 1984-2014. However, the radiometer only provided wind speed data. The authors observed that POT results on altimeter datasets were comparable with buoy measurements and they feel with increasing altimeter missions the dataset will further enhance. The radiometer created some incompetency in measurements during heavy rain and other extremes and hence is not preferred for extreme value analysis

Boudia and Santos (2019) assessed the wind potential in the Algeria region of Africa. The study was based on 33 years of ERA-Interim dataset. The characterization of wind speeds was performed by the GEV technique. The validation concerning 42 stations across Africa was performed. Probability density plots of wind speeds were plotted for ERA-interim and in-situ records. From the study, it was found that the Algerian Sahara is windier than northern Algeria. The mean wind speed of 2.3 m/s is expected predominantly from the northwest direction. The northern portion has the potential of generating wind energy up to 4MWh/day in the windiest period that is from February to April. The southern portion has a higher potential of about 6MWh/day with March to April being the windiest period.

Mohan and Bhaskaran, (2019) evaluated the surface wind from 35 CMIP5 models for the period from 2006 to 2016. A multi-model mean corresponding to four RCPs was derived for ACCESS1.0, CanESM2, CMCCCMS, HadGEM2-AO, HadGEM2-CC, HadGEM2-ES, MPIESM-MR, MIROC-ESM, MRI-CGCM3, and NorESM1-M models. The study focused on the skill level of these models in assessing the day to day wind patterns. They used monthly wind speed data of a 1°x1° grid to analyze its performance against merged satellite altimeter data. The future changes corresponding to RCP 4.5 and RCP8.5 were studied for the periods 2026 to 2045 and 2080 to 2100 with respect to the historical period of 1993 to 2005. The skill scores found by the authors for the multi-model mean match well with the radiative forcing of these models for recent decades. The authors found there a decrease in the change in mean wind speed by 0.25 to 0.5 m/s for RCP4.5 and a decrease of 0.3 and 0.5 m/s for RCP 8.5 for the Arabian Sea and Bay of Bengal region. Hence bias correction was suggested.

Sawadogo et al., (2019) projected the potential impacts of climate change on the wind energy potential of West Africa. The study was based on 11 multi ensemble multi models simulations based on RCMs from the CORDEX project. Datasets like ERA-Interim, ERA-20C and in-situ observations were used for validation. Plots of probability density functions are obtained from simulated results. The RCM performance of surface wind speeds was not at par with GCM results at some stations. The variation in annual wind speed indicated the Guinean zone has low wind speeds and Wind Power Density (WPD). However, the Sahel zone of West Africa had the most potential based on WPD values. The authors conclude the RCMs simulations overestimated WPD and the increase in WPD due to global warming might not have sufficient effects on cites with low WPD for future wind power generation.

Ulazia et al., (2019) evaluated the wave energy trends on a long-term basis to assess their effect on the capture width of Wave Energy Converters (WECs). The study was based on ERA-20C data calibrated against ERA-Interim and validated with in-situ data at the Northeast Atlantic Ocean. Seasonal changes of the 20th century were assessed across 32 years for the Atlantic Ocean. The results show a reduction in capture width ratio by 20% for oscillating wave surge-type WECs as a result of an increase in wave energy flux by 3 and 2 kW/m per decade in winter and spring respectively.

Zhang et al., (2019) studied the changes in near-surface wind speed in china from 1958 to 2015. Multiple datasets like JRA55 (Japanese 55-year dataset), ERA-Interim from ECMWF and NCEP/NCAR data were used in this study. For the study, daily anemometer wind speeds were collected from National Meteorological Information Center (NMIC). The spatial and temporal distribution of averaged winds of multiple years from different databases were plotted and analyzed. The study showed the wind speeds across northern China were stronger than the southern part. Comparison with in-situ records showed JRA55 data matched well. The long-term wind studied also indicated a decrease in wind speed of 0.109 m/s/decade for China from 1958-2015 the decrease is more dominant since 2000.

2.2 LITERATURE ON NUMERICAL MODEL STUDIES

With the improvement and refining of wave models we have (third-generation) state of the art wave models which can be developed using tools like, WAVEWATCH III (WWIII) (Erikson et al., 2015), Simulating Waves Nearshore (SWAN) (Nayak et al., 2012), Wave Modelling (WAM) (Umesh et al., 2017), MIKE 21 (Aboobacker et al., 2009; Remya et al., 2012 and Kumar et al., 2018) etc. The third-generation model uses a more detailed nonlinear wave-wave interactions source terms and relaxes most of the constraints on the spectral shape in simulating wave growth. Various tools have been used by researchers worldwide with some merits and demerits. Numerical studies performed are discussed below.

Reistad, (2001) studied climate change effects on the wave climate, which subsequently might affect offshore operations and sea explorations. Waves and Storms of North Atlantic (WASA) was a research project to study the climate fluctuations over a longer time. As WASA could not successfully predict future changes, numerical model STOWASUS-2100 was an attempt that relied on wind and pressure data for the estimation of wave climate along with changes in wind and surges. STOWASUS-2100 was based on simulations of two 30 years cycles (1970-1999 and 2060-2089) using the ECHAM4 atmospheric model. There were several climate model simulations performed to study the changes in pressure, temperature and wind in a region. Statistical analysis was performed to study the variation in significant wave height. Validation was done based on observed and hindcast data. Higher variations were observed in the Norwegian Sea and the Barents Sea. North Sea wave heights with 100 years return period may increase by 0.5 m and the northern part of the Norwegian Sea might have wave heights increase up to 1.5 m.

Jose and Stone (2006) performed a wave simulation study along the Gulf of Mexico. The nearshore parameters were forecasted using MIKE 21. National Center for Environmental Prediction (NCEP) wind data from the National Oceanic and Atmospheric Administration (NOAA) was used as input. The northern boundary of the Gulf had finer resolution close to 2 km. The authors obtained good estimates during

fair weather sea. However, weather events such as Hurricanes and tropical storms were not captured due to the inaccuracy of wind input. The forecasts under predicted the extreme weather wave heights as compared to buoy measurements taken at stations located off the Louisiana coast.

Moeini and Shahidi (2007) performed a spectral model hindcast study on the wave parameters on Lake Erie using SWAN and MIKE 21 SW numerical tools. The models were subjected to varying wind conditions. The accuracy along with computational efficiency was measured. For hindcasting of waves, buoy collected data of Lake Erie from the period of 2002 to 2005 was used. Linear and nonlinear wind input were given on a nonstationary third-generation model in the Cartesian coordinate system. Bathymetry data, wave dissipation due to white capping and bottom friction conditions were considered. Calibration of the models was done by measured data of wind and waves from various stations. It was observed from the results that models slightly under-predicted the value of the peak wave period and over predicted the wave height. The results were verified with the measured data and standard deviation were mentioned. The authors conclude that the numerical method SWAN is superior to MIKE 21 SW for significant wave height estimation and MIKE 21 outperformed SWAM during the peak wave period estimation.

Strauss et al., (2007) compared two wave models developed in SWAN and MIKE 21 SW for Gold coast Australia. Gold coast is a sandy coastline with variable wave climate and longshore sediment transport. The boundary condition for the MIKE and SWAN model was based on modelling exercise extracted from NOAA's WaveWatch3 model. Both the model results were validated against buoy measurements. The authors found that the nearshore activities were well captured by the models. However, the inclusion of wind speed above 10 m/s did not improve the model performance.

Grabemann and Weisse (2008) studied the possible future changes in the North Sea due to anthropogenic climate change for 30 years (2071-2100). Numerical modelling was performed using WAM with an ensemble of wind data. Uncertainties are modelled with

two GCMs (HadAM3H and ECHAM4/OPYC3). The representative study for the existing climate was done based on 30 years of data (1961 to 1999) hindcast. Emission scenarios considered are A2 and B2 suggested by IPCC AR4, hence a total of four scenarios were tested. Finer resolution Regional Coupled Atmosphere-Ocean model (RCAO) was incorporated into WAM simulations. Extreme changes in climate were obtained by analyzing the differences in the four scenarios. As there is a variation in amplitude and spatial pattern of climate change signals for different models and different scenario it is difficult to rely on one model. It was concluded that the frequency of storm events is the reason for extreme wave heights. Despite the uncertainties, a moderate increase in wind speed at the end of the century is expected in the eastern part of the North Sea.

Aboobacker et al., (2009) developed spectral wave characteristics for nearshore off Paradip Port during monsoon and extreme events. Datawell directional wave buoy measurements from 1996 to 1997 off Paradip was used for the study. The wind data available from reanalyzed NCEP/NCAR winds is used for model studies which were developed using MIKE 21. The model could produce wave characteristics for different seasons off the Paradip region. The measured and model-simulated results were compared which were reasonably good. The correlation coefficient for wave heights was 0.87 with a bias of -0.25.

Holmbom, (2011) set up a small scale wave model for the Baltic Sea using MIKE 21. Three different wind inputs were tested to get the best fit with the measured data. The wind data considered were from nine Swedish Meteorological and Hydrological Institute (SMHI), Satellite measurements in terms of ocean surface wind velocity from Cross-Calibrated, Multi-Platform (CCMP) and Geostrophic winds from synoptic weather stations. The numerical model output was validated against five in-situ measurements. Statistical analysis showed that the CCMP wind data set gave better results than the other two wind fields. The authors also mention that the model was for offshore measurements and had fewer uncertainties for estimates of wave height less than 0.5 m and it underestimates wave period below 4s.

Nayak et al., (2012) assessed the effects of bottom slope on wave-induced setup during a cyclone event along Kalpakkam, located at the south-eastern side of India. SWAN was the numerical model used for this study. Initially, a sensitivity study was performed considering the JONSWAP wave spectrum for ocean boundary with a wave height of 9 m, wave period of 12 s and a wind speed of 20 m/s. Various models with different gird resolutions and beach slopes were analyzed. Further, the effect of cyclone 'NARGIS' on the Kalpakkam coast was studied. Near slope regions with gentle slopes showed very less variation in significant wave heights. The results showed a maximum setup of 0.4 m for 'NARGIS' near Kalpakkam coast with max. significant wave height 2.6 m and period 8.3 s at steep slopes. The estimate of wave parameters for the mild slope was reduced by 50% to that of steep slopes.

Remya et al., (2012) performed wave hindcast experiments for the Indian Ocean domain using MIKE 21. The bathymetry was developed based on GEBCO data. Blended wind data of ECMWF and QuickSCAT was given as input to the model for the year 2005. Satellite altimeter data along with buoy data was used for validation. The authors concluded that the effects of swell are significant in the Bay of Bengal region and it is less effective in the Arabian Sea region as other phenomena like sea breeze and Shamal swells take over. The validation results were satisfactory but, better results can be expected if a larger domain is considered.

Teena et al., (2012) have worked on estimating wave heights based on Generalized Extreme Value (GEV) and Generalized Pareto Distribution (GPD) on the eastern Arabian Sea location. The wave height was obtained at the one-hour interval at 15 m water depth off Honnavar coast for 31 years. The wave model was developed using MIKE 21 SW and was validated against buoy measured data during 2009. From the dataset, annual, monthly and weekly maximum wave heights were used for GEV analysis. The probability Weighted Method (PWM) is used for both GEV and GPD analysis along with the maximum likelihood method and method of moment for GPD parameter estimation. Comparison of wave heights obtained from various methods for

24

10, 50 and 100 years return period was performed. The authors concluded that the PWM based valued for GPD is reliable than the Maximum Likelihood method. Annual maximum based GEV predicted data well compared to GPD Peak Over Thresholds. For return periods the variation was within 9% for GEV and GPD analysis. The wave height with 100 year return period for the monsoon period was (~5.9 m) 1.55 times the value of pre-monsoon period data which was 2 times that of post-monsoon data.

Aydoğan et al., (2013) focused on estimating the wave energy potential of the Black Sea. Their focus is on the possibility of wave energy as an alternative source for fossil fuels. The spectral wave model was developed using MIKE 21 for 13 years (1996-2009). The simulation resulted from ECMWF wind speeds helped in preparing wave Atlas for this region. Validation was done using five in-situ records. The results indicated a decrease in wave energy along the coast from west to east. Annual wave energies were obtained and they found the Thracian shores of Turkey as a promising location to harness wave energy in the region studied.

Abdollahzadehmoradi et al., (2014) assessed the wave energy potential of the Marmara Sea using MIKE 21 SW module. The wind data input was from ECMWF. The MIKE model was calibrated to match the in-situ measurements taken at the Ambarli district of Istanbul. The parameters were altered to get a good correlation with the observed data. The study estimates a mean annual wave power of 0.84 kW/m for the year 2012 at the Marmara Sea. The offshore wave period was 2.5 s while the nearshore wave period was 2 s at the coastline.

Anoop et al., (2014) assessed the surface waves in the shallow water region of the Arabian sea both spatially and temporally. The stretch from Karwar to Ratnagiri along the west coast of India was their area of interest. Buoy measurements at these locations from 2011 to 2012 were considered by the authors for assessing temporal variations. The spatial variation was subsequently performed using the ERA-Interim dataset of ECMWF. Except for the monsoon, the variation of 10% in wave parameters was observed temporally. This temporal variation was within 26% during the monsoon

period. Similar trends were observed spatially where the variation was within 10% during non-monsoon. And the monsoon period had a spatial variation of about 20 %. The temporal and spatial variation was consistent along the 270 km coastline considered.

Appendini et al., (2014) performed a hindcast study on 30 years of data for the Gulf of Mexico region. The hindcast information was used to characterize mean and extreme waves climate in the study area. The MIKE model was based on ETOPO 1 bathymetry and NCEP winds from NOAA. Validation was performed using (National Data Buoy Centre) NDBC data and altimeter data from 6 satellite missions like ERS-1, ERS-2, TOPEX, GEOSAT, JASON-1, and ENVISAT. The authors concluded that the winter fronts were the major contributors to the wave climate of the Gulf of Mexico. An increase in wave height at a rate of 0.07 to 0.08 m/yr in September and October was observed as an effect of increased cyclone intensity over the last decade. However, the role of the Atlantic swell was not considered in their work.

Sandhya et al., (2014) contributed by developing a wave forecasting system at Puducherry coast which will help in marine-related operations. Two-dimensional energy density spectra which is time-varying was developed using a tool WWIII this data was used as boundary conditions for the SWAN model. Blended wind data from remotely sensed QuickSCAT retrievals was merged with ECMWF analyzed winds, which contributed by predicting waves for global oceans. Validation of the SWAN model was done based on the buoy (DWR-MkIII). The statistical correlation obtained is 0.8 which indicates a good correlation between measured and predicted data. SWAN under predicted the wave height in December 2008 which was because of weak wind input. Similarly, it overpredicted November 2007 wave heights as the 'SIDR' Cyclone hit the Bay of Bengal but its effect was least felt on the Puducherry coast. The authors mention that the study area is under the influence of strong distinct swell activities coming from the Northern Indian Ocean. The deficiency of the nested model is in the prediction of waves with a frequency above 10 s which was because of boundary inefficiency of WW3, the overall performance of the nested model was satisfactory.

Erikson et al., (2015) projected the wave climate with two CMIP5 climate scenarios for Eastern North Pacific. They performed a hindcasting study for data from 1979-2005. Three hourly wind speeds from four GCMs were used in this study. RCP 4.5 and RCP 8.5 were the scenarios considered in their study. Historical simulations of nearshore wave parameters were compared with buoy measurements. The CMIP5 models considered for the current study are BCC_CSM11.1, INMCM4, MIRCO5, GFDLE_SM2M. WaveWatch 3 (WW3) was the numerical wave model used in the study. An extreme value analysis of significant wave heights was performed using Generalized Pareto Distribution (GPD). Wave parameters with a return period of up to 100 years were evaluated for RCP 4.5 and RCP 8.5. The results for the current century indicate a decrease in mean annual wave heights along the North American west coast and south of Hawaii. North of Hawaii and the Gulf of Alaska will experience increasing trends when both the RCPs were considered.

Kumaran et al., (2015) conducted a study on wave climate to locate a suitable location for offshore structure in the Lakshadweep group of islands. Numerical model studies were performed using MIKE 21 SW module. Available wind data from ECMWF is used for hindcasting offshore wave characteristics. Two model studies were performed, one where the wind to wave transformation model (regional model) considering North Indian Ocean and the second model where fine resolution wave to wave transformation model (local model) of Agatti Island was created. The regional bathymetry was based on GEBCO and CMAP bathymetry for the regional model along with echo sounder data by NIOT was used for local model input. A regional model with flexible mesh was calibrated using AD09 buoy data installed at 1500m water depth. The significant wave height simulated and observed were compared and they were comparably similar. Calibration of the local model was done using CB02 buoy data. The local model slightly underestimates significant wave height when compared with the observed data. The authors concluded that the local model can be further used for locating a suitable site for offshore structure.

Kumar and Naseef, (2015) assessed the performance of the ERA-Interim dataset for Indian nearshore waters. The authors used modelled dataset as ship observations are not effective in large area capture and altimeter data have a low temporal resolution. The evaluation was performed on the east and west coasts of India. Validation was based on a year's buoy measurement taken at six different locations along the Indian coast. The statistical parameters assessed were R, RMSE, bias, and SI which was based on the significant wave heights (H_s) and wave period measured at six buoy locations. The overall analysis showed the ERA-Interim overestimated H_s with a difference of about 15% along the west coast. ERA-Interim, underestimated H_s by 33% at the east coast which experiences frequent cyclone. Hence the author suggests using ERA-Interim dataset values for design application only after proper validation.

Patra et al., (2015) investigated offshore wave characteristics during cyclones storms at the Bay of Bengal region. Wave modelling was done using MIKE 21 SW module. This study was performed for the year 2008-2009 considering NCEP wind fields and ETOPO1 bathymetry. The modelled results were compared with IMD measurements which recorded 5 cyclones during the selected period. The simulated wave heights were in good agreement with measured wave heights with a correlation coefficient of 0.86. The results were also compared with some empirical relations like Sverdrup-Munk-Bretschneider (SMB) equations which overestimated the values.

Pentapati et al., (2015) emphasize the estimation of potential changes in significant wave height due to climate changes in the Mumbai High region. Mumbai High has the highest number of offshore oil platforms (more than 200) in India. Past and future wave heights were estimated with MIKE 21 SW numerical modelling. Reanalyzed Data of NCEP for obtaining past wave conditions from 1971-2010 was used as input for numerical model simulation. For forecasting 40 years wave conditions, they used GCMs output of the CanESM2 project of CMIP5. Bias correction of RCP 8.5 is done before simulation, to standardize the future wind with historical GCM data. Flexible mesh in MIKE 21 was developed by ETOPO2 bathymetry data for deep water and CMAP for coastal water. Long-term effects were assessed using distributions such as

Weibull, Generalized Extreme Value and Generalized Pareto Distribution. Authors estimated that wave heights may increase by 10 to 28% in the northern part of Mumbai High and from zero to 10% in southern sites.

Amrutha et al., (2016) performed numerical model analysis using SWAN and WW3. The model performance was evaluated concerning to buoy measurements off the Karwar coast. SWAN has larger nearshore applications and WW3 is capable of global and regional modelling. Hence SWAN model is nested along with WW3 for the Arabian Sea domain in this study. ERA-Interim wind data was used during modelling with ETOPO1 bathymetry. The WW3 model overestimated the wave period in deep waters by 23.7% when the source term 2 package was used. However, the nested model was in good agreement with nearshore observation with an R-value of 0.96. The observation was better during the non-monsoon period when compared to the monsoon period and this model was effective in forecasting the Ocean state for the Karwar region.

Hemer and Trenham, (2016) assessed the performance of the global dynamic wind-wave climate derived from CMIP5. For this study eight CMIP5 models, three CMIP3 models and their ensembles were used. Wave parameters were assessed across thirteen areas of the global ocean. The hindcast study was compared along with ECMWF products and NCEP climate forecasts. WW3 wave model was used for wave climate simulation based on GCMs. The performance of models was measured using metrics like Mielke measure (M-score) which is nondimensional, followed by Normalized Error Matrix (NEM-score). The model performance was ranked based on thirteen areas divided around the global. The ensemble-based simulations provided a good rank for the Indian Ocean domain followed by GCMs like HadGEM2. The authors, however, do not claim any high-performance GCM forced wave simulation. They also mention that the effect on the model resolution in its performance is minimal.

Jadidoleslam et al., (2016) prepared a wave power atlas for the Aegean Sea near Turkey based on the ERA-Interim dataset from 1999 to 2013. The numerical model used in the

study was MIKE 21 SW module. Nine buoy observations were used for calibration. Wave power was calculated on a monthly and seasonal scale. The spatial variability of wave power along the Turkey coast was assessed. Along with wave power, the authors performed statistical analysis on simulated and observed wave heights and wave period. The direction aspect of wave power was captured in wave rose diagrams. From the study, the authors found February as the powerful month with wave power potential reaching up to 9 kW/m. However, the month of May showed the least potential. The maximum average energy was for wave heights in the range of 1.5 to 3 m with energy periods between 4.5 to 6 s. From the study performed on 10 different points north to middle southern had maximum mean power. These regions were between Crete and Kasos islands as per the study area considered.

Patra and Bhaskaran (2016) have performed a detailed study for the head region of the Bay of Bengal based on the satellite altimeter data collected from 8 satellite missions for 21 years and compared it with numerical model results. Annual and seasonal variability in wind speeds and significant wave heights were studied based on daily altimeter data obtained from IFREMER/CERSAT. The numerical model developed in WWIII showed values close to the satellite measured data, modelling was based on NCEP wind datasets from Climate Forecast System Reanalysis (CFSR) from 1997 to 2010. The bathymetry of the study was from Earth Topography version 1 (ETOPO1). The Bay of Bengal dominates seasonal winds governing the wind-wave climate when compared with the Arabian sea. Spatial distribution of annual variation results indicate wind speed and significant wave heights are maximum during monsoons for the Bay of Bengal region.

However, these percentage variation results of wind speed and significant wave height showed contrasting trends (east-west dipole) for the head bay considered. Additionally, spatial variability in the dataset was studied using Empirical Orthogonal Function where the principal component helped them understand the trend in variation for two decades. It was concluded by correlating Mean Sea Level Pressure (MSLP) to the contrasting trend in wind speed and significant wave height for the eastern and western side of the head Bay of Bengal region.

Rajasree et al., (2016) predicted the shoreline shifts along the Udupi region in their study. The study was based on two methods, initially based on satellite imageries followed by a numerical model study of shoreline for past and future predictions of 35 years. They also performed an alternate computation study using the Artificial Neural Network (ANN) to understand future changes. The study is on an uninterrupted shoreline of 6.5 km along the Udupi coast. Historical satellite imageries from 1979 to 2014 (35 years) is initially used for the study. A downscaled version of GCM is numerically modelled with CORDEX wind data as input after bias corrections and bathymetry derived from CMAP. MIKE 21 SW module was used to simulate the wave heights and wave periods for 35 years. Future studies are based on RCP 4.5. Outputs were validated against buoy data of 3 years. Statistical analysis revealed a rise in wave height by about 37% based on numerical modelling studies. The authors conclude based on the satellites imageries that the coast is subjected to continuous erosion with an average rate of -1.46 m/yr. Numerical modelling indicated an erosion rate to be -2.21 m/yr. and ANN predicted an increase by -1.66 m/yr.

Satyavathi et al., (2016) predicted the possible changes in significant wave height and spectral time period for a return period of 100 years along the west coast of India. They suggest that the climate change effects on design waves can be studied based on two-time slices of 30 years each, past using reanalyzed wind data and future using GCMs. Statistical analysis was performed to obtain the wave height and wave period after 100 years based on Pareto distribution. 21 offshore locations along the west coast of India about 50 km offshore was considered for the study. NCEP/NCAR reanalyzed wind data from 1971 to 2010 was the input for the MIKE 21 SW model with ETOPO2 and CMAP based bathymetry. For forecasting (2011-2050) a GCM developed form CCCMA as a part of the CMIP5 experiment was used. Buoy data measured for 3 years was used for validation. Design waves were evaluated based on GEV and GPD best fit of these was selected based on the Kolmogorov- Smirnov statistic test. GPD proved to have the lowest test statistic as both wave height and wave period fitted well for all locations.

The results obtained indicate that as wave height increases, the wave period also increases except for regions at the southern tip where the complex wind wave system between the Indian Ocean and the Arabian Sea. Probability density function plots were obtained to justify the projected future change. Wave directional changes caused by air circulation changes were highlighted with the help of the rose diagram. The significant wave heights might increase within a range of 7% to 45% and the wave period within 14% to 51% along the west coast of India confirming the severe wave climate.

Divinsky and Kosyan (2017) objective were to perform a Spatio-temporal variability analysis for the Black Sea. The climate data from 1979 to 2015 was considered in the study. Numerical modelling was done using MIKE 21 of DHI. Wind wave fields from ERA-Interim was the input to the model. The model was further verified by buoy measurements, a stationary platform, and altimeter data. Statistical analysis in terms of bias, RMSE, SI, etc. was performed for the data processed along the Black Sea. Wave energy fluctuations were assessed with the spatial distribution of wave energy along the Black Sea. The study revealed that strong and extreme storm affected the climate in the western part of Sea and the eastern part had moderate storms. The contribution of north-eastern waves on wave energy showed an increasing trend over 37 years.

Pradhan et al., (2017) investigated the shoreline changes associated with the dynamic tidal inlets of Chilika lagoon. A numerical study of wave parameters was performed using measured bathymetry, beach profiles, and sediment characteristics and utilizing the MIKE 21 SW model. The objective was to quantify the sediment transport rates. The results were validated against measured values that were in close agreement. The results indicated erosion in the middle and north spit and deposition in the southern spit. The authors conclude that alongshore transport is predominant in Odisha as compared to Andhra Pradesh and Tamil Nadu.

Roshin and Deo (2017) investigated wave changes after 100 years along the 7000 km long coast of India as a result of climate change. Numerical wave models are studied and statistical analysis was performed. Wind data from Coordinated Regional Climate

Downscaling Experiment (CORDEX) was collected for two-time series, past (1979-2005) and future (2006-2033) each of 27 years. Selected 39 offshore stations are 50 km from the coast at a water depth ranging from 20 to 2000 m. MIKE 21 SW was used for modelling based on unstructured meshing. Bathymetry was generated based on CMAP and digitized NHO charts. For better prediction model variables like roughness, breaking and white capping were considered. The extreme value probability distribution function is used as a statistical tool for long-term wave height prediction. GPD was the distribution function used for the obtained past and future wave heights. The threshold for wave heights is obtained from the POT method. Three wave rider buoys were deployed at 20 m from the coast, whose three years of measured data was used for validation.

Wave heights are compared as past and projected mean wave heights at different locations. Annual and mean wave height variation trend for a specific location was studied year wise. The probability density function for wave height at certain locations was also obtained decade wise, which indicated larger waves in future. One location showed a decrease in wave height and the possible reason being, it was a shallow gulf pocket. The authors found that the wave height does not depend on depth, however, the changes in wave height might be the result of nonlinear wave propagation at shallow depths. In general wave heights obtained in eastern locations show less increase when compared to the western coast of India.

Saraçoğlu et al., (2017) highlight the importance of wave climate in studies related to coastal erosion, structure design, and sediment dynamics. MIKE 21 SW numerical model was used to evaluate the Black Sea region from 1996 to 2008. Buoy measurements along five different locations along the Turkey coast were considered for calibration. MIKE numerical model was set by bathymetry obtained from Turkish Naval forces and ECMWF wind data. The output obtained was highly consistent with wind and deep water wave atlas of Turkish coasts. The significant wave height was in the range of 10 m with a wave period varying between 2 to 10 s.

Sirisha et al., (2017) predicted wave conditions for the north Indian Ocean for winters and extreme conditions. The approach adopted for wave modelling involved using ECMWF wind data for near-shore along with ten buoy measurements. The error statistics of the outputs from ECMWF winds were performed. The results were validated using buoy measurements observed during cyclones like Sidr, Khai Muk, and Nisha. The authors main objective was to verify the extreme event forecasts given by ESSO-INCOIS. The results showed BoB winds showed better results than AS winds. Error statistics analysis showed the forecast was reliable and the best match was with Nisha cyclone observations. The authors point out that the forecasts were best in a wave range of 1 to 2 m. they also suggest that refinement of the atmospheric model can enhance the results in coastal areas.

Umesh et al., (2017) simulated and validated wave spectra for ocean wave using numerical model SWAN for the Puducherry coast. Wind data from ERA-Interim winds for the outer domain and QuickSCAT-NCEP blend winds for the intermediate domain were considered and their effect on wave spectra was studied. Three different multi-scale nested models were used for simulation, they are nothing but grids with different horizontal resolution. Numerical experiments for the coarser grid were performed using the WAM prediction model, the WAM model helped in providing boundary information of 2D wave energy spectra. ETOPO1 bathymetry and wind data which is responsible for generating waves were used during modelling. The monthly peak energies obtained from the SWAN model for a finer grid evaluated for both the wind datasets used in the study and was compared with the buoy measured data. The performance of the model was assessed by statistical error analysis where it was compared with buoy measured data. The study was also extended for comparison of results obtained for storm conditions with calm conditions. The multi-scale nested model results reviled blended winds gives a better representation of Puducherry coast and the model gave good results for southwest monsoon and hence the model can be used for operational use.

Casas-Prat et al., (2018) simulated a global ocean wave climate based on wind speeds

34

and sea ice concentrations for the Arctic ocean. WW3 numerical wave model was developed using CMIP5 historical data from 1979 to 2005 and future projections based on RCP 8.5 for 2081-2100. The model resolution varied from 100 km offshore to 50 km nearshore. BCC-CSM1-1, MIROC5, GFDL-ESM2M, EC-EARTH are the CMIP5 datasets used along with ERA-Interim and CFSR winds. The study resulted in historical wave climates which were overestimated with positive bias. The future winds also showed an increase in wind speed for the Arctic region with an exception of the GFDL-ESM2M dataset. The authors mention that projected wave heights could increase up to 6.4 m in September in the Arctic ocean. Overall the model results indicated higher wave activity in the Arctic region compared to lower latitude regions.

Ilia and O'Donnell (2018) compared the performance of SWAN and MIKE 21 third-generation models in determining coastal circulation and wave processes. The models were developed for New Haven Harbour in Connecticut, U.S. where the effect of three breakwaters on the wave parameters was assessed. The major difference for the modelling approach adopted is that for time integration, MIKE 21 uses an explicit approach while SWAN is based on a fully implicit method. Time step and grid size were kept constant to have uniformity between the two models. The simulated model outputs were compared with measured records of the storm during the winters of 2015. An R^2 of 0.6 was obtained for both models. MIKE 21 showed better results during storm peaks. The authors mention that both the model's performance was poor when the wind blew from coast to sea. The breakwater dissipated more energy in MIKE 21 model as compared to SWAN. The computational time taken by both models were similar.

Kumar et al., (2018) examined the annual changes in significant wave height (H_s) along the Indian mainland for 15 years. In their study, 19 locations were identified around the Indian coast at a water depth of 55 m. MIKE 21 wave model was used for the study with CMAP bathymetry data. The wind from ECMWF was used as input. A sensitivity analysis was carried out comparing the obtained results with buoy measurements. Comparison of the hindcast with AD02 buoy for the year 2012 gave a good correlation

at the AS region. The monsoon trend of H_s was higher, and the average trend in the western Gulf was higher when compared to the eastern gulf. The paper also highlights that the variation in surface wind speeds by 10% can lead to a 10-20% error in H_s estimates. The authors obtained an annual mean H_s at the western shelf and eastern shelf locations of about 1.2 m and 1 m respectively. The trends in H_s observed from 1998 to 2012 was 1.14 cm/yr in the western shelf and 1.03 cm/yr in the eastern shelf seas. They also pointed out that the results should be considered with care as the closing boundary considered in the study was 40ºS.

Zilong et al., (2018) focus on obtaining nearshore wave height from predictive equations by a method called the response surface method. Here, the nearshore wave heights were predicted based on offshore wave records. The directional decoupled parametric formulation in MIKE 21 was used as the study focus on nearshore wave propagation. The water levels were given as input to the model along with the offshore measurements. Sample points were selected on the response surface and the best fit was obtained. Based on wave energy flux conservation and coefficients which were undetermined, predictive equations were obtained. Predictive equations sensitivity was assessed based on nearshore measurements taken for a shorter duration. The predictive equations were for the non-breaking region which gave a correlation of 0.85.

Barbariol et al., (2019) performed a long-term and global statistical assessment of maximum wave heights. The authors have combined numerical model outputs with extreme statistics on ocean waves for 25 years. The ERA-Interim reanalyzed product is validated against buoy measurements of the North Pacific Ocean. Assessment of ERA-Interim with the latest product called ERA-5 is also performed. The wave heights of the global ocean (Atlantic, Pacific, and Indian) were provided by 50th and 99th percentile values along with 50-year return period values. The authors claim that this study is one of its kind as it assesses the maximum values of sea states quantitatively.

Chowdhury and Behera (2019) assessed the GCMs performance to simulate waves. GCMs from CMIP5 and Regional circulation models (RCMs) from Coordinated

Regional Climate Downscaling Experiment (CORDEX) were used in wave modelling of the Indian Ocean domain. The results were evaluated based on ERA-Interim reanalysed data. The study was based on RCPs like RegCM4(GFDL), RCA4(IPSL), RegCM4(CSIRO), RCA4(CNRM) and an ensemble model as well. Bias correction of these data was done using the quantile mapping method before using as input data in MIKE 21. The results showed that there is no significant advantage of using fine resolution GCM in simulating regional wave climate. In deep waters, GCMs and RCMs showed a good correlation with R about 0.9 when compared with ERA-Interim. However, in shallow waters, GCMs was better than RCMs when compared with ERA-interim with values of R of 0.6 and 0.2 respectively. It was observed that climate-driven models simulations were estimating the mean values better than the extremes. Amongst the climate models used ensemble GCM showed the best result for the Indian Ocean domain.

Cucco et al., (2019) assessed the role of temporal resolution while modelling sea surface transport which is induced by wind. They carried out numerical model studies for the Gulf of Oristano. The measurements taken from anemometers which were located at the coast at different locations were used. Also, wind-induced sea surface transport was measured using 16 drifters for nearly two years. A three dimensional hydrodynamic model with high resolution was used. This FEM model provided simulations of wind-induced water circulations. The model was forced by hourly winds obtained from the field observations and were compared with simulated drifter trajectories. The simulated drifter trajectory was then assessed against the observed drifter trajectory. The sampling time varied from 1 min to 1 day. The results showed wind speeds with lower resolutions of 1 min did not affect the model results as compared to 1-hour datasets. Hence, using the lowest sampling intervals temporally may not guarantee accurate outputs in oceanic predictions.

Lemos et al., (2019) performed a study using an ensemble of wave climate projections for the mid 21st century (2031-2060). The ensemble constituted a WAM wave model, CMIP5 four GCM dataset and RCP 8.5 projections. In-situ measurements (72 stations)

along with reanalyzed data was used for comparison. The authors observed a considerable effect of climate change in the mid-21st century global wave climate. An increase in wave parameters like mean significant wave height, wave energy flux and mean wave period was observed. The WAM model proposed gave realistic estimates of the global wave climate.

Liu and Zhao, (2019) performed a global ocean wave propagation study using the SWAN wave model with ERA-Interim winds from 1979 to 2016. The study takes into account swells along with the wind-waves. The monthly averaged wind speed for the global oceans are plotted based on ERA-20C data from 1980 to 2010. Some critical regions like North Pacific, North Atlantic, and the Southern Ocean were modelled in SWAN. The simulation indicated that southeastward and southward moving swells are predominating in the North Pacific and North Atlantic regions. Southern Ocean experiences swell which moves northeastwards. The authors also located swell pools in topical Oceans.

Noujas et al., (2019) performed numerical model studies on an embayed beach at Vengurla along the west coast of India. A numerical model was developed using the LITPACK module of MIKE 21 to study the shoreline evolution for 26 years. The model input parameters like wave data were based on buoy records of the year 2015, the bathymetry data and sediment data collected at the same period was also used. Tidal gauge data is also imputed to the model. The initial coastline of 2015 was based on satellite imagery. The shoreline evolution of future years (26 years) was predicted using LITCONV tool in LITPACK. The results indicated that from 1990–2016 the Vengurla has experienced accretion of 1.6 m/yr and 1.0 m/yr in the southern and northern sectors respectively. The future coastline is predicted to advance by 10 m along with the southern sector, accretion of 80 m along with the northern sector. Hence the authors suggest that the sand dunes should not be disturbed for any construction purpose as it will affect the coastline.

2.3 SUMMARY OF LITERATURE

This section highlights the importance of operational oceanography relevant to marine related applications. The growth in the shipping industry has encouraged more and more marine structures which, in turn, has encouraged studies related to wave forecasting. Long-term data analysis in terms of hindcasts and forecasts are essential prerequisites in the design of the marine structure. This section also discusses numerical wave modelling using MIKE 21 being successfully adopted for various regions around the globe. The common practice of using wind as input from global datasets can be seen. Validation for a shorter period using in-situ measurements helps in the assessment of the numerical model's efficacy. The numerical wave model has been used for wave forecast studies, asses renewable energy prospects, extreme event analysis, shoreline studies, estuary dynamics etc. Hence, the methodology for the present research is framed in similar lines.

Based on the kinds of literature reviewed the wave climate on the east coast of India is more severe than on the west coast. The monsoons result in rough seas and during fair weather season that is the rest of the year wave climate will be calm. At present, more emphasis is not given to the West coast of India due to less extreme events observed. The historical data based on reanalysed products have performed well but there is some uncertainty involved while choosing the model for the future, considering climate change effects. Hence, the efficacy of CMIP5 models is assessed through statistical tools from which a best-suited model for the Indian domain can be obtained.

The literature review points out that a numerical model study with wind speed reliability analysis can also be extended to assess the wind-wave climate. This, in turn, helps in mapping the renewable energy potential along the Indian coast. The developed numerical wave model can also be applied to study the long-term shoreline changes along the coast. Hence, in the present study, the objectives are extended to explore the applicability of this numerical model to assess the wind and wave energy potential along the coast and to study the shoreline changes along Mangaluru.

2.4 PROBLEM IDENTIFICATION

The projected global sea-level rise is expected to be at a rate of 8 mm/year to 16 mm/year during the years 2081 to 2100 according to IPCC (2007). Most of the Indian landmass has a sea-level only a few meters high. An independent wave model for the Indian domain is a work in progress. Hence, this research can focus on selecting the best performing global model dataset which fits to the Indian Ocean domain. Formulation of a numerical model for simulating wave climate is essential. Literature globally used MIKE 21 SW module for numerical modelling which can be explored. There are many problems along the Indian coast associated with the wave climate. Shoreline changes and wave climate variation during the monsoon and applicability of the numerical model to assess these variations can be evaluated. With a focus on renewable energy, the wind and wave energy potential along the Indian coast for a specific return period can be estimated. The coastal protection works constructed is generally without considering the climate change effects. Hence, there is a need to study the wave parameters along the Karnataka coast considering climate change effects and their response on the coastal structures.

2.5 RESEARCH OBJECTIVES

The following objectives are framed based on the research gaps:

1. To simulate the historical wind-wave climate along the Indian domain using MIKE 21 numerical wave model driven by wind speeds from ERA-Interim global dataset and validating the model set up with in-situ measurements.

2. To perform long-term analysis of waves based on historical simulated wave heights and its comparison with in-situ records for the Mangaluru coast. Additionally, modelling of shoreline changes along the coast.

3. Assessment of wind and wave climate at nearshore locations along the Indian coast based on ERA-Interim global hindcast dataset.

4. To perform historical data analysis from 1980 to 2005 based on monthly wind speed data from 38 different CMIP5 global datasets and correlating it with ERA-interim global dataset to arrive at the best performing CMIP5 models for the Indian domain.

5. To evaluate the performance of best CMIP5 models with four RCPs (2.6, 4.5, 6, 8.5) based on average daily wind speed data from 2006 to 2018 and to forecast the wave climate along the Karnataka coast.

2.6 SCOPE OF THE WORK

An understanding of long-term variation in wave climate is a necessity when an engineer has to design a coastal or an offshore structure. The variations inclusive of the climate change effect should be taken into account when the structure is designed for a particular return period. The population density in coastal India is larger due to various factors, making it very sensitive to the effects of climate change. The low lying areas along the Indian coast are most vulnerable to coastal flooding and land subsidence aggravating the problem and poses a serious threat to the coastal population.

Most of the wave forecast study is region-specific. A numerical model study with wind speed reliability analysis can be extended to assess the wind-wave climate. The diminishing supply of fossil fuels and the increase in global energy demand has shifted

the focus on renewable energy which is environment-friendly. The focus is now on sustainable development which is inevitable without harnessing renewable energy sources. The wave characteristics which affect other coastal phenomena like sediment transport has to be studied for the sustainable development of the coast. Hence, the methodology for the present study is framed so that the above-mentioned problems can be solved by the numerical wave model study.

CHAPTER 3
MATERIALS AND METHODS

This chapter presents the methodology involved in wind speed data analysis and the development of the numerical model developed for the wave climate analysis of the Indian domain.

3.1 METHODOLOGY

In the present study, the following action plan has been followed.

Objective 1: The ERA-Interim wind dataset is validated with in-situ records at BD11 and AD02 installed at the east and west coast respectively. Further, based on reanalyzed ERA-Interim hindcast wind data, MIKE 21 SW numerical model simulated significant wave heights (H_s) are validated against in-situ wave heights taken at Karwar location for the year 2011 and offshore Goa (OB02) for the year 2005.

Objective 2: A long-term analysis based on five probability distributions is studied for the Mangaluru region and the best performing Weibull distribution ($\alpha=1.3$) is applied to the simulated H_s to obtain the hindcast. The estimates for a return period of 10 and 50 years are compared with the long-term analysis performed on in-situ records at the same location. The simulated wave parameters are used to study the shoreline changes from 1980-2015 at the Mangaluru coast using the LITPACK module of MIKE.

Objective 3: Assessment of wind-wave climate at nearshore water depths along the Indian coast from MIKE numerical model driven by ERA-Interim wind speeds.

Objective 4: Monthly average wind speed data of 38 different CMIP5 models are correlated against the ERA-Interim dataset based on hindcasts from 1980-2005. The results are compared with the help of the Taylor diagram. The best performing models for the Indian domain are arrived at.

Objective 5: To forecast the near future wave climate, RCP projected daily wind speeds are compared with ERA-Interim data from 2006-2018. The wave climate is forecasted based on the closest to reality RCP projections. The near future wave climate with a return period of 10 and 50 years is simulated using a numerical wave model.

Fig. 3.1 Methodology flow chart

Legend:
- Hindcast (1980-2005)
- Nowcast (2006-2018)
- Forecast (up to 2070)

Flow chart elements:
- ERA-Interim Global wind data
- C-MAP Bathymetry for Indian domain
- In-situ data (validation)
- Numerical wave model (MIKE21 SW)
- Wave parameters (1980-2005)
- In-situ data at Mangaluru (5 years)
- Long-term analysis
- Shoreline changes along Mangaluru (LITPACK)
- Assessment of wind-wave energy along Indian coast
- Location specific design significant wave height for return period of 10 and 50 years
- ERA-Interim dataset
- Statistical analysis on monthly wind speed
- CMIP5 dataset (38 models)
- Best performing CMIP5 model for Indian domain
- RCP projections from four best datasets
- Statistical analysis on daily wind speed
- ERA-Interim dataset
- RCP closer to the prevailing wind speed trends for Indian domain
- Numerical wave model (MIKE21 SW)
- Forecast of location specific significant wave height for return period of 10 & 50 years

44

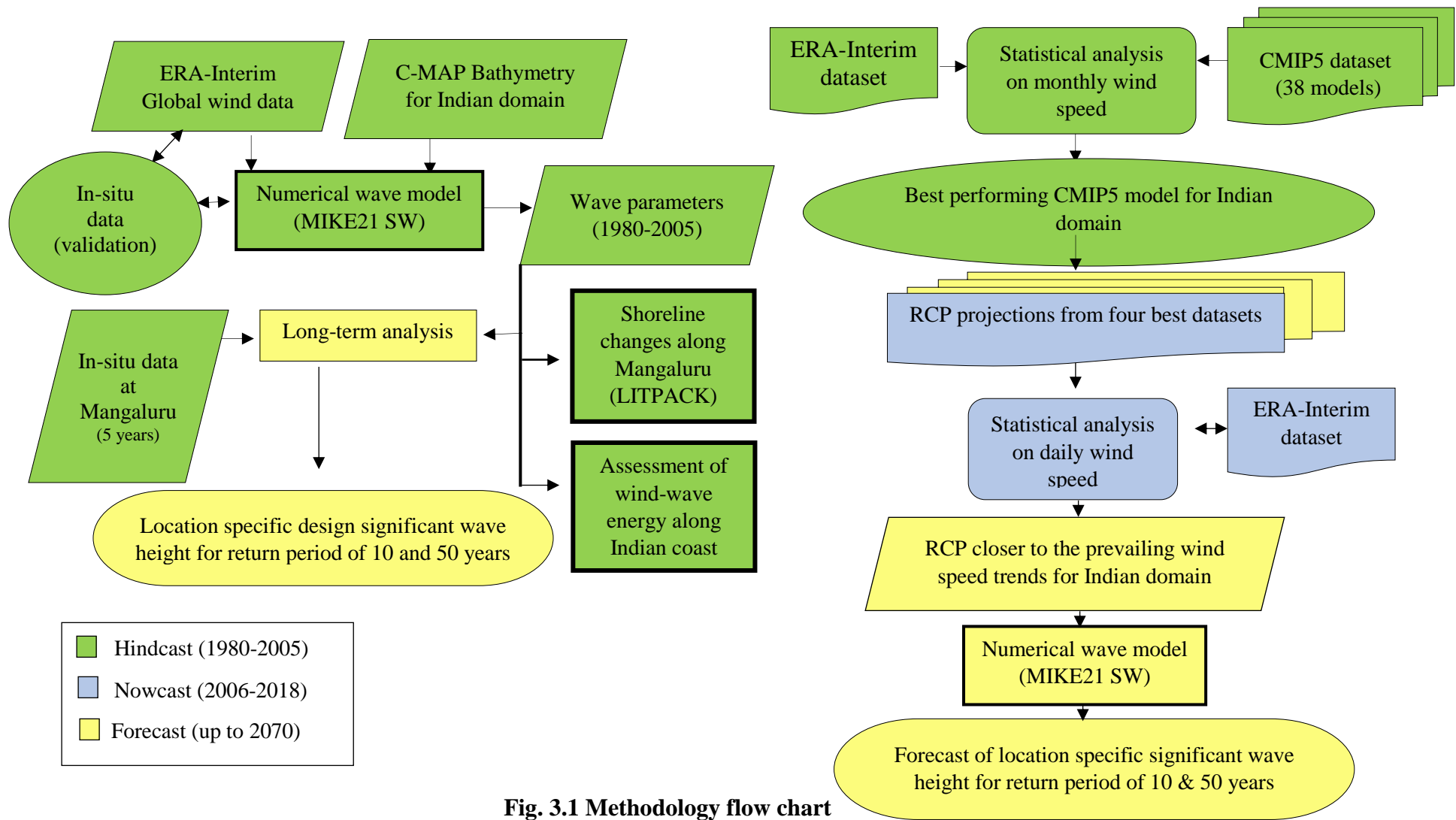## 3.2 WIND SPEED DATA ANALYSIS

3.2.1 Data collection and processing

Oceanographic hindcast and forecast products are mostly mathematical equations models based on the ocean and atmospheric processes. Large computation facilities are required for studies of this magnitude which will be taken up by government metrological agencies supported by other bureau or agencies. In the present study, the first objective is a historical data comparison of ERA-Interim with in-situ measurements. The MIKE 21 SW model is driven by ERA-Interim winds which is a product of ECMWF. Daily wind speed data for 26 years after downloading has to be processed. The wind speed data from the global datasets are extracted from their respective public web interface. The coordinates of GCM (Figure 3.2) corresponds to 30º N 40ºE -4º S 95ºE (Indian domain). This huge dataset of raw data has to be processed before using it as input for numerical modelling. The required wind data is obtained in Network Common Data Form (.netCDF) from different datasets, consistency of data plays a vital part. The wind speeds downloaded (U_{10} and V_{10} components) are measurements corresponding to 10 m height from the mean sea level. The resultant wind speed is calculated from U_{10} (zonal) and V_{10} (meridional) components as $\sqrt{U_{10}{}^2 + V_{10}{}^2}$ Zhang et al., (2019). These measurements help in predictions for future and also current sea state estimation. A consistent spatial resolution of 0.5º x 0.5º is maintained across datasets in the present study. The boundaries are set with respect to coordinates 30º N 40ºE -4º S 95ºE (Figure 3.2). The daily wind speed data with about 1213056 data points are then reduced to a monthly average of 312 values corresponding to 26 years.

Processing of these data is performed using a tool called FERRET developed by National Oceanic and Atmospheric Administration, U.S. which works in the LINUX platform. FERRET is a versatile tool that can analyse, process and visualize climate data. The downloaded data is imported to FERRET which is followed by operations like re-gridding, obtaining resultant wind speed and monthly average wind speed followed by exporting the data into the required format (Annexure 1). This processed data is then extracted in text form; further statistical analysis is performed using programming language 'R' by plotting Taylor plot.
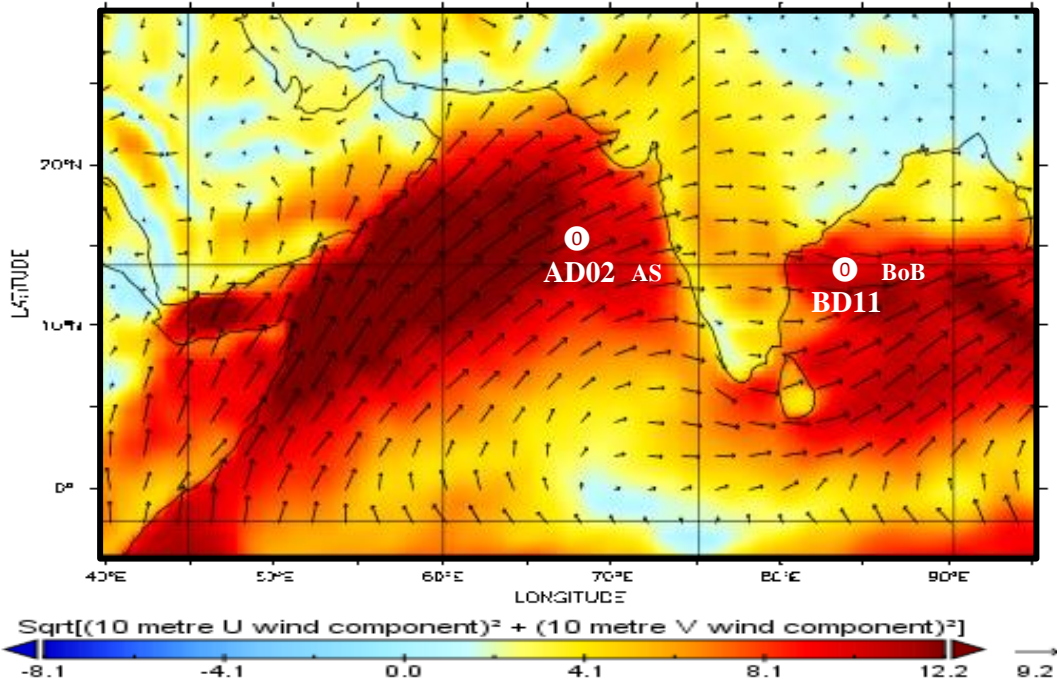
Fig. 3.2 Typical resultant wind speed (m/s) variation along the Indian domain considered for the study (- 4º to 30º N 40º to 95ºE)

3.2.2 Validation

Operational Oceanography deals with measurements of oceanic variables like waves, currents, wind, tides, etc. for a certain duration. Validation of the datasets is mandatory to evaluate the global datasets performance; this can be done using in-situ measurements.

The validation is against buoy measurement recorded by AD02 and BD11 (Fig. 3.2) deployed offshore of Goa coast (69.01°E, 15.02°N) and Tamil Nadu coast (84.00°E,13.50°N). The daily wind speed data measured for a year is compared with ERA-Interim wind speeds. The buoy measured wind speed at 3 m from sea surface level whereas, ERA-Interim wind speeds are at 10 m height (Hithin et al. 2015; Boudia and Santos, 2019). Hence, the required conversion is performed by commonly used Hellmann exponential law (Suvire, 2011)

$$\frac{V}{V_o} = \left| \frac{H}{H_o} \right|^{\alpha} \qquad (3.1)$$

Where,

V is the speed at height H= 3 m and V_o is the speed at height H_o = 10 m

Frictional factor α = 0.125 (for Lakes, ocean and smooth hard ground)
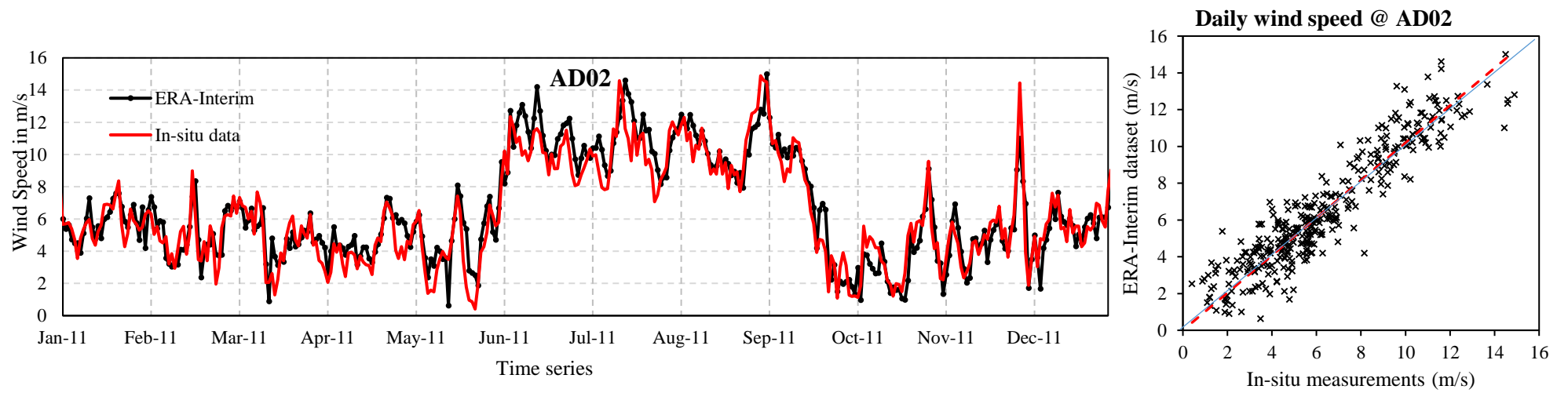
Fig. 3.3 Daily wind speed variation and Scatter plot at AD02 along with corresponding ERA-Interim values for the year 2011
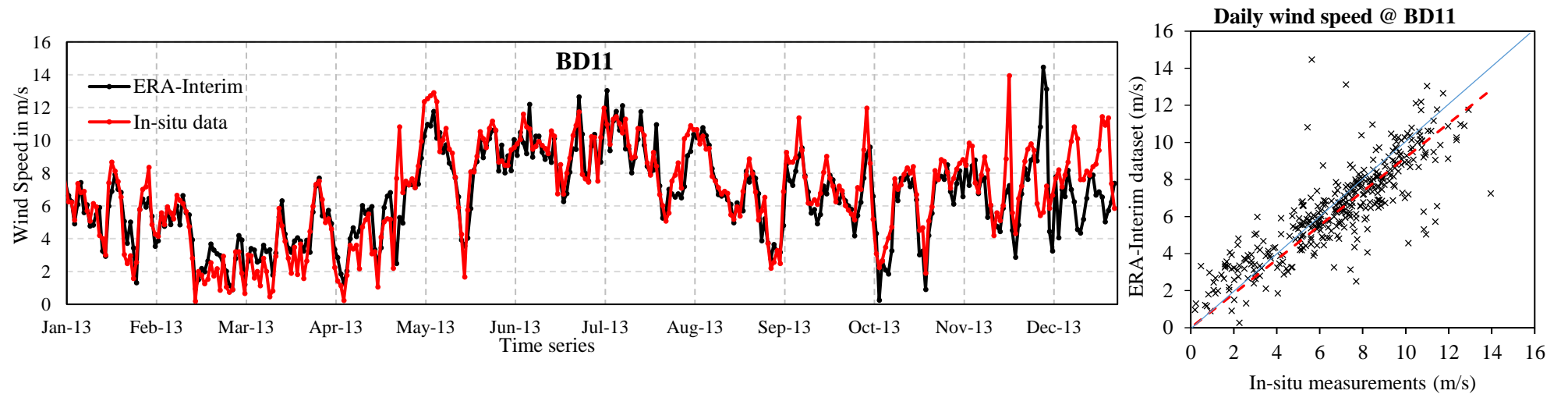
Fig. 3.4 Daily wind speed variation and Scatter plot at BD11 along with corresponding ERA-Interim values for the year 2013

Location-specific buoy data is obtained from INCOIS for the required period. Various statistical indices in the form of Correlation Coefficient (CC) and Root Mean Square Error (RMSE) will provide an estimate of the accuracy of the modelled wind speed. The daily wind speeds from ERA-Interim are compared with the offshore locations on the east and west coast of India (Figure 3.3 and Figure 3.4) which showed an excellent match. AD02 had an R-value of 0.93 and RMSE 1.20 m/s for the year 2011. BD11 had an R-value of 0.84 and an RMSE of 1.59 m/s for the year 2013. Daily modelled wind speed performance is good which is reflected in the scatter plots.

3.3 NUMERICAL MODELLING

Solutions to the wave propagation problems can be effectively obtained by numerical modelling. In the present study, the numerical model is developed using MIKE 21 a commercially available tool. This third-generation wave model (SW module) is based on unstructured meshes that work on the cell-centred finite volume method (DHI, 2015; Chowdhury et al., 2019). MIKE21 SW simulates wave parameters spatially by solving energy and mass balance equations. Wind waves in the MIKE model are represented as action density spectrum $N(\sigma,\theta)$, Where σ is angular frequency expressed as $2\pi f$ and θ being the wave propagation direction. The wave action balance equation can be either represented in cartesian coordinate form or spherical coordinate form. The cartesian coordinate system is preferred for small scale applications where the conservation equation is as shown below,

$$\frac{\partial N}{\partial t} + \boldsymbol{\nabla}.(\tilde{v}\boldsymbol{N}) = \frac{S}{\sigma} \qquad (3.2)$$

Where,

$N\ (\bar{x},\ \sigma,\ \theta,\ t\ )$ is the density function, with time 't', $\bar{x}$ is (x,y) in Cartesian coordinate, $S=S_{in}+S_{nl}+S_{ds}+S_{bot}+S_{surf}$ with S_{in} being momentum transfer due wind, S_{nl} represents the nonlinear wave-wave interaction mechanism, S_{ds} is energy dissipation due to white capping, S_{bot} is the energy dissipation attributed due to bottom friction and S_{surf} is energy dissipation depth induced wave breaking parameter, $\tilde{v}= (c_x,\ c_y,\ c_\sigma,\ c_\theta)$ is wave group propagation velocity in four-dimensional phase space of $\bar{x},\ \sigma,$ and θ with a fourth-dimensional differential operator ∇ (Sørensen et al., 2005).

MIKE 21 numerical wave model gives more emphasis to the detailed parameterization

of the wave-wave interaction which is non-linear (Abdollahzadehmoradi et al., 2014). The growth and decay of waves along with the transformation of wind-generated waves and swells can be simulated using this software based on unstructured meshes (Appendini et al., 2014). Holmbom, J. (2011) highlights the similarity of MIKE 21 with that of SWAN in terms of the process of wave generation but, the difference is that SWAN considers rectilinear or curvilinear mesh. MIKE, on the other hand, uses the Eulerian model with unstructured mesh which makes it more flexible. MIKE 21 is one of the world's leading tool to be used for modelling marine engineering problems (Ilia and O'Donnell, 2018). Sørensen et al., (2005) mention these models focused on the formulation of source function based on physical phenomena which enhanced its application in coastal regions. Zilong et al., (2018) from their research found that both offshore and nearshore wave conditions can be effectively modelled using MIKE 21 Spectral Wave (SW) module.

In MIKE 21, the cell-centred finite volume method is used for spatial discretisation of the conservation equation (Sørensen et al., 2005). The fully spectral formulation and directional decoupled parametric formulation are the two governing equations in MIKE 21 SW. Amongst the two governing equations fully spectral formulation is preferred as it is based on wave action conservation equation (Eqn. 3.2). Generally, the spectral wave models include the following processes - i) Wave generation by wind input ii) Nonlinear interaction iii) White capping (wave breaking in deep water) iii) Bottom friction iv) Depth-induced wave breaking (wave breaking in shallow water) vi) Refraction and shoaling. However, computation efficiency in terms of time can be reduced by directional decoupled parametric formulation (Zilong et al., 2018). The module is based on a wave action balance equation where time integration is done by the effective multi-sequence explicit scheme.

3.3.1 Input parameters

The accuracy of the simulated output of wave parameters is dependent on the bathymetry of region and wind speed data. To obtain the input bathymetry, initially, the global domain (Figure 3.2) is traced using the google earth pro tool. The boundaries are set concerning coordinates 30º N 40ºE -4º S 95ºE. The Ocean boundaries are considered to be a closed boundary. C-MAP provides digital bathymetry features in the MIKE

readable format which is based on databases like General Bathymetric Chart of Oceans (GEBCO). This traced boundary along with land and water file in .xyz format is then imported through manage scatter data option of MIKE zero. Further, the triangular mesh is generated using generate mesh command. A coarser mesh of the order of few kilometres is created for the offshore region and the nearshore regions had finer mesh with sizes in meters. Smoothing of the generated mesh is performed followed by the interpolation command in the MIKE mesh generator tool. After smoothening and interpolation this bathymetry has 6152 nodes and 11656 elements. This bathymetry file (.mesh) is then exported in MIKE readable format (Figure 3.5(a)) which can be used in the SW module.

The wind forcing is also a very important input that affects the numerical model performance. The simulation of waves will be achieved by running a numerical wave model forced by wind speeds derived from ERA-Interim for the past data (hindcast), and CMIP5 GCM dataset for future predictions (forecast). The downloaded wind data needs to be processed where it is converted into MIKE readable format. The wind file should be in a time series form (.dfs0) for the required domain. The .netCDF GCM wind data was read and processed using the excel spreadsheet of Microsoft. A code is developed in the virtual basic application tool of the excel spreadsheet to automate the data conversion process (Annexure II). Later the time series tool of MIKE is used to get the wind data in the required format year wise. The processed file is exported to the ASCII form. The grid series tool in MIKE is used to import this ASCII file and the wind data is saved in .dfsu2 format. This .dfsu2 file with wind forcing is used to drive the MIKE numerical wave model (Figure 3.5(b)).

The computational time varies depending on the simulation period and the core capacity of the system. The output parameters (Figure 3.5(c)) are extracted as area series (.dfsu format) capturing the entire domain. The required point data from the area series can then be extracted (in .dfd0 format) by specifying the coordinates. The key integral output parameters such as significant wave height (m) and wind speed (m/s) values are extracted and compared with in-situ measurements for validating the numerical model. Additional parameters such as mean wave period (s), water depth (m) and wave power (kW) are extracted from the simulated results to assess the wind-wave climate.
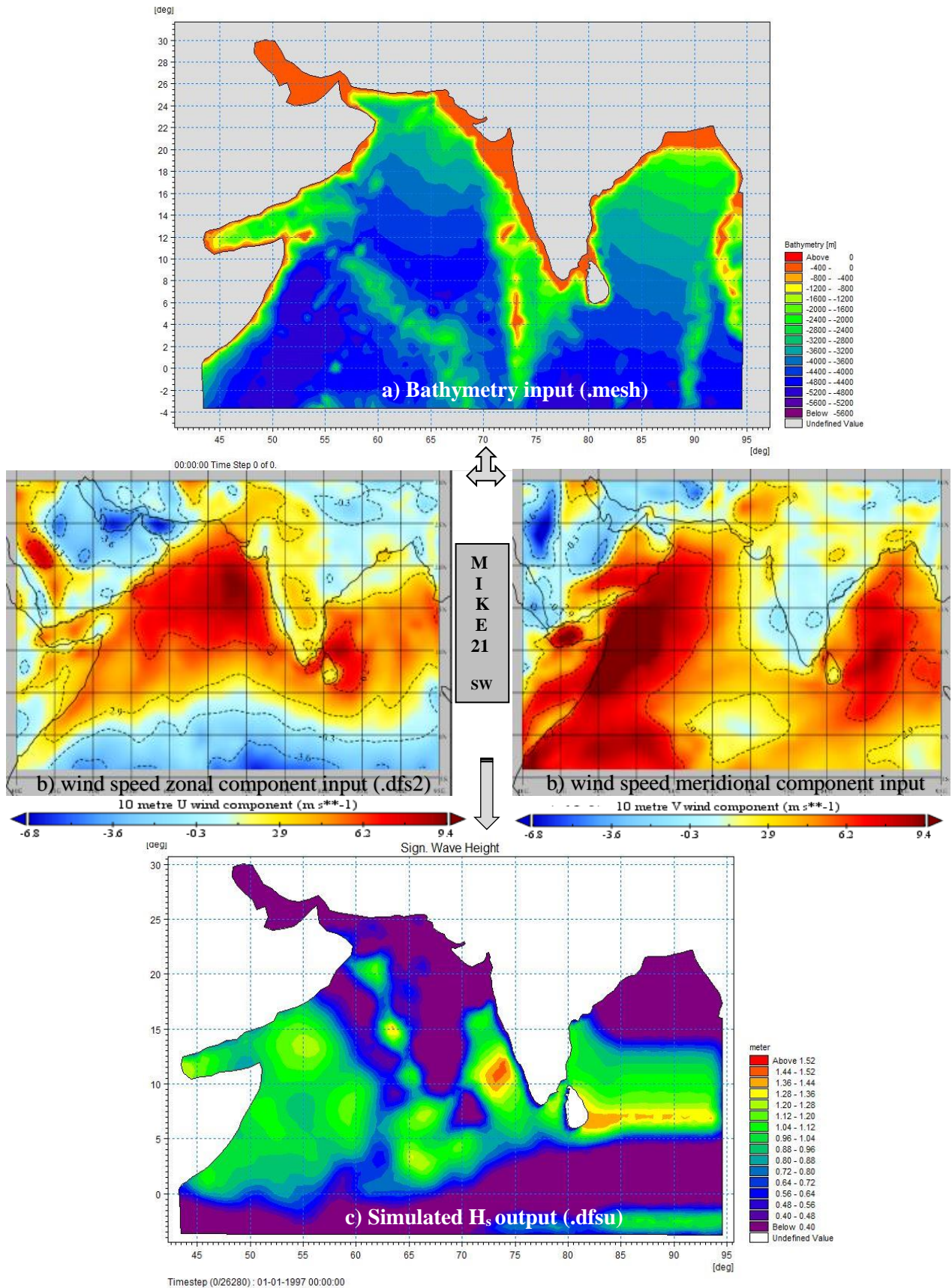
50

Fig. 3.5 The sequence of MIKE 21 modelling

As the wind forms the primary input for wave generation, the basic model equation is chosen as fully spectral and the time formulation is prescribed as a non-stationary

formulation. Spectral discretisation in MIKE can be further specified as frequency and directional discretisation. Logarithmic frequency discretisation with 25 frequencies and 360 degrees rose directional discretisation with 16 directions are assigned to the model. The higher-order solution technique was the chosen scheme for discretisation of the geographical and spectral-domain as it has better accuracy. Water level changes and current variations are not considered while modelling in this study. Ice coverage is negligible in our domain and hence not considered. Diffraction effects are not considered. The other parameters are tuned according to our model requirements.

Holmbom, (2011) suggest that in deep waters, processes like wind generation, quadruplet wave-wave interactions, and white capping are dominant. The initial conditions are as per JONSWAP fetch growth expression. In coastal waters, bottom refraction/shoaling, surf breaking and triad wave-wave interaction are dominant while bottom friction and current refraction significantly affect the outputs. White capping is the most sensitive parameter along with wind inputs (Moeini and Shahidi, 2007). Dissipation coefficients in MIKE 21 can be specified as C_{dis} and δ_{dis}. As the present study focuses on the coastal region, some of the calibration parameters are kept constant during modelling. These calibration parameters are assigned based on many model runs performed. The scatter plots of few trails with varying wave breaking and dissipation coefficients are shown in Annexure III. Table 3.1 shows the calibration parameters assigned to the model so that the simulated significant wave heights are closer to the in-situ measurements at the specified locations.

Table 3.1 Details of the MIKE 21 SW numerical model

In-situ location	Numerical model details					
	Name	Wave breaking	bottom friction	Current friction	C_{dis}	δ_{dis}
Karwar	Model1	0.7	0.04 m	3	4.5	0.5
OB03	Model2	0.6	0.04 m	5	7	0.3

3.3.2 Validation of model setup

It is one of the common and popular approaches to verify the model outputs in the form of wave heights through in-situ measurements (Sirisha et al., 2017, Kumar et al., 2018, Zilong et al., 2018, Takbash et al., 2019).
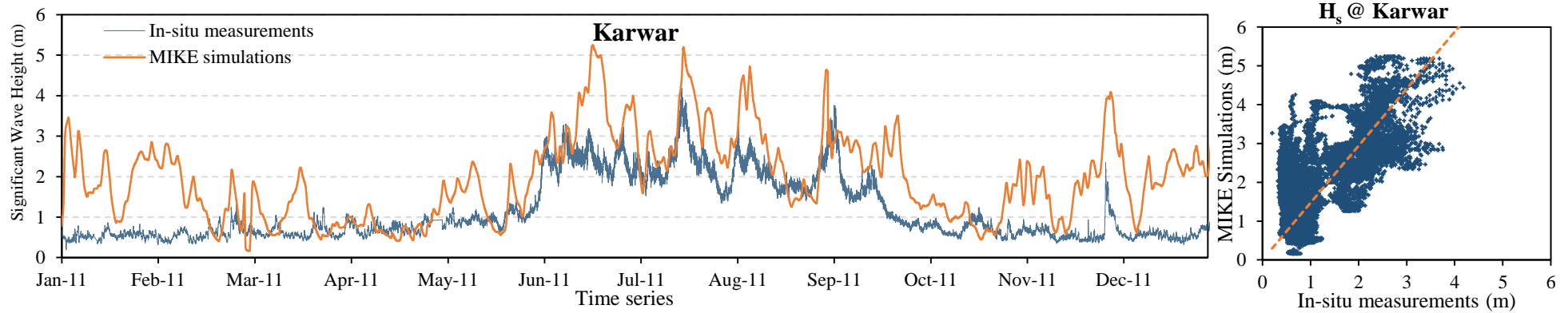
Fig. 3.6 Variation of H_s and Scatter plot at nearshore Karwar station along with corresponding MIKE simulations for 2011
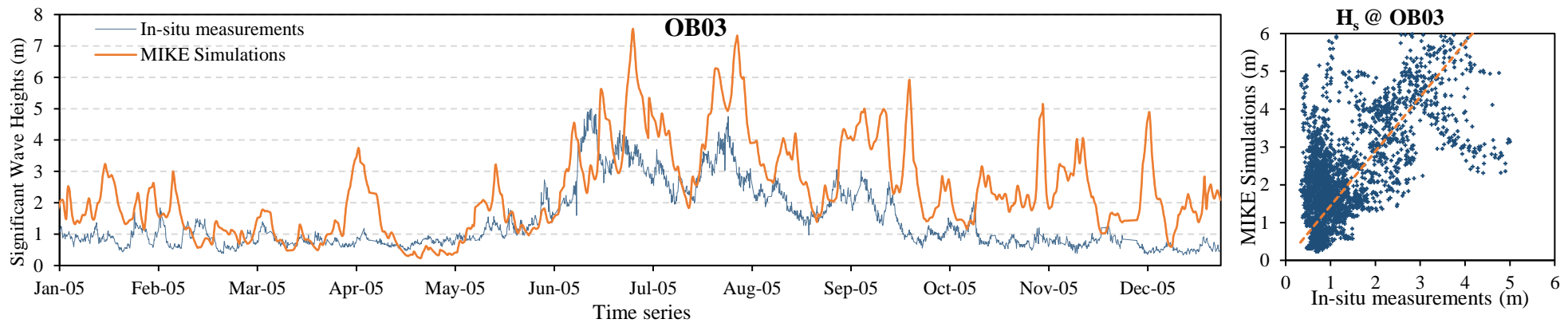

Fig. 3.7 Variation of H_s and Scatter plot at offshore station OB03 along with corresponding MIKE simulations for the year 2005

The model output has been quantitatively validated based on in-situ measurements. The simulation period is set depending on the buoy data availability for validation hence start and end period of the simulation is accordingly set. For the Karwar nearshore region, an R-value of 0.67 and an RMSE of 1.13 m is observed for the year 2011. The offshore location OB03 had an R-value of 0.66 and an RMSE of 1.42 m for the year 2005. The scatter plot is indicating that MIKE simulated significant wave heights are on a higher side when compared with in-situ measurements of wave heights (Figure 3.6 and Figure 3.7). The variation of significant wave heights is fairly captured and the MIKE numerical model majorly overestimated the wave heights in both locations. The model output at the buoy location is found satisfactory considering that the coarser-resolution and wider domain datasets being used in this study.

3.4 COMPARISON OF WIND DATASETS

ERA-Interim provides both hindcast and nowcast of various oceanic parameters but, ERA-interim datasets do not provide predictions for the future. Hence, CMIP5 datasets are considered for future prediction of wind speeds. CMIP5 comprises various model developing groups worldwide which provide various climatic projections. In the present study, historical wind speeds obtained from ERA-Interim are compared against different CMIP5 model historical wind speed data which is the fourth objective of the present study. The best performing CMIP5 model for the Indian ocean domain is further used in the present study to obtain wave forecasts for specific return periods. Historical data analysis comprises of wind speed data of 26 years (1980-2005), which is from 38 CMIP5 models (Table 3.2) and it is compared with the ERA-Interim dataset. Here, the ERA-Interim dataset is considered as controlled data set as their wind speeds matches well with the in-situ data as mentioned in the earlier section 3.2.2. The spatial resolution of CMIP5 models is different as it is developed by different modelling agencies.

Comparison between such a large dataset and arriving at a feasible dataset is a laborious task. Hence, Taylor (2001) came up with a graphical solution for comparing patterns of different global climate models. These diagrams are known as Taylor diagrams and are extensively used globally by climatologists. IPCC (2001) specifies the relative skill of these diagrams in gauging different climate models.

Table 3.2 Details of CMIP5 models used for comparison

Sl. No.	Model	Institute	Spatial Resolution (Long.×Lat.) in degrees	RCPs available			
				2.6	4.5	6	8.5
1.	NorESM1-ME	Norwegian Climate Centre, Norway.	2.5×1.875		✓		
2.	NorESM1-M				✓		✓
3.	MRI-ESM1	Meteorological Research Institute, Japan.	1.125×1.125				✓
4.	MRI-CGCM3			✓	✓	✓	✓
5.	MIROC4h	Atmosphere and Ocean Research Institute, National Institute for Environmental Studies & Japan Agency for Marine-Earth Science and Technology.	0.56×056		✓		
6.	MIROC5		1.41×1.39	✓	✓	✓	✓
7.	MIROC-ESM		2.81×2.77	✓	✓	✓	✓
8.	MIROC-ESM -CHEM			✓	✓	✓	✓
9.	BNU-ESM	Beijing Climate Center, China Meteorological Administration	2.81×2.77		✓		✓
10.	BCC-CSM1.1m				✓		✓
11.	BCC-CSM1.1				✓		✓
12.	IPSL-CM5B-LR	Institut Pierre-Simon Laplace, France	3.75×1.875		✓		✓
13.	IPSL-CM5A-LR			✓	✓	✓	✓
14.	CNRM-CM5-2	Centre National de Recherches Meteorologiques, Meteo-France, France	1.41×1.40				
15.	CNRM-CM5			✓	✓		✓
16.	GFDLCM3	NOAA Geophysical Fluid Dynamics Laboratory, USA.	2.5×2.0	✓	✓	✓	✓
17.	GFDLCM2.1				✓		
18.	GFDL-ESM2M			✓	✓	✓	✓
19.	GFDL-ESM2G			✓	✓	✓	✓
20.	GISS-E2-R-CC	NASA Goddard Institute for Space Studies, USA	2.5×2.0		✓		✓
21.	GISS-E2-R			✓	✓	✓	✓
22.	GISS-E2-H-CC				✓		✓
23.	GISS-E2-H			✓	✓	✓	✓
24.	ACCESS1.3	Commonwealth Scientific and Industrial Research Organization (CSIRO), Australia and Bureau of Meteorology (BOM), Australia	1.875×1.25		✓		✓
25.	ACCESS1.0				✓		✓
26.	CSIRO-Mk .3.6.0	Commonwealth Scientific and Industrial Research Organization (CSIRO), Australia	1.875×1.86	✓	✓	✓	✓
27.	HadGEM2-ES	Met Office Hadley Centre, U.K.	1.875×1.25	✓	✓	✓	✓
28.	HadGEM2-CC				✓		✓
29.	HadGEM2-AO			✓	✓	✓	✓
30.	HadCM3		3.75×2.5		✓		
31.	MPI-ESM	Max Planck Institute for Meteorology, Germany.	1.875×1.85		✓		✓
32.	MPI-ESM-MR			✓	✓		✓
33.	MPI-ESM-LR			✓	✓		✓
34.	INM-CM4	Institute for Numerical Mathematics, Russia	2.0×1.5		✓		✓

35.	CanESM2	Canadian Centre for Climate Modelling and Analysis, Canada	2.81×2.79	✓	✓	✓
36.	CMCC-CMS	Euro-Mediterraneo sui Cambiamenti Climatici, Italy	3.75x3.7		✓	✓
37.	CMCC-CM		0.75×0.75		✓	✓
38.	CMCC-CESM		3.75x3.4			✓

The pattern similarities in the Taylor plot is established in terms of correlation coefficient (R), standard deviation (σ) and centred Root Mean Square Differences ($\bar{E}$ or *RMSD*). The statistical analysis is based on the expressions shown below (Taylor, 2001),

Standard deviations (σ),

$$\sigma_r{}^2 = \frac{1}{N}\sum_{n=1}^{N}(r_n - \bar{r})^2 \qquad (3.3)$$

$$\sigma_f{}^2 = \frac{1}{N}\sum_{n=1}^{N}(f_n - \bar{f})^2 \qquad (3.4)$$

Where,

$\bar{r}$ is the mean value corresponding to reference field r (ERA-Interim dataset)

$\bar{f}$ is the mean value corresponding to test field f (CMIP5 datasets)

σ_r and σ_f are standard deviations of reference and test fields.

Correlation Coefficient (R),

$$R = \frac{\frac{1}{N}\sum_{n=1}^{N}(f_n - \bar{f})(r_n - \bar{r})}{\sigma_f \sigma_r} \qquad (3.5)$$

Centred Root Mean Square Difference ($\bar{E}$),

$$\bar{E}^2 = \frac{1}{N}\sum_{n=1}^{N}[(f_n - \bar{f}) - (r_n - \bar{r})]^2 \qquad (3.6)$$

In the present study, the Taylor diagram is plotted on average monthly wind speed data across 26 years. Statistical analysis and Taylor diagram are plotted using programming language 'R'.
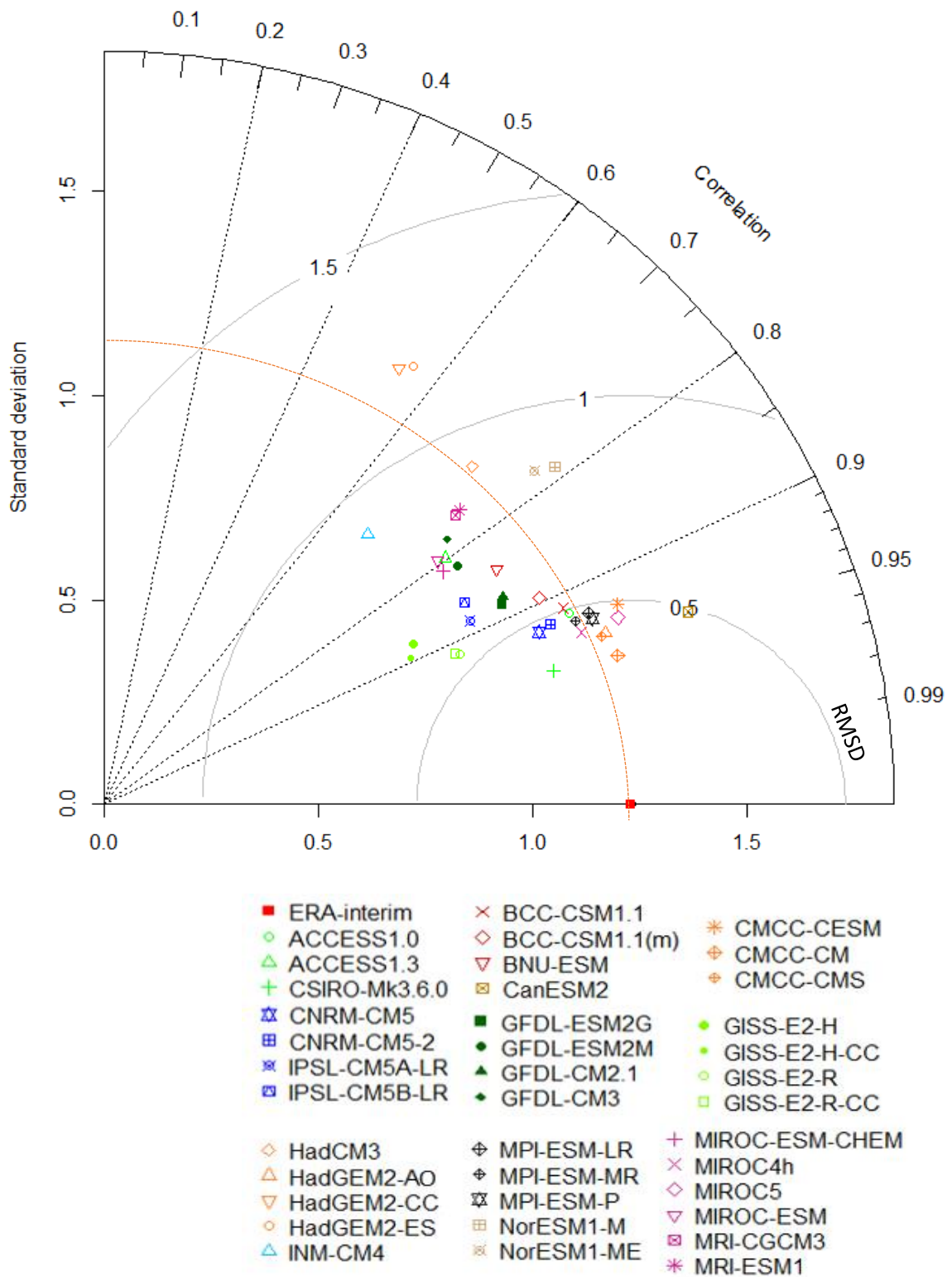
Fig. 3.8 Taylor diagram corresponding CMIP5 models and ERA-Interim

Monthly average wind speeds from historical data (1980 -2005)
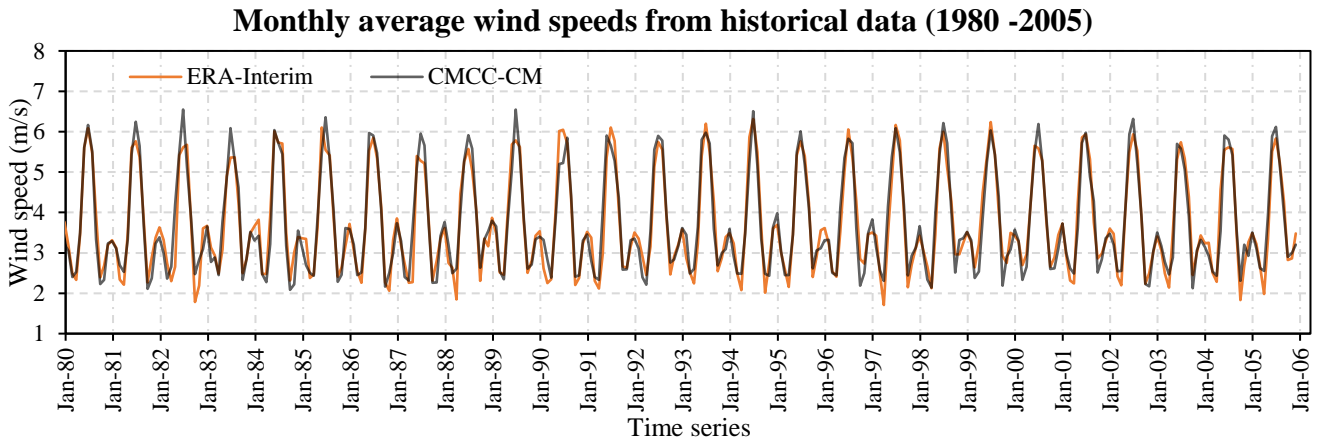
Fig. 3.9 Wind speed variation of historical data from ERA-interim and CMCC-CM GCM.

Monthly average wind speeds from 1980-2005
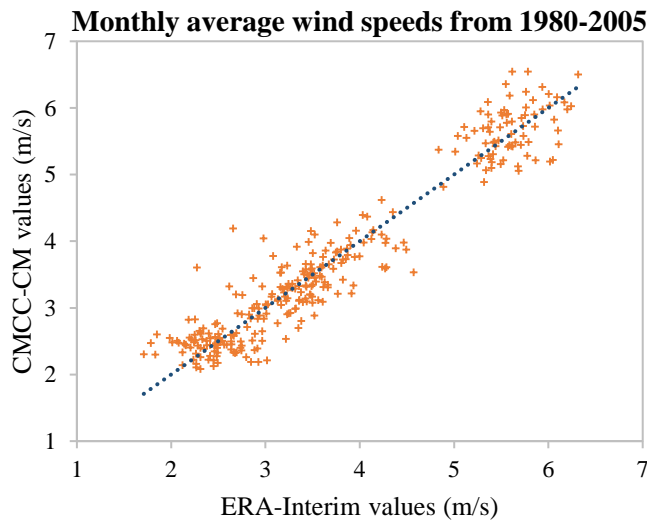
Fig. 3.10 Scatter plot

From the above Taylor plot (Fig. 3.8) and time series plot (Fig. 3.9), it is clear that amongst the 38 different CMIP5-GCMs, CMCC-CM matches well with ERA-Interim wind speeds. Statistical analysis showed a correlation of 0.96, a standard deviation of 1.25 and an RMSD of 0.3 m/s. The historical plots on a temporal scale depict the monthly variation of wind speed values (Fig. 3.9). Here it can be observed that higher wind speed from June to September across 26 years which reflects in terms of harsh wave climate.

CMCC-CM an Italian GCM with a spatial resolution of 0.75°x 0.75° provides projections for RCP 4.5 and RCP 8.5 only. As the fifth objective is to find a relevant RCP amongst all four RCPs, the four best GCMs which are in good agreement with ERA-Interim wind speeds are considered for further analysis.

The four best datasets (CMCC-CM, CSIRO-mk3.6.0, HadGEM-AO, and MIROC5) are chosen based on the Taylor plot above plotted on monthly mean wind speed variation across 26 years for the Indian domain. The performance of these CMIP5 daily wind speed data across available four Representative Concentration Pathways (RCPs) is assessed for a nowcasting period of 13 years (2006 – 2018).
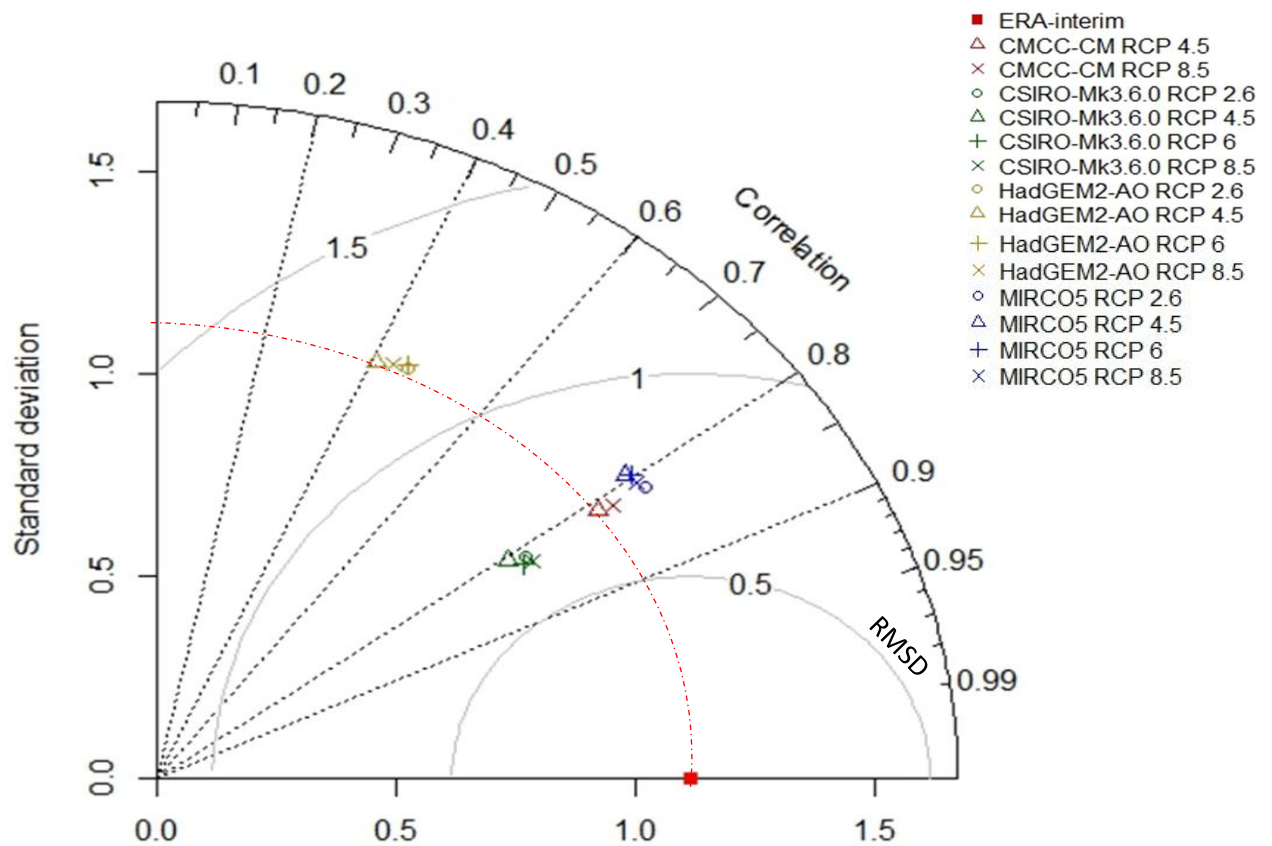
Fig. 3.11 Taylor plot for wind speed datasets across 13 years

From the Taylor plot amongst the 14 CMIP5 projected datasets, CMCC-CM for RCP 4.5 is closest to the ERA-Interim reanalyzed daily wind speed data. The Correlation Coefficient is 0.81, standard deviation 1.13 and RMSD of 0.75 m/s.

The objective here was to obtain the best GCM model amongst the available database of CMIP5 projections for the Indian domain. Figure 3.11 indicates that the present wind speed variability is close to CMCC's RCP 4.5 projections incorporating present emission scenarios for the Indian domain. The daily variability between these two datasets is shown in Figure 3.12 and Figure 3.13 below.
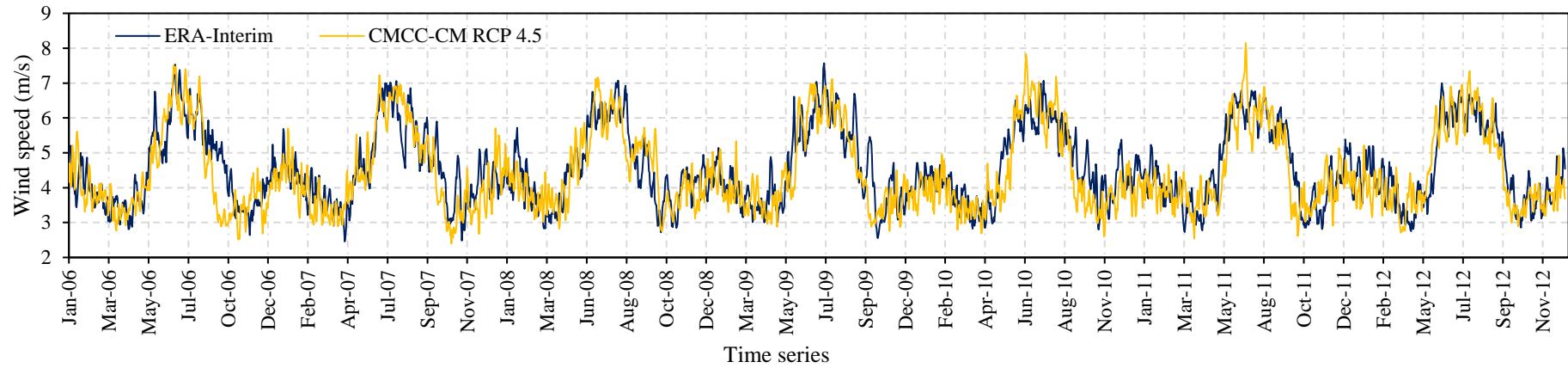
Figure 3.12 Variation of daily mean wind speeds of ERA-Interim and CMCC-CM RCP 4.5 from 2006 to 2012

Figure 3.13 Variation of daily mean wind speeds of ERA-Interim and CMCC-CM RCP 4.5 from 2013 to 2018

The variability plots with daily temporal changes indicate two successive peaks yearly across 13 years. The peak values of wind speed are from the south-west and north-east winds which are predominant in the Indian domain. CMCC-CM projections are a slight overestimate of wind speeds, especially during the years 2010 and 2011. The maximum daily wind speed of 7.6 m/s and 8.1 m/s are observed 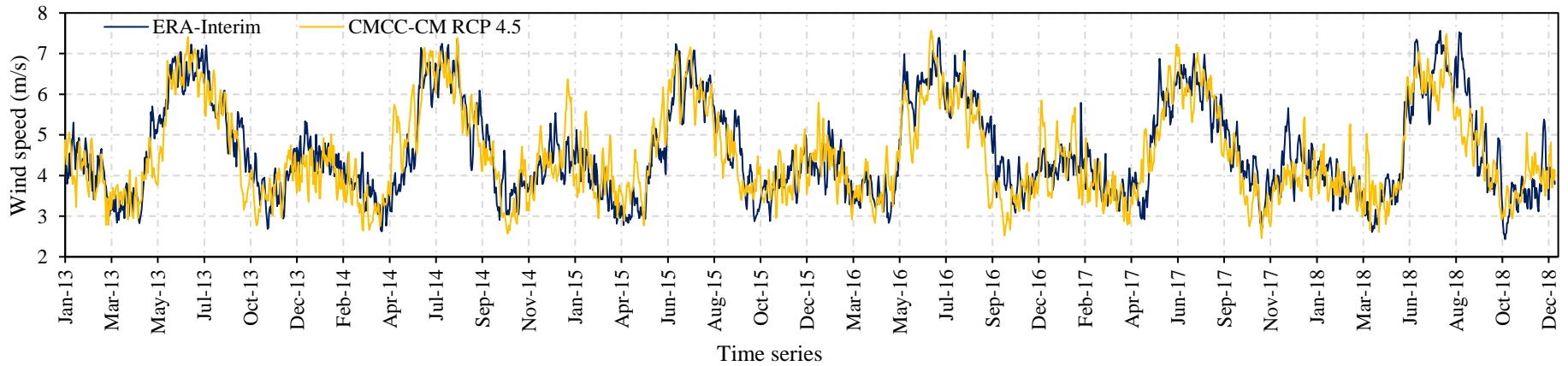for ERA-Interim and CMCC datasets respectively. Hence, amongst the CMIP5 dataset, CMCC-CM RCP 4.5 follows the current wind speed pattern and can be used to forecast wave climate.

Therefore, the GCM wind speeds of CMCC-CM RCP 4.5 with a spatial resolution of 0.75º x 0.75º will be used as input for simulating the near future wave climate using MIKE 21 numerical wave model.

3.5 SUMMARY

The chapter discusses the methodology adopted in the present study. Wind data analysis is initially performed where reanalyzed ERA-Interim daily wind speeds performance is compared with in-situ measurements. ERA-Interim wind speeds showed an excellent match with correlation coefficients of 0.93 and 0.84 at buoy locations AD02 and BD11 respectively. Hence, ERA-Interim wind speeds are used for the hindcast study performed using MIKE 21 SW. The details of the numerical model developed in the MIKE 21 SW module is explained in this chapter.

Further, for the forecast studies, CMIP5 global wind speeds from 38 different modelling agencies are used. To arrive at the best performing model amongst the 38 different CMIP5 models a performance evaluation of the dataset is performed against the ERA-Interim dataset. From this analysis, CMCC-CM with RCP 4.5 emerged as a best-performing dataset for the current period in the Indian domain with a correlation coefficient of 0.81, a standard deviation of 1.13 and an RMSD of 0.75 m/s. CMCC-CM RCP 4.5 modelled wind speed dataset is used as an input in MIKE 21 SW to forecast the wave climate up to the year 2070.

4.1 GENERAL

The long-term analysis is being effectively used worldwide to predict wave heights based on extreme wave statistics (Li et al., 2012; Erdik and Beji, 2018). Long-term statistical analysis based on various distributions contributed to arrive at an expected wave height for a given return period. Long-term wave analysis is performed as it serves two purposes, firstly it helps in organizing the wave data and secondly, extreme value wave heights can be extrapolated based on low probabilities of exceedance (Erdik and Beji, 2018). The long-term analysis is a traditional design criterion performed based on a statistical analysis of existing data or probability-based methods. Long-term wave analysis comprises several probability distributions that can be used. These include distributions such as Log-normal distribution, Gumbel distribution, Fretchet distribution, Exponential distribution, and Weibull distributions. One cannot give physical reasons for choosing a particular distribution, this can be based on the best fit to the dataset chosen. Although all distributions have a theoretical base, they are used here essentially as an empirical fit to the data. The extreme distribution functions for data fitting used in the present study are listed below (Table 4.1).

Table 4.1 Summary of Distribution Models (Kamphuis, 2010)

Distribution	Equation	Y	X	A	B
Log-Normal	$P = \Phi\left(\dfrac{\ln H - \overline{\ln H}}{S_{\ln H}}\right)$	$\Phi^{-1}(P) = Z$	$\ln(H)$	$\dfrac{1}{S_{\ln H}}$	$-\dfrac{\overline{\ln H}}{S_{\ln H}}$
Gumbel	$P = \exp\left(-\exp\left(-\dfrac{H-\gamma}{\beta}\right)\right)$	$-\ln\left(\ln\dfrac{1}{P}\right)$	H	$\dfrac{1}{\beta}$	$-\dfrac{\gamma}{\beta}$
Fretchet	$P = \exp\left(-\exp\left(-\dfrac{H-\gamma}{\beta}\right)\right)$	$-\ln\left(\ln\dfrac{1}{P}\right)$	$\ln(H)$	$\dfrac{1}{\beta}$	$-\dfrac{\gamma}{\beta}$
Exponential	$P = 1 - \exp\left(-\left\{\dfrac{H-\gamma}{\beta}\right\}^{\alpha}\right)$	$\left(\ln\dfrac{1}{Q}\right)$	H	$\dfrac{1}{\beta}$	$-\dfrac{\gamma}{\beta}$
Weibull	$P = 1 - \exp\left(-\left\{\dfrac{H-\gamma}{\beta}\right\}^{\alpha}\right)$	$\left(\ln\dfrac{1}{Q}\right)^{1/\alpha}$	H	$\dfrac{1}{\beta}$	$-\dfrac{\gamma}{\beta}$

In describing the distributions, it is convenient to adopt the following notation for the parameters used to define any specific distribution: 'γ' is the location parameter which

locates the position of the density function along the abscissa; 'β' is the scale parameter which controls the degree of spread along the abscissa (variate axis) and 'α' is the shape parameter which determines the basic shape of the particular distribution.

Here, Extreme wave analysis is performed based on Peak Over Threshold (POT) method from which the best-fit probability distribution is obtained. In the POT method, a population of storms is selected based on the arbitrarily selected threshold value of wave heights (Neelamani et al., 2007). The basic definition of storms can be the time when wave height exceeds this threshold. This simple distribution is fitted to those observations which exceed a suitable level and it is expected that this fitted distribution is close to real distribution in extreme parts. Hence, during level selection, one should take care that the selected level should be high enough for the tail to have the standardized form. Meanwhile, it should not be too high as it may result in a few observations above it. The maximum wave heights or the peak values during each storm are the only data points used in the POT method (Kamphuis, 2010).

The intention is to provide a straight line fit to the dataset when it is plotted on a particular probability paper. In the case of probability distributions, the scales are known prior and only two parameters are needed in each case. Here, the least-squares method in its most basic form is directly applicable (Neelamani, 2009). The best-fit line $y = Ax + B$ is obtained where all the data points are in terms of coordinates *(x, y)*. The slope of this line is represented as *A* and *B* is the intercept of the line. In any case, the least-squares procedure can readily be extended to provide estimates of *A, B,* and *γ* or *A, B* and *α* or both. This involves an iterative procedure that entails no serious difficulty. The corresponding estimated values of the parameters of the distribution, if required, are obtained from the slope and intercept by the expressions given in Table 4.1.

The design wave height ($H_{S(T_R)}$) for a return period of (T_R) years is evaluated. The number of events per year required for analysis is calculated from Eqn. (4.1) for the dataset considered. Where λ is the mean rate of extreme events. It is defined as the ratio of the number of events N_T to the period *K* years as,

$$\lambda = \frac{N_T}{K} \qquad\qquad (4.1)$$

For Weibull distribution, the design wave height ($H_{S(T_R)}$) is calculated by Eqn (4.2) below

$$H_{S(T_R)} = \gamma + \beta \, ln \left(ln \frac{1}{Q} \right)^{\frac{1}{\alpha}} = \gamma + \beta \left(ln\{\lambda_{T_R}\} \right)^{\frac{1}{\alpha}} \tag{4.2}$$

The wave parameters such as design wave height for any given return period can be evaluated once the distribution is optimized.

The long-term analysis is initially performed on the in-situ wave data recorded at coastal waters off the Mangaluru coast. Further, the best performing distribution is applied to the simulated wave heights obtained from MIKE 21 numerical model forced with ERA-interim wind speed data.

4.2 LONG-TERM ANALYSIS ON IN-SITU MEASUREMENTS

In-situ measurements have spatial constrain and are generally taken for a shorter duration. A surface type wave recorder was in operation off Mangaluru Port along the west coast of India. The data is made available for a period of five years, i.e., from October 1999 to April 2004 by NIOT Chennai. The wave recorder was installed at a distance of 1.5 km offshore, at a water depth of 10 m (12º55′N, 74º49′E). In order to analyse extreme waves, the entire dataset of significant wave heights recorded at every three hourly intervals was considered. This data is further grouped using the POT method. The methodology also involves generating past waves by forcing a numerical model with hindcast winds obtained from the ERA-interim dataset. Further statistical analysis is carried out for such projected wave data.

Extreme wave analysis for grouped data is obtained from the entire measured dataset with three threshold wave heights (H_t) as 1.5 m, 2.5 m, and 3.5 m. From the extreme wave heights of the whole 5 year in-situ measurements, the above-mentioned probability methods are expected to give precise estimates. Figure 4.1 shows the plots of five probability distributions. The best fit line for these points is determined using the method of least squares as mentioned earlier. The method of least squares is a well-known technique and is used in the present study.

65

From the distribution plots of grouped data, it can be seen that the data points are very close to the trend line. In each of the distribution, it can be observed that the higher values of the wave heights are showing a linear trend which can be further extrapolated using the Eqn. 4.2 to get the design wave heights for the particular return period. The coefficient of determination (R^2 value) is highest (Figure 4.1) for the Weibull distribution with α=1.3. Hence, the design wave height as per Weibull distribution is calculated and is mentioned in Table 4.2 below.
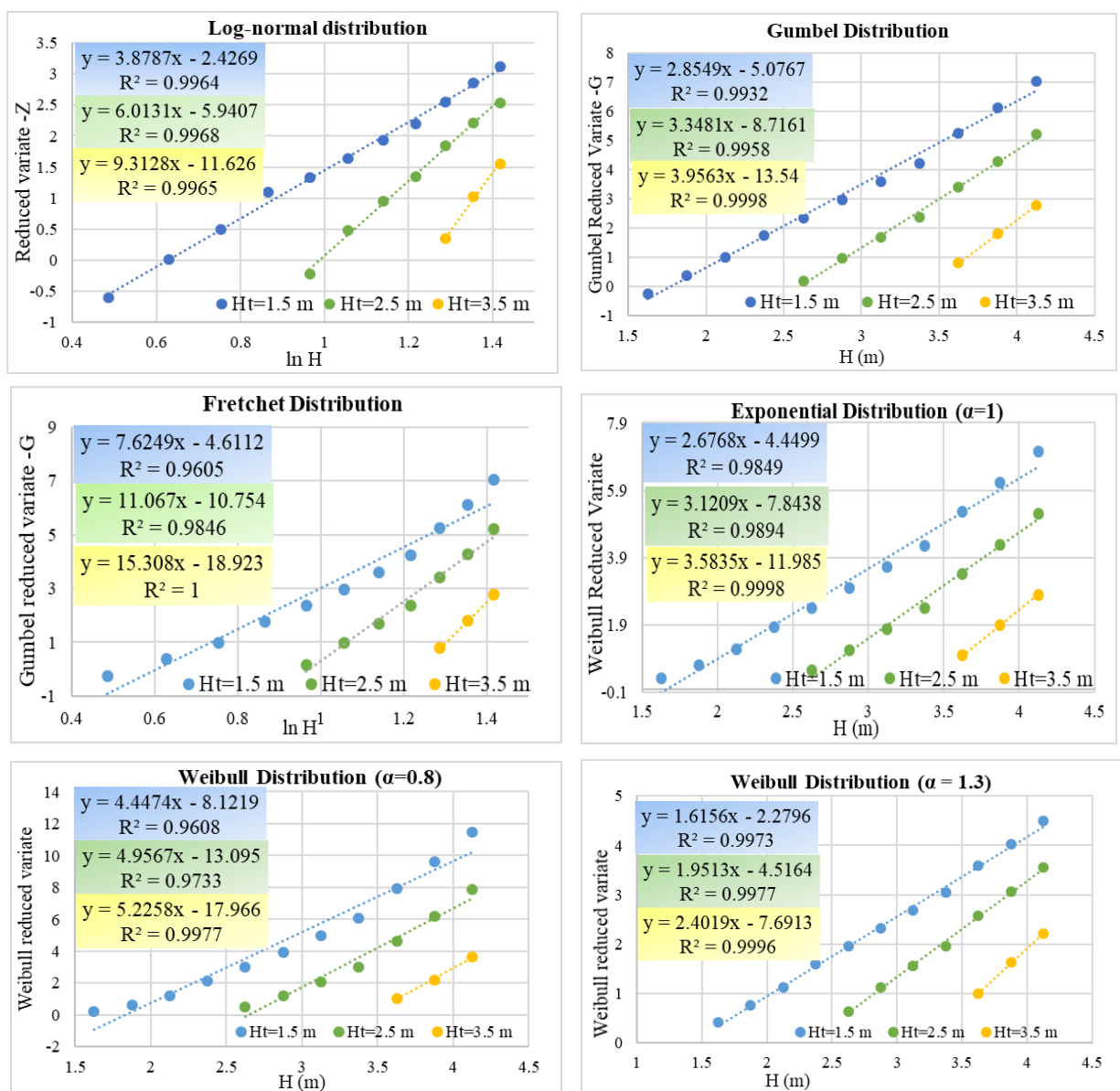

Fig. 4.1 Statistical distribution plots for grouped in-situ measurements

66

Table 4.2 Predictions of H_s from grouped data of in-situ measurements

Weibull distribution (α =1.3)					$H_{S(T_R)}$ in meters for different Return periods	
H_t (m)	λ	α	β	γ	10 yrs.	50 yrs.
1.5	459.2	1.3	0.62	1.41	7.07	7.77
2.5	73.2	1.3	0.51	2.31	6.91	7.53
3.5	6.6	1.3	0.42	3.20	6.84	7.39

Table 4.2 presents the results of the extrapolation (Eqn. 4.2) of design wave heights for return periods of 10 and 50 years, for the best performing Weibull distribution with α=1.3 for the three different values of the threshold wave height (H_t=1.5, 2.5 and 3.5 m).

From the above extreme wave analysis performed on in-situ measurements, Weibull distribution for α=1.3 will be further used for long-term analysis of simulated significant wave height based on hindcast values of ERA-Interim dataset for Mangaluru coast region.

4.3 LONG-TERM ANALYSIS ON SIMULATED HINDCAST WAVE HEIGHT

The results obtained from the extreme value analysis of in-situ measurements have established the applicability of this method for wave analysis. Hence, the same approach to fit Weibull distribution is adopted to the Mangaluru coast (12º55′N, 74º49′E) and to obtain the design wave height for the desired return period based on wave hindcasting. To simulate the significant wave heights (H_s), the third generation Spectral Wave (SW) module of MIKE 21 is used in this study. From the simulated wave heights, 12 hours interval significant wave height (H_s) is extracted from the dataset for 38 years (1980-2018). Extrapolation of wave heights for return periods of 10 and 50 years, is analyzed using Weibull distributions (α=1.3) for the threshold wave heights (H_t) of 1.5 m, 2.5 m, 3.5 m, 4.5 m, 5.5 m, and 6.5 m. The wave height values should be assessed to provide the best fit for the distribution (Figure 4.2).

The design parameters such as β and γ which are required for the estimation of design wave height is shown in Table 4.3, where A and B are the slope and intercept values of distribution graphs.
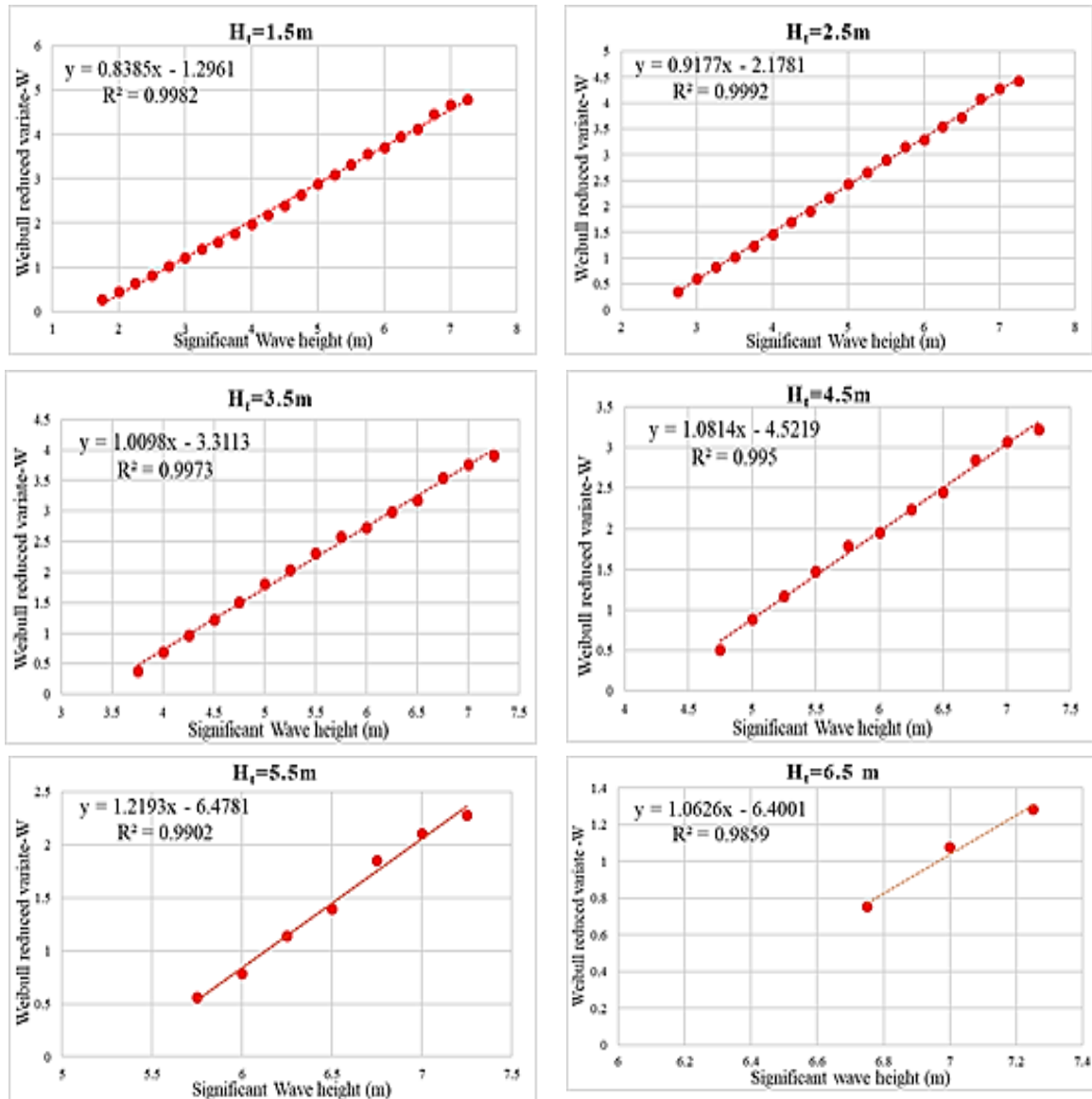

Fig. 4.2 Weibull distribution (α =1.3) for varying threshold wave heights

Table 4.3 Design parameters estimated from simulated results

H_t	1.5	2.5	3.5	4.5	5.5	6.5
A	0.84	0.933	1.01	1.08	1.22	1.06
B	-1.29	-2.18	-3.31	-4.52	-6.48	-6.40
β	1.19	1.08	0.99	0.92	0.82	0.94
γ	1.54	2.37	3.27	4.18	5.31	6.02
R^2	0.998	**0.999**	0.997	0.995	0.990	0.986

From Table 4.3, it is found that the highest R^2 value of 0.999 occurs for a threshold wave height of 2.5 m for the Weibull distribution (α =1.3). The Extrapolated design wave heights calculated for the same is highlighted in Table 4.4. The design wave height is calculated for return periods of 10 and 50 years using Eqn. (4.2) as discussed in the earlier section.

Table 4.4 Comparison of significant wave heights

Dataset	β	γ	$H_{S(T_R)}$ in meters for different Return periods	
			10	50
38-years hindcast	1.09	2.37	7.09	7.94
In-situ data	0.51	2.31	6.91	7.53
Percentage increase in design wave height (%)			2.60	5.44

From the long-term wave analysis performed an increase in design wave height values is observed for results obtained from simulated hindcast data to that of 5-year in-situ measurements. The increase in design wave height with a 10 year return period is 2.60 % and 50 year return period is 5.44 % for the Mangaluru coast. This increase in design wave heights is because of the larger spatial resolution global reanalyzed ERA-Interim dataset which captures changes in wind circulation due to climate change.

4.4 SHORELINE CHANGES ALONG MANGALURU COAST

The shoreline studies help us to understand the complex factors that decide the dynamic equilibrium of the shoreline and its impact on the coastal population and various structures. The regional coastlines are affected by the wave climate which varies on a long-term basis (Chowdhury and Behera, 2017). The change in the hydrodynamic circulation as a result of constructing breakwaters diverts littoral currents, as well as sediment flow resulting in accretion at up-drift and erosion at the down-drift side. The seasonal variations of sediment transport help to evaluate the annual sediment transport and accordingly the shore protection strategy can be planned (Arockiaraj et al., 2018). The volume of sediment transported and the shoreline changes along the coast perpendicular to New Mangalore Port (NMP), Panambur located on the west coast of India is simulated using numerical shoreline module LITPACK. The coastline from Bengre to Sasihithlu of about 25 km (12º51'N 74º49'E to 13º4'N 74º46'E) is considered in the present study as shown in the figure below.
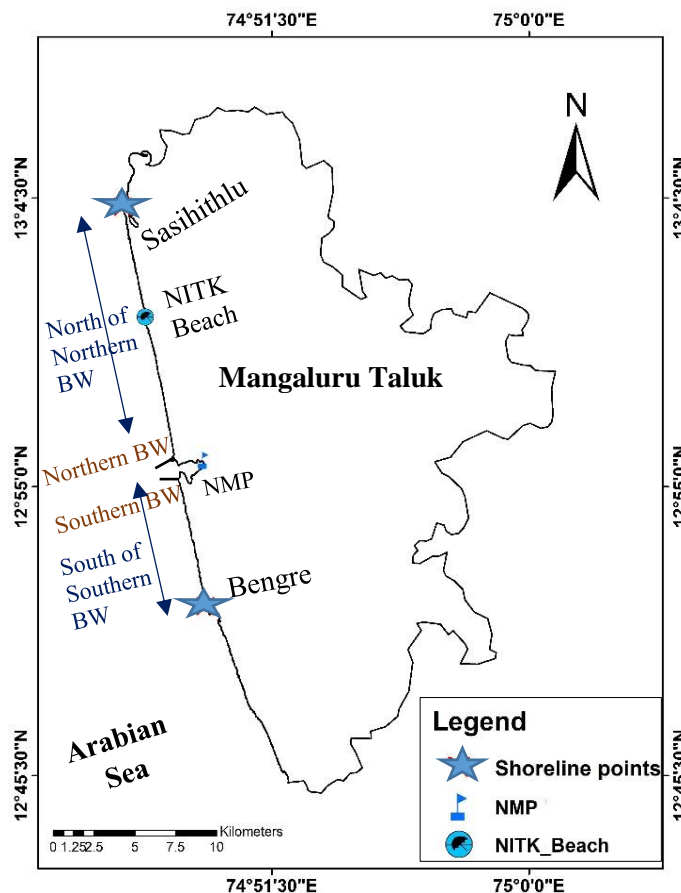

Fig. 4.3 The study area - shoreline adjacent to NMP

4.4.1 New Mangaluru Port

The New Mangalore Port (NMP) is the only major Port in Karnataka state. It is deep water all-weather Port located at Panambur, Mangaluru which was initiated in 1962. The Port has grown over the years and the traffic handled has increased up to 39.4 million tonnes during 2013-14. The Port activities are managed by New Mangalore Port Trust (NMPT). The coordinates of the port are Latitude 12°55' North and Longitude 74°48' East. The Port is approached through a 7.5 km long approach channel with water depths in the outer channel being 15.4 m and that of the inner channel being 15.1 m. The Port has a total land area of approximately 822 ha and a water spread area of 120 ha. The maximum wind speed so far recorded has not exceeded 62 kmph.

The predominant direction of waves at open sea within the vicinity of Mangalore Port during the monsoon months of June to September is Southwest and West. Whereas, the predominant wave direction during the fair-weather months is NorthWest and North. Two number of rubble mound breakwaters, each on the northern and southern portion of the approach channel was constructed. Each breakwater has a length of 770 m, it was constructed in three stages with a spacing of 1,362 m at the root. The breakwaters terminate at a depth of about -6.0 m CD. Past experiences have shown that construction along the coast has changed the coastal environment (Mishra et al., 2001). Hence, the shoreline adjacent to NMP is studied in the present study (Figure 4.3).

4.4.2 Numerical modelling

The shoreline changes are predicted using the coastline evolution tool (LITPACK) modelled based on the historical wave outputs from 1980-2015. The hindcasted wind-driven wave parameters such as wave height, wave direction and wave period are numerically modelled using MIKE 21 SW module. The wave climate from 1980 to 2015 is simulated using the wind as the forcing parameter, derived from the ERA-interim global dataset. The significant wave height, wave period and wave direction is extracted for NMP location using the data extractor tool of MIKE Zero. The wave data is extracted for two points, one at the north of the northern breakwater (BW) and the other at the south of the southern breakwater.

71

The wave parameters derived from the MIKE 21SW model serves as a necessary input for the LITPACK module. LITPACK is a 2D sediment transport module by MIKE (DHI, 2014). LITPACK modelling system has integrated modular structure with modules like LITDRIFT, which is used to estimate the sediment transport across the profile and LITLINE a shoreline evolution model. LITDRIFT gives the distribution of sediment transport across the profile, which is integrated to obtain the gross longshore sediment transport rate (Mishra et al., 2014). The sediment transport is estimated using the equation below,

$$q_t = q_b + q_s \qquad (4.3)$$

Where q_t is total sediment transported, q_b is bedload sediment transport and q_s is sediment transport in suspension (MIKE, 2017).

The total annual sediment transport Q_{annual} is found as the sum of the contributions from all wave incidents.

$$Q_{annual} = \sum_{i=1}^{NSETS} Q_s(i).Duration(i) \qquad (4.4)$$

Where *NSETS* is the total number of wave incidents, Q_s is the sediment transport.

In LITLINE analyses, sediment transport is resolved by the continuity equation mentioned below,

$$\frac{\delta y_c}{\delta t} = \frac{1}{h_{act}} \frac{\delta Q}{\delta x} + \frac{Q_{sou}}{h_{act}\Delta x} \qquad (4.5)$$

Where y_c is the distance from the baseline to the shoreline, Q is the volume of longshore sediment, t is time, h_{act} is the height of active cross-shore profile, x is the long-shore position, Δx is long-shore discretization step and Q_{sou} is the source or sink term expressed as volume or Δx.

The position of the shoreline is calculated based on wave climate as an input in time-series format (.dfs1). In addition to wave data, other inputs like sediment properties and the cross-shore profile are included. The bathymetry derived from CMAP is also a critical input to the model as the cross-shore profile is extracted based on this (.mesh) file (Figure 4.4a). These extracted profiles are used to develop a cross-shore profile using the profile series (.dfs0) option in MIKE Zero. Cross profile is nothing but a series

of data related to bathymetry. The other input to the line series includes mean sediment diameter, fall velocity and roughness factor. The model can be calibrated by varying the fall velocity and roughness parameters. The mean grain diameter plays a significant role in longshore drift, so the sediment characteristics are set to default conditions with sediment description varying from a diameter of 0.2 to 0.4 mm from fine sand to silt and clay, 0.075 to 0.002mm diameter, up to a depth of 10 m. The influence of different structures such as breakwater, groynes, and jetties on the coastline can also be included in the module. In the numerical model, two breakwaters of NMP is specified as jetty of length 1952 m (southern side) and 1882 m (northern side) from the fixed baseline. The sediment transport across south and north of breakwater and shoreline changes are evaluated for a 5-year interval from 1980 to 2015.
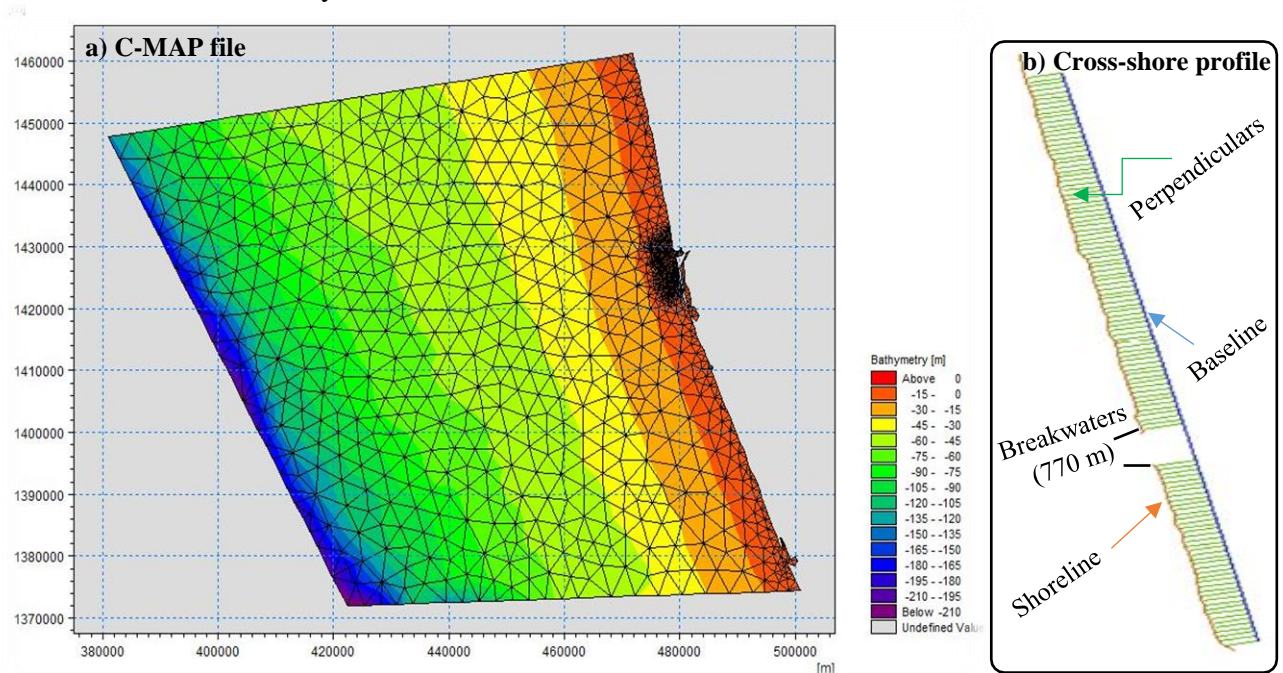

Fig. 4.4 CMAP bathymetry and cross-shore profile developed for the coast

The LITLINE results are validated with the LANDSAT-8 images of 3 days (17th of April, 06th of July and 29th of December) representing the seasonal changes for the year 2015. From USGS, LANDSAT images are downloaded to extract the shoreline to be used as input to LITPACK (https://earthexplorer.usgs.gov/). For this purpose, available cloud-free remote sensing data are analyzed using digital image processing techniques. The LANDSAT images are downloaded for the year 1980 from the LANDSAT 5 for extracting the initial shoreline alignment and images from 2015 of

73

LANDSAT 8 for validating the simulated results. The shoreline is drawn using a visual interpretation technique. Additionally, a baseline is drawn approximately parallel to the shoreline. The shoreline position is defined by the distance from this baseline and also by the angle to the normal to the coast which is 258°. The entire baseline is divided into equally spaced grid points and the perpendicular from the points gives the distance to the shoreline (Figure 4.4b). The perpendicular distance from the baseline to the coastline is exported from ArcGIS and is fed into the Initial Coastal Alignment utility tool of MIKE Zero.

4.4.3 Volume of sediments and shoreline changes

The results obtained from LITPACK module based on hydrodynamic forcing from MIKE 21 SW are discussed below. Across the northern and southern profiles of the NMP breakwaters studied, LITDRIFT provided the monthly average volume of sediments in m^3 for 35 years. The effects of wave climate on the dynamic equilibrium of the coast are analyzed using outputs from the LITLINE module. Figure 4.5 and Figure 4.6 show the volume of sediment accreted or eroded along northern and southern profiles of breakwater along the NMP.

The positive sign indicates the volume of sediment accreted and the negative sign indicates the volume of sediment eroded. The northern profile (portion north of northern breakwater) and southern profile (portion south of southern breakwater) follows a regular reversal pattern of erosion and accretion across 35 years. The reversal is an indication of the seasonal movement of sediments as per the previous studies by Rao et al. (2001). From the plots, it can be seen that a peak in accreted volume in the month of May before the onset of monsoons exists. The monsoon period from June to September experiences severe erosion along the coast. During the post-monsoon season, it is seen that the coast experiences peak accretion. The northern profile experiences a huge quantity of sediment transported in the order of 10000 to 15000 m^3 every month. However, the southern profile has an overall less quantity of sediment transported (5000 to 6000 m^3) as compared to the northern profile indicating the beach build-up.
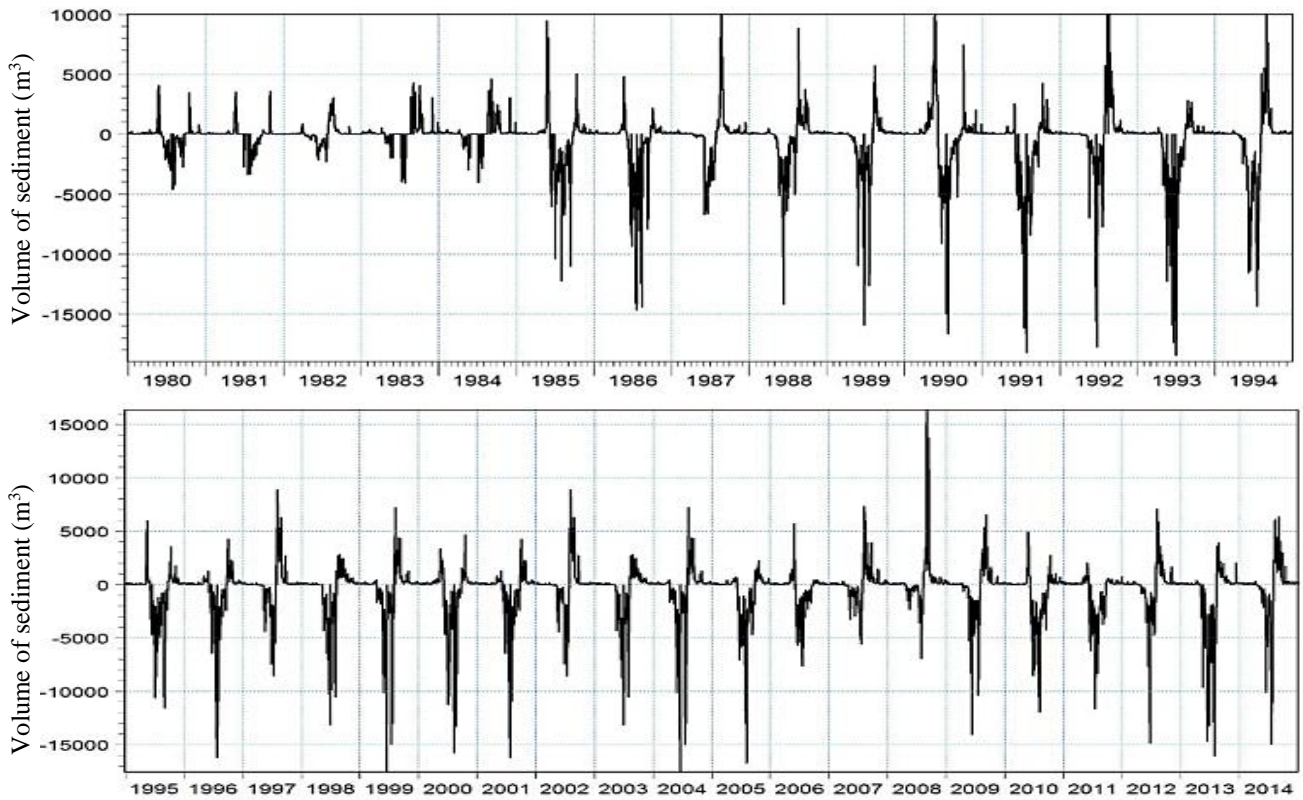
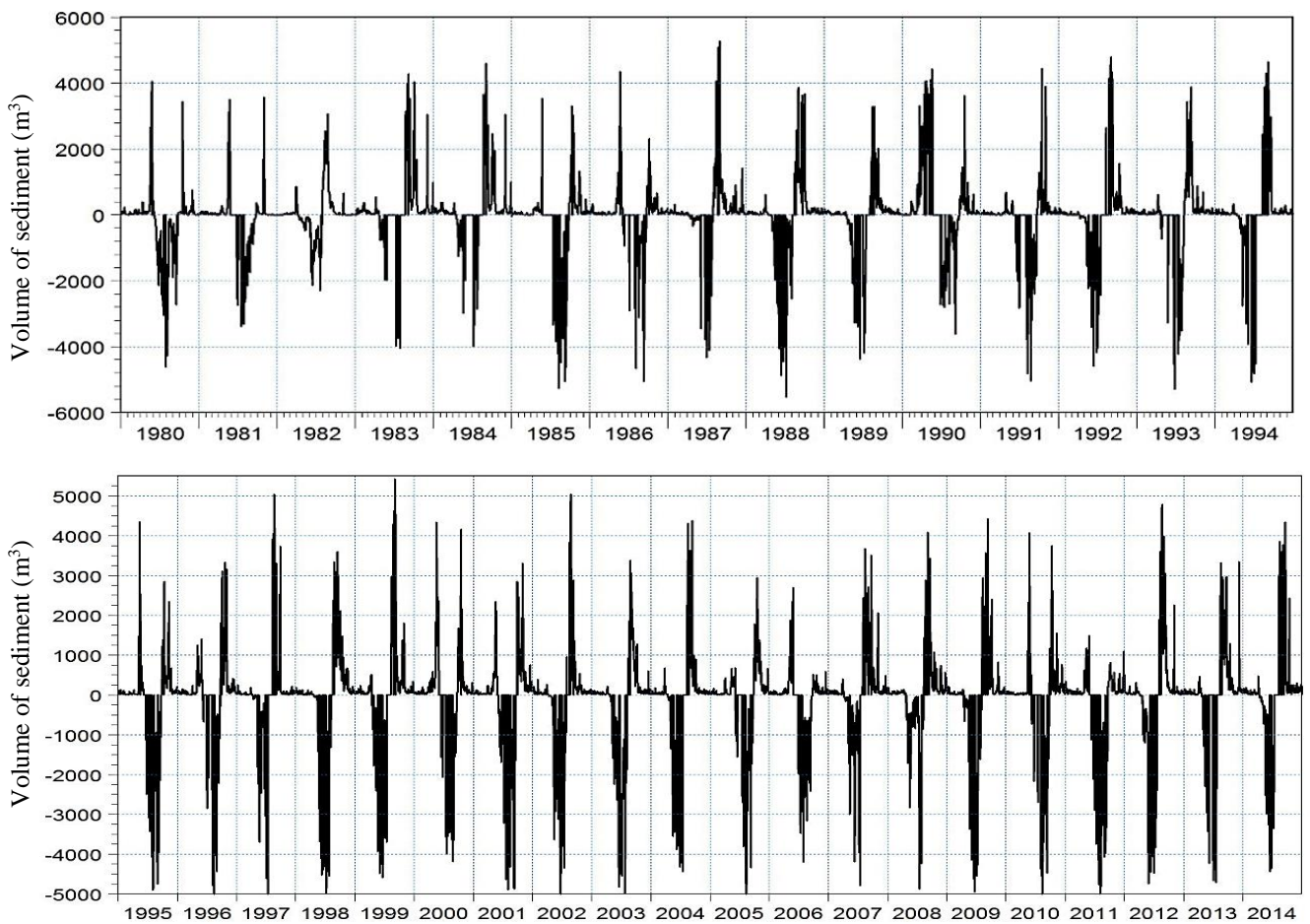**Fig. 4.5 The volume of sediment accreted/eroded in the north of northern BW**

Fig. 4.6 The volume of sediment accreted/eroded in the south of southern BW
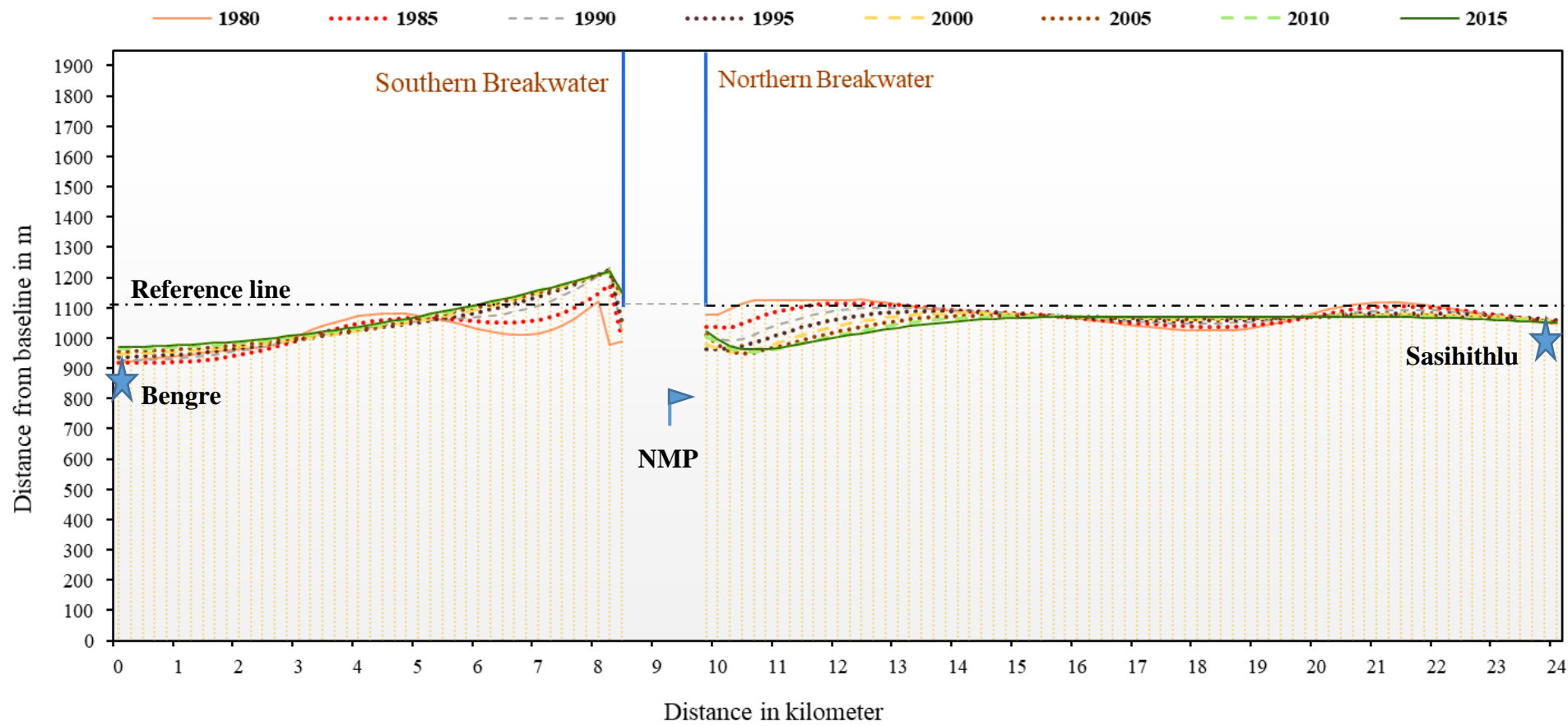
75

Fig. 4.7 Shoreline changes from the year 1980 to 2015

The shoreline studies performed using LITLINE indicate that there is a significant change in the shoreline (Figure 4.7) over 35 years (1980-2015). The study helps in assessing the breakwater's role in changing the shoreline dynamics. Perpendiculars from the base of the 770 m long breakwater are drawn to assess the shoreline changes over 35 years. The past shoreline changes indicate considerable episodes of erosion and accretion along the coast. The coast perpendicular to northern breakwater is comparatively stable when compared to the southern breakwater. The shoreline of 2015 indicates the highest erosion of about 100 m near the extreme south of southern breakwater (Bengre) and a beach built-up of about 100 m at the base of southern breakwater. The coast north of northern breakwater has reached stability after consecutive erosion and accretion in the previous decades. The shoreline of 2015 indicates that the maximum erosion of about 150 m near the base of northern breakwater. The magnitude of the eroded coastline averaged about 50 m is observed along the rest of the coastal stretch for 2015. Sasihithlu the extreme coastline point studied experienced an erosion of about 75 m during 2015.
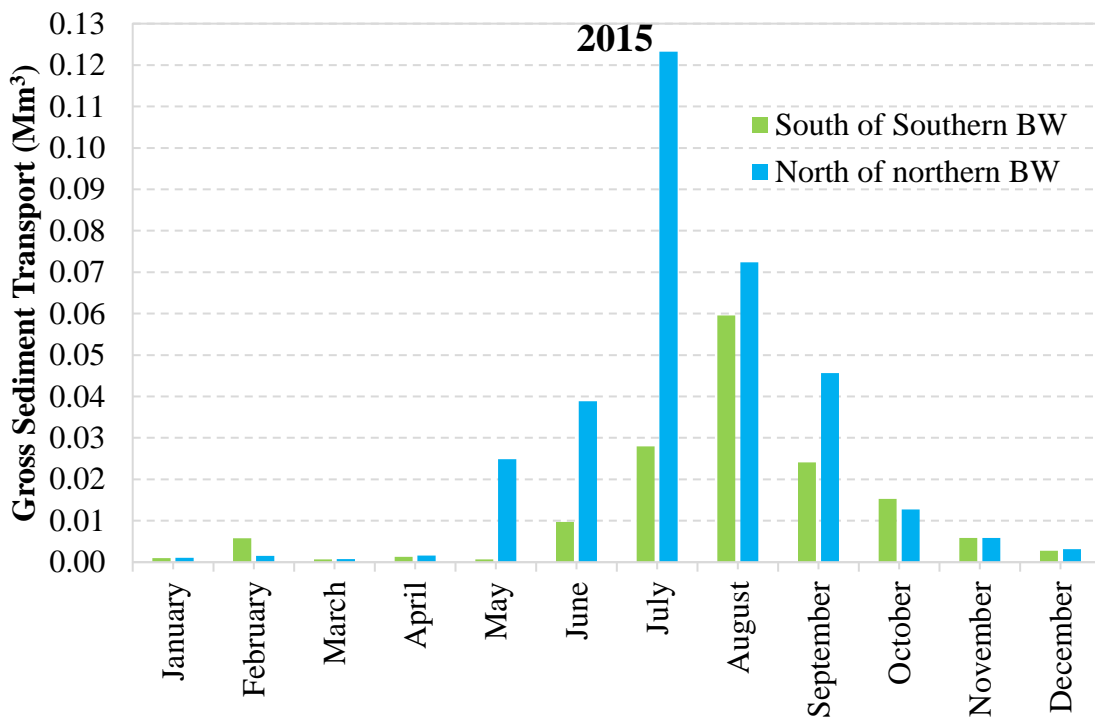
4.4.4 Monthly sediment transport

Fig. 4.8 Monthly Gross sediment transport along the shoreline

77

From the shoreline evolution study (Figure 4.7) the year 2015 showed maximum accretion and erosion. Hence, Monthly gross sediment transport is evaluated and is represented in Figure 4.8. The sediment transport is less in the pre-monsoon month of January to May. With the arrival of the monsoon, the sediment transport rate increases and reaches a maximum value in the month of July and August. In the south of southern breakwater, the maximum transport of 0.1232 Mm^3 is observed in the month of July. And north of northern breakwater had maximum sediment transport of 0.0595 Mm^3 observed in the August month of 2015. The north of northern breakwater has higher values as the coastal length studied is higher towards the north when compared with the south of the southern breakwater. The gross sediment transport during the post-monsoon season is less along the shoreline.

4.4.5 Validation

The validation is performed based on the satellite images taken for the pre-monsoon, monsoon and post-monsoon seasons of 2015 (Figure 4.9 and Figure 4.10). The simulated shoreline distances matched well with the satellite measurements correlation with R-value of 0.96, 0.89 and 0.97 for the 17th of April, 06th of July and 29th of December respectively.
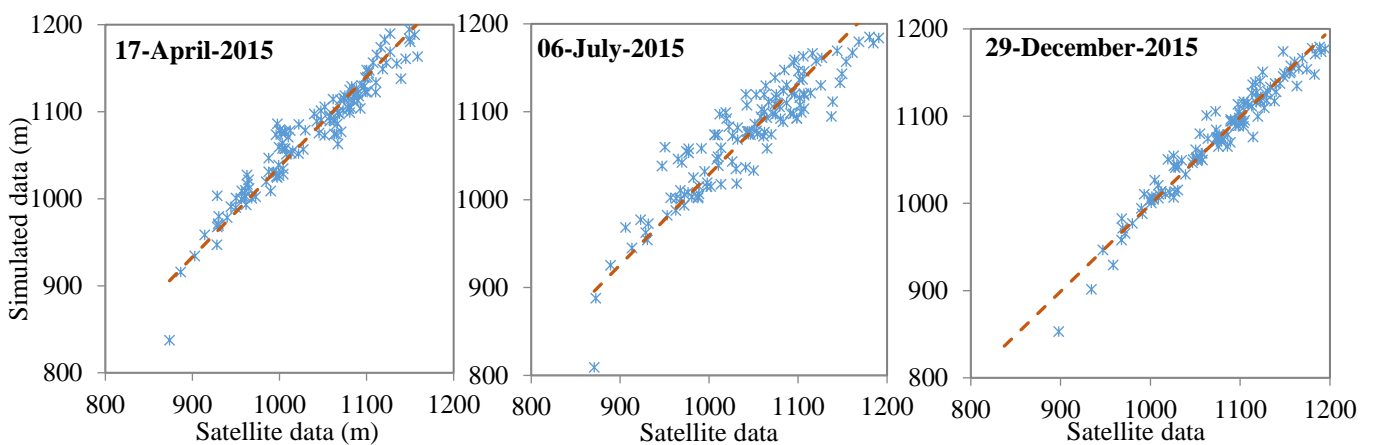
Fig. 4.9 Scatter plots
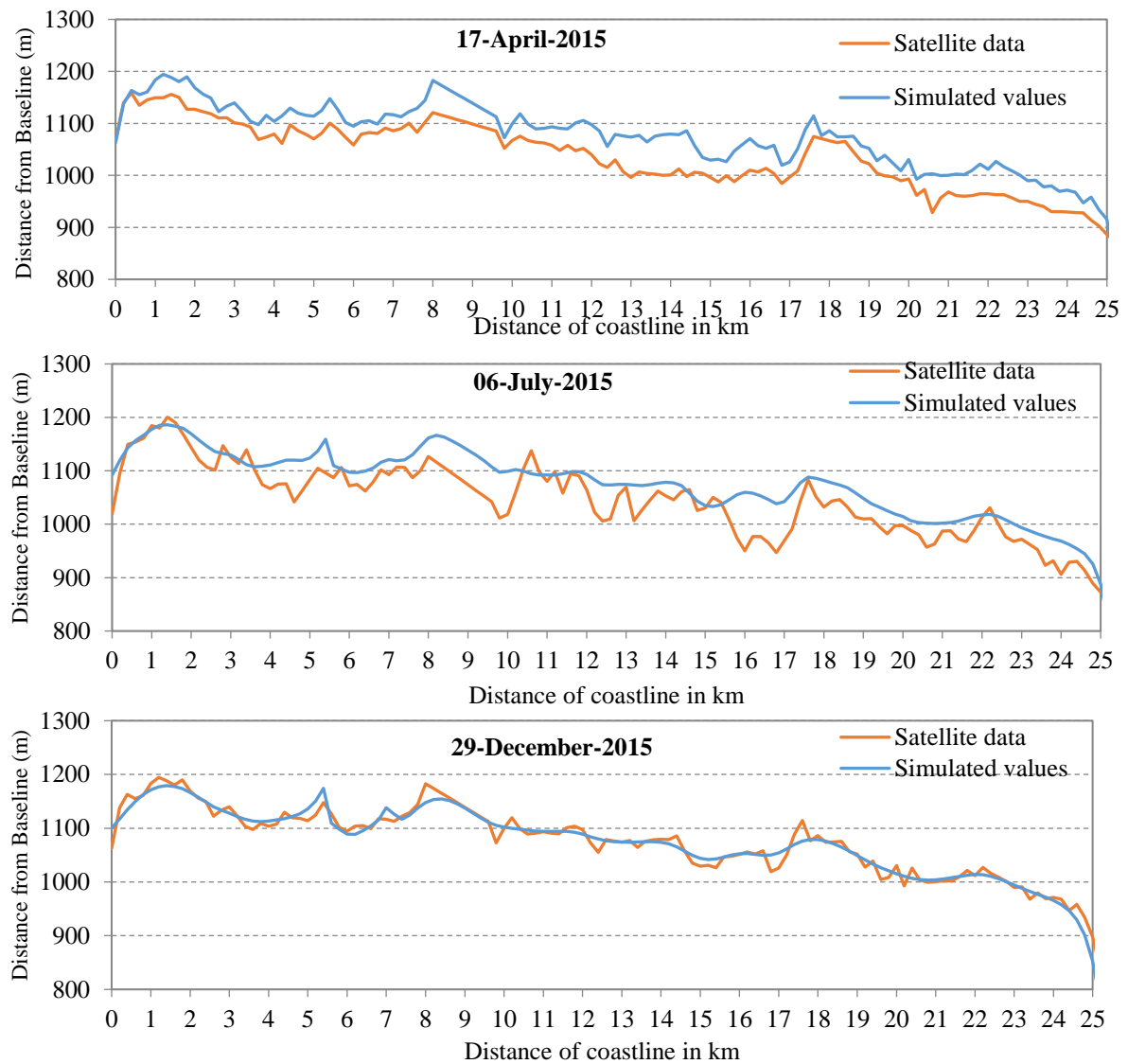
Fig. 4.10 The plot of MIKE simulated shoreline values against satellite measurements

The LITPACK module results driven by wind-wave forcing of MIKE21 SW is fairly successful in analyzing the shoreline dynamics. The model performance is good when validated against satellite records which is fair as the tidal variations are not included in the present study. Based on the study across 35 years, there is a slight increase in the volume of sediment transported yearly. The coastline studied has erosion and accretion being predominant from May to October. In the rest of the season, the beach is in equilibrium. The predominant onshore-offshore transport of sediments is responsible for keeping in equilibrium Rao, S. (2002). The numerical model outputs are in agreement with the previous studies by Rao et al. (2001,2002 and 2007) performed on the adjacent coast.

4.5 SUMMARY

In this chapter, long-term wave analysis is performed on the in-situ measurements recorded at the Mangaluru region for 5-years. Long-term analysis of significant wave height is performed based on five probability distributions. Amongst the five probability distributions Weibull distribution (α=1.3) performed well and is applied on simulated hindcasted significant wave heights for the Mangaluru region spanning 38 years. The design wave height with a return period of 10 years and 50 years is evaluated for in-situ measurements and simulated wave height records of 38 years. The results showed an increase in design wave height value for simulated record in comparison with the in-situ record. An increase of 2.6% and 5.44% in design wave heights for return period 10 and 50 years respectively is observed in the Mangaluru region in the present study. This design wave height can be used for the analysis and design of coastal structures in this region.

A shoreline analysis is performed on the coastline adjacent to NMP using LITPACK tool of MIKE 21. The profile north of northern breakwater and south of southern breakwater from Bengre to Sasihithlu is studied based on wave hindcast from 1980 to 2015. The shoreline evolution at a 5-year interval is studied along the coast to understand the erosion and accretion patterns along the coast. The southern profile experienced an erosion of 100 m near the Bengre region and accretion of 100 at the region near the southern breakwater during 2015. The region near the northern breakwater experienced an erosion of 150 m and erosion of 75 m at Sasihithlu during 2015. The southern profile had a maximum sediment transport of 0.1232 Mm^3 in July of 2015 and the northern profile had maximum sediment transport of 0.0595 Mm^3 in August of 2015. The results are validated against satellite measurements with R-value of 0.96, 0.89 and 0.97 for pre-monsoon, monsoon and post-monsoon seasons of 2015.

CHAPTER 5
ASSESSMENT OF WIND-WAVE CLIMATE ALONG THE INDIAN COAST

5.1 GENERAL

The ambitious efforts to reduce the anthropogenic greenhouse gases emission by the second half of the 21st century can be achieved by reducing the use of fossil fuels (Curto et al., 2019). IPCC in its report expects 80% of the world energy demand to be fulfilled by renewable energy by 2050. Extracting ocean energy is a viable alternative to meet energy demand but also solves coastal protection problems (Manasseh et al., 2017). A successful ocean energy extraction project can be made possible only by careful and detailed wave resource assessment (Xu et al., 2020). Wind power forecasting using numerical prediction models on a global to local scale is important for potential future development in the field of wind power generation (Foley et al., 2012). Analyzing the wind-wave climate not only help Oceanographers but also helps decision making agencies for coastal management and to assess the prospects of ocean energy.

The mainland of India separates the North Indian Ocean into two semi-marginal seas, the Bay of Bengal and the Arabian Sea that has the potential to tap Ocean renewable energy (Sannasiraj and Sundar, 2016). Counties such as America, Europe, China and India are developing strategies to include Ocean energy into their energy mix (Aderinto and Li, 2019). Tropical regions such as India have the potential to extract ocean energy but there are several challenges for renewable energy extraction (Felix et al., 2019).

5.2 OCEAN ENERGY

The unobstructed wind energy from the sea and addition ocean energy through waves, tides or thermal can be extracted. This renewable energy extracted from the ocean can be termed Offshore Renewable Energy (ORE). Offshore renewable energy as a clean energy source has emerged and options of integrating wave energy converters to offshore wind turbines are given more emphasis as it is economical (Pérez-Collazo et al., 2015). Most of the countries are investing in renewable energy which is extracted from offshore wind turbines and wave energy converters. ORE has a total potential to exponential exceed the world's total energy demand (Ellabban et al., 2014).

5.2.1 Wave energy converters

Surface gravity waves contain a vast supply of energy worldwide which can be harnessed (Morris-Thomas et al., 2007). Since the first concept of wave energy convertors 200 years ago this field has seen significant progress as there exists a variety of concepts of wave energy converters. Wave energy converters (WECs) are designed in such a way that they can capture the incident wave energy effectively. Wave energy converters are preferred at water depths less than 100 m (shallow depths) so that dissipated wave energy can be harnessed. Based on the basic technology WECs can be classified as i) Oscillating water column device, ii) Overtopping device and iii) Oscillating devices. Apart from the hydrodynamic property of the device a complete analysis of the system of convertors up to its connection with the electricity network grid has to be studied.

5.2.2 Offshore wind turbines

There is a huge amount of wind energy that is untapped. As far as the Indian scenario is concerned offshore wind energy prospects are yet to be explored (ManiMurali et al., 2014). The objective of capturing a clean energy economy can be achieved by installing wind turbines offshore. Some of the European regions with higher population density have invested in bottom-mounted offshore wind turbines and lower water depths (Ackerman and Söder, 2002). Based on the rotary operation principle wind turbines can be classified as a vertical axis wind turbine and horizontal axis wind turbine. Offshore wind turbines foundation plays a vital role in its stability and cost of the project. Offshore wind turbines can either be on a ballast stabilized, mooring stabilized, buoyancy stabilized platform (Thiagarajan and Dagher, 2012). In the near future, offshore wind farms promise to be an important source of energy when compared with onshore farms (Bilgili et al., 2011).

5.3 MIKE 21 NUMERICAL WAVE MODEL

The numerical model of the Indian domain modelled in the MIKE21 SW module is used for assessing the wind-wave climate. The daily wind speed ERA-Interim data from 1980 to 2018 is used as an input for the numerical model. The bathymetry is derived

from C-MAP. The model input parameters are assigned as discussed in the earlier section 3.3.1. The wind-wave climate is simulated for 38 years. The mean values of wave parameters in terms of significant wave height, peak wave period and wave power are extracted at nine locations as shown in Figure 5.1. The mean wind speed and the distance of the selected locations from the coast and the water depth at the locations are extracted and are tabulated in Table 5.1. The plot composer tool of MIKE zero is used to obtain the time-series plot at each location with information on significant wave height, wind speed and wind direction.
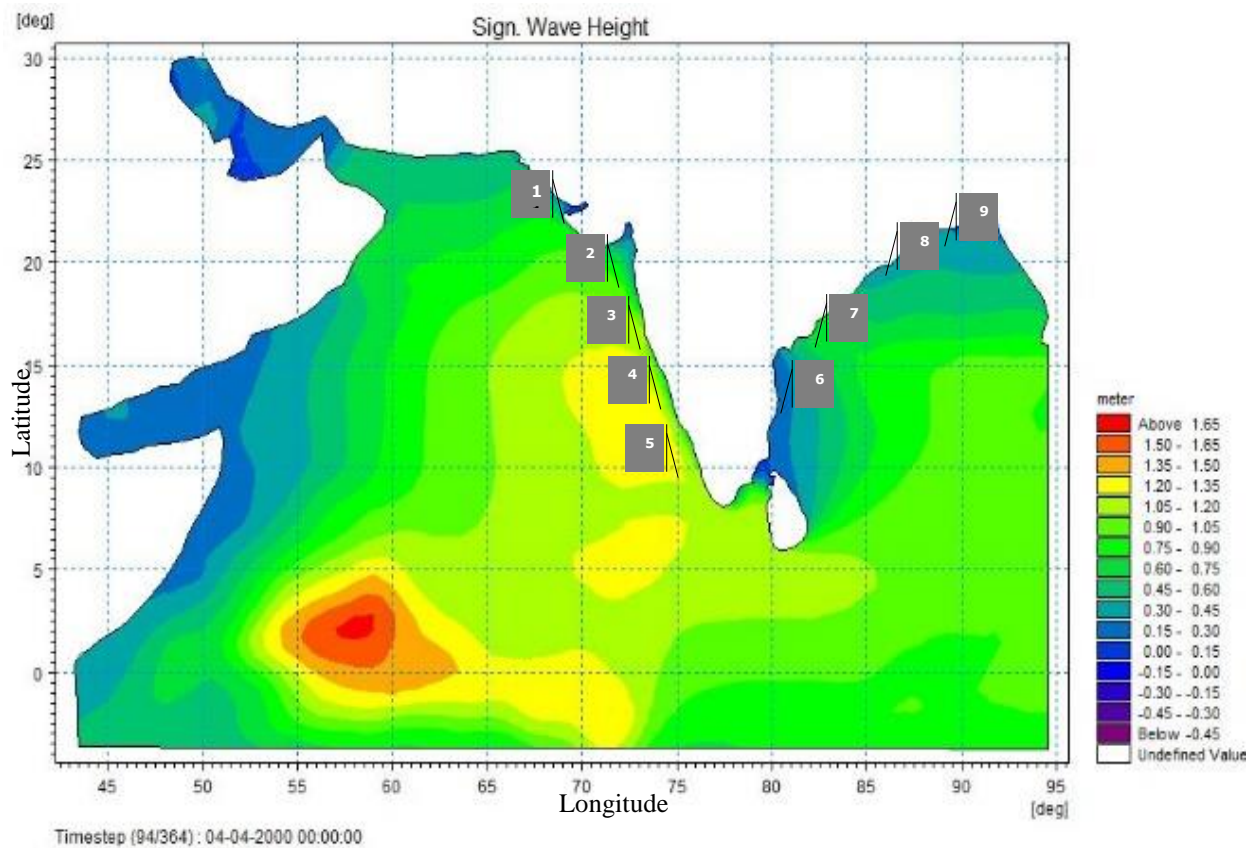
Fig. 5.1 Typical variation of H_s on 04/04/2000 over the Indian domain with a nearshore location

In the present study, the focus is on the feasibility of offshore structures on a fixed platform at low water depths which can operate wind turbine. The cost of the offshore structure is proportional to the water depth (Clauss et al., 1992). Hence, the location selected in this study has water depths varying from 45 to 55 m. The fixed offshore platforms can be a gravity type, jacket type, suction bucket type or monopile type

structure. The frequency of extreme events occurring at a specific location has to be taken into account while designing the platform. Additionally, the wave power at selected nearshore locations is also evaluated to assess the feasibility of a combined ORE platform along the Indian coast at lower water depths. The spatiotemporal wind forcing provided ERA-Interim is used to assess the nearshore wind and wave energy potential along the Indian coast. The wave energy potential is evaluated based on mean wave power (kW/m) obtained from the equation below,

Wave Power, $$P_{energy} = \rho g E C_g \qquad (5.1)$$

Where E is energy density, C_g is group celerity of waves, ρ is the density of water and g is the acceleration of gravity.

Figure 5.1 shows the details of nine nearshore locations studied. The MIKE21 numerical simulated hindcast results at nine locations are summarized in Table 5.1. The typical variation of significant wave height (m), wind speed (m/s) and wave direction in the nine nearshore locations are shown in Figure 5.2 to Figure 5.4.

Table 5.1 Mean values of wind-wave parameters simulated using MIKE numerical model for locations considered in the study

| Location no.	Lat. (ºN)	Long. (ºE)	Location (off the coast)	Mean Significant wave height (m)	Mean Peak wave period (s)	Mean Wave power (kW/m)	Mean wind speed (m/s)	Water depth/ Distance from coast (m/km)
1	22.094	68.701	Gujarat	0.86	7.56	7.57	2.87	50.01/20
2	17.903	72.446	Maharashtra	0. 91	7.67	8.70	2.07	50.44/40
3	15.375	73.454	Goa	1.28	7.01	13.67	5.90	51/25
4	12.904	74.423	Karnataka	1.30	7.07	12.27	6.12	46.70/30
5	9.501	74.944	Kerala	1.52	7.22	14.93	6.14	56/80
6	12.446	80.377	Tamil Nadu	0.83	5.11	3.06	5.75	56/20
7	16.294	81.582	Andhra Pradesh	0.73	5.70	2.97	4.62	51.4/5
8	19.732	86.329	Odisha	0.54	6.18	1.87	1.39	54.13/12
9	20.921	88.427	West Bengal	0.49	6.30	1.66	1.33	54/60
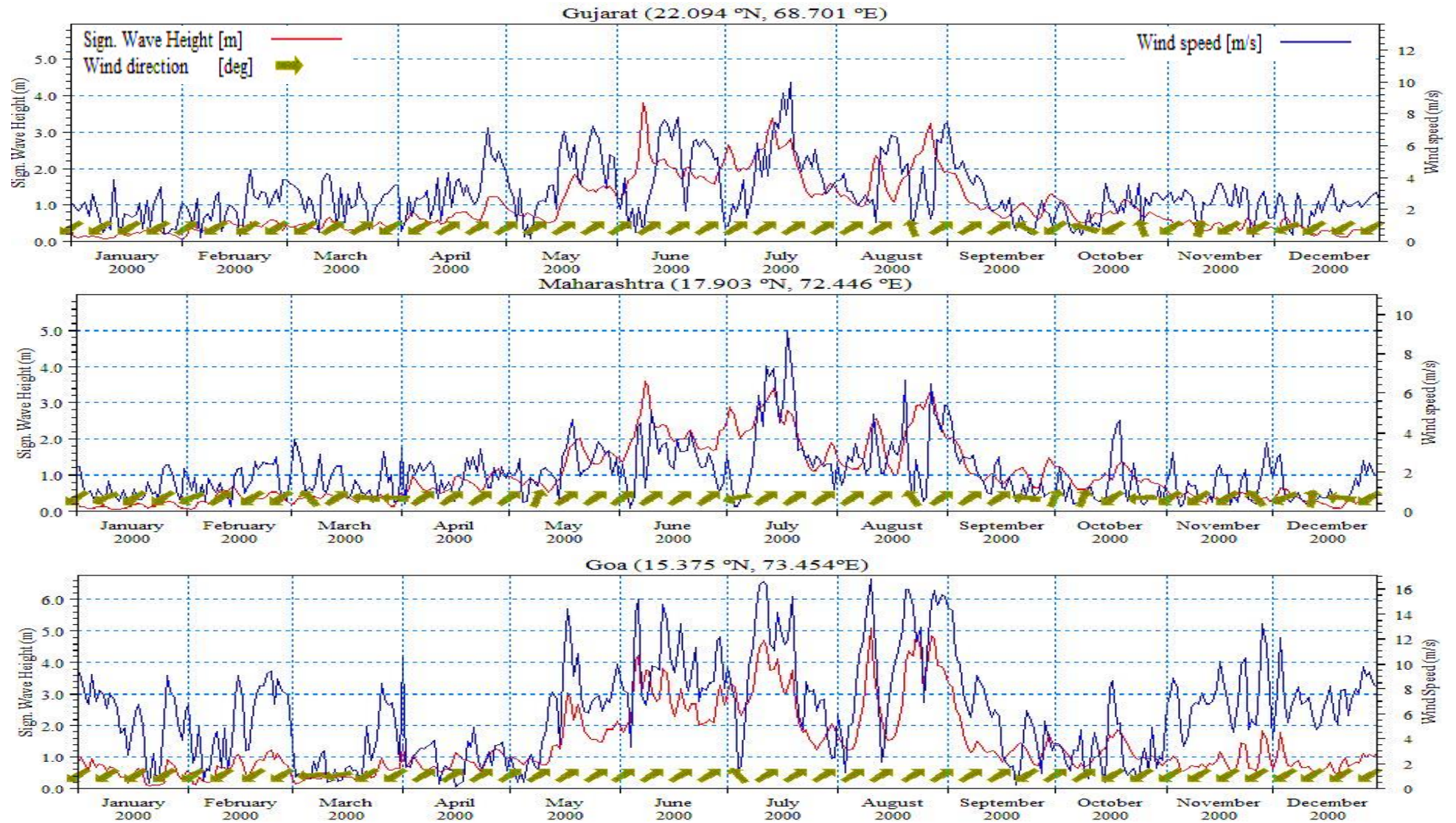
Fig. 5.2 Variation of wind-wave climate across Gujarat, Maharashtra, and Goa for the year 2000
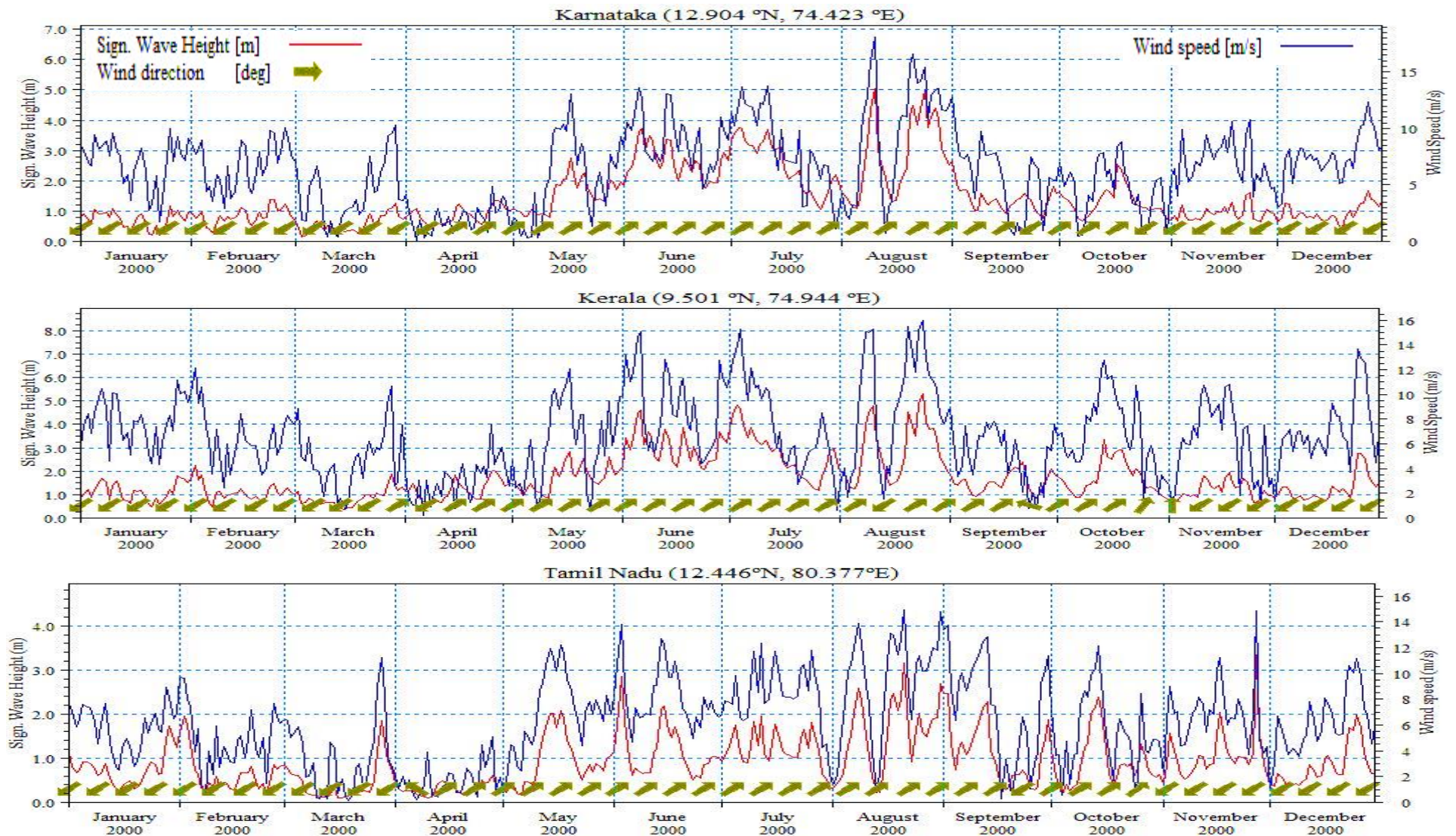
Fig. 5.3 Variation of wind-wave climate across Karnataka, Kerala and Tamil Nadu for the year 2000
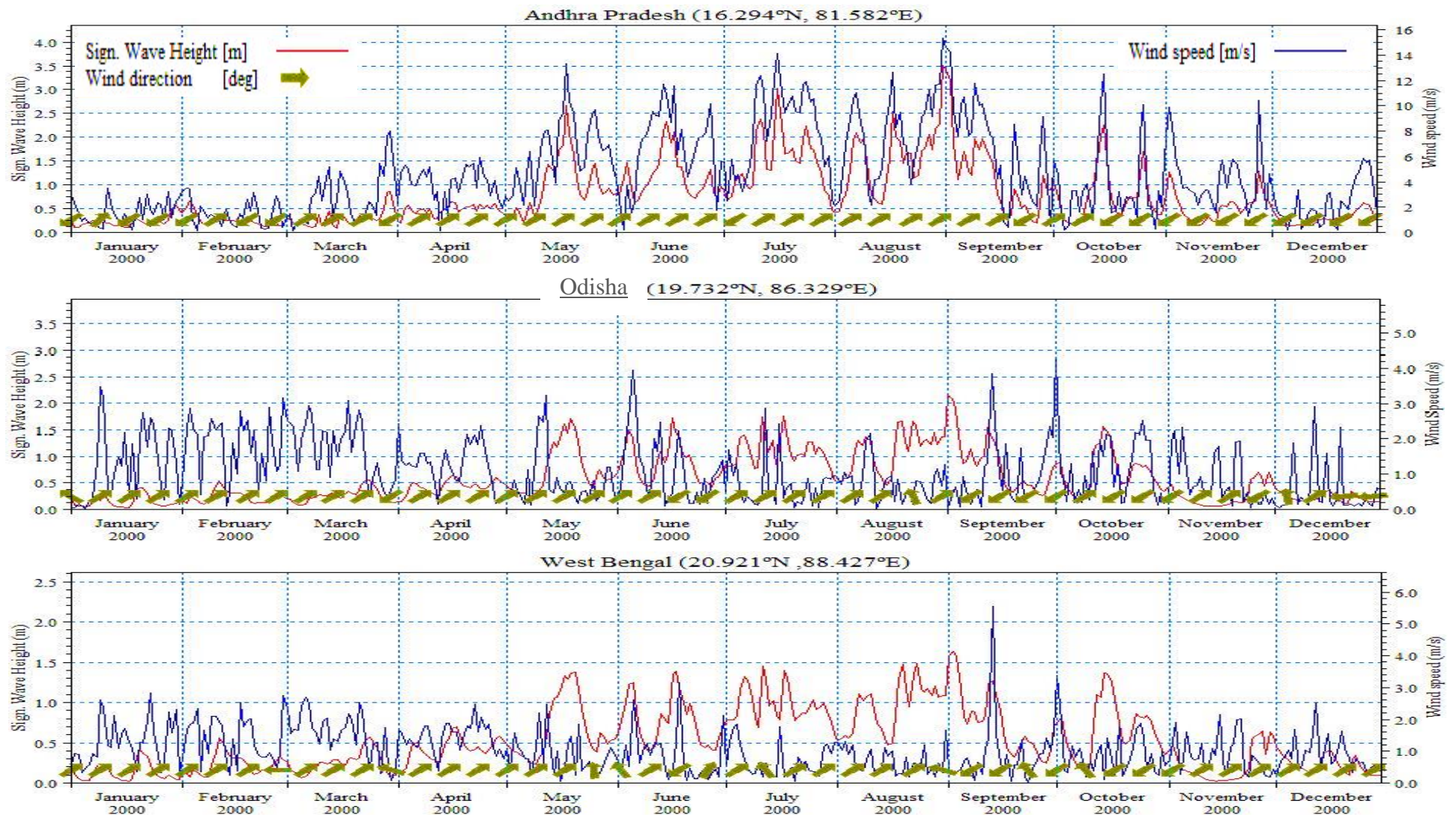
Fig. 5.4 Variation of wind-wave climate across Andhra Pradesh, Odisha and West Bengal for the year 2000

5.4 RESULTS AND DISCUSSION

From the hindcast analysis based on daily wind speed for 38 years, the Gujarat location has fair wind potential as the location majorly experiences wind speed above 3 m/s. The hindcasting study showed a maximum wind speed of 25.92 m/s. The wind directions over this region consistently ranged between 45° and 225°. The second location off the Maharashtra coast experiences higher winds only during monsoons which are above the cut-in speed of 4 m/s for wind turbine operation (Boudia and Santos, 2019). The inconsistent wind direction also adds to the unlikely wind potential across seasons.

The remaining three southern coastal locations on the west coast have similar wind and wave climate with mean wind speed close to 6 m/s across seasons. Based on the 38-year hindcasting data, maximum wind speeds experienced are 24.46 m/s, 29.80 m/s and 18.66 m/s off Goa, Karnataka and Kerala coasts respectively. The higher wind speeds also reflect the wave climate which is dominated by wave heights above 1m.

The east coast has two southern coasts off Tamil Nadu and Andhra Pradesh which has a mean wind speed above 4.5 m/s. The time series shows peaks at regular intervals which is indicative of better wind energy potential. The other two locations such as off Odisha and West Bengal experience a relatively calm wind climate with wind speeds below 3 m/s. The east coast of India is prone to extreme winds during cyclones which is more frequent when compared to the west coast of India increasing the risk to devices during the extreme events at the two sites.

Analysis of wave climate across the nine locations studied indicates that the wind and wave climate is severe in the monsoon months of June to September (JJAS). The regions with yearly mean wave power of 15 kW/m have the potential to generate wave energy (Nelson, 2015). The mean wave power at all the sites is less than 15 kW/m which is deficient to harness wave energy effectively at competitive prices (Chybowski and Kuźniewski, 2015). However, Korde and Ringwood (2016) mention that there are efforts to make cost-effective wave energy extraction with low energies. The power output expected from WECs rated below 1000 kW is not significant in the Indian ocean domain (Rusu and Onea, 2017). Therefore, considering all these aspects, at present

extraction of wave energy might not be economically viable at the selected nearshore water depths. Wave energy extraction might be practical in offshore locations whose potential can to be assessed by numerical model studies.

Overall, the locations of the southern states such as, off Goa, Karnataka, Kerala, Tamil Nadu, and Andhra Pradesh have fair wind energy potential which can be effectively harnessed through offshore wind turbines. As the nearshore locations assessed are having water depth below 55 m fixed offshore wind turbines like gravity type, jacket type, suction bucket type or monopile type structure can be the options to choose from.

5.4 SUMMARY

This chapter discusses the wind-wave potential along nine locations along the Indian coast. The wave climate output from MIKE 21 performed based on ERA-Interim hindcast wind data for 38 years is used. The wind-wave climate typical variation for the year 2000 is graphically represented in this chapter. Based on the average values across 38 years amongst the nine locations off Goa, Karnataka, Kerala, Tamil Nadu, and Andhra Pradesh have fair wind energy potential.

CHAPTER 6
PREDICTION OF WAVE CLIMATE

6.1 GENERAL

Coastal regions are critical zones owing to high population density, infrastructure and installation facilities. It is very essential to have a proper assessment of wind-wave characteristics relevant to ocean engineering problems. Dynamically changing wind intensity and direction has direct implications on associated wave parameters.

6.2 KARNATAKA COAST

Karnataka has a coastline of about 320 km length which passes through three coastal districts namely Uttara Kannada, Udupi, and Dakshina Kannada (Fig. 6.1). These coastal districts cover an area of about 1,91,791 km^2 and have a population has of 43,63,617 based on census data (Rani et al., 2015).

Karnataka's coastline of 249.6 km is affected by erosion and only 56.77 km is protected as per state reports as mentioned in Kumar et al., (2006), which means about 89% of the coast is prone to erosion. As per a report on the Challenged Coast of India, the length of coastal settlements in Karnataka within 500 m from the coast is 100.61 km. Additional length occupied for commercial establishments is about 16.62 km. Vulnerability Atlas specifies Karnataka as a moderate Damage risk zone for wind and cyclones with a probable maximum storm surge height of 4.5 m (Guidelines, 2010). Karnataka's coastline comprises of river mouths, long beaches, bays, creeks, lagoons, cliffs, spits and sand dunes. There are around 90 beaches with different aesthetic potential amongst which 22 are unfit due to coastal erosion, port activities, fisheries and industries as per state of the environment report. (CZM, 2003). This report also mentions about 22 urban agglomerations and 1044 villages on the coast. The state has one major port called the New Mangaluru Port (NMP) and nine minor ports along the coast. Additionally, there are about 110 fish landing centres catering a fisherman community population of about 1,67,429 as per the Central Marine Fisheries Research Institute (CMFRI) census report of 2010. Karwar has India's third-largest Naval base INS Kadamba occupying a 45 km^2 area along the coastline.
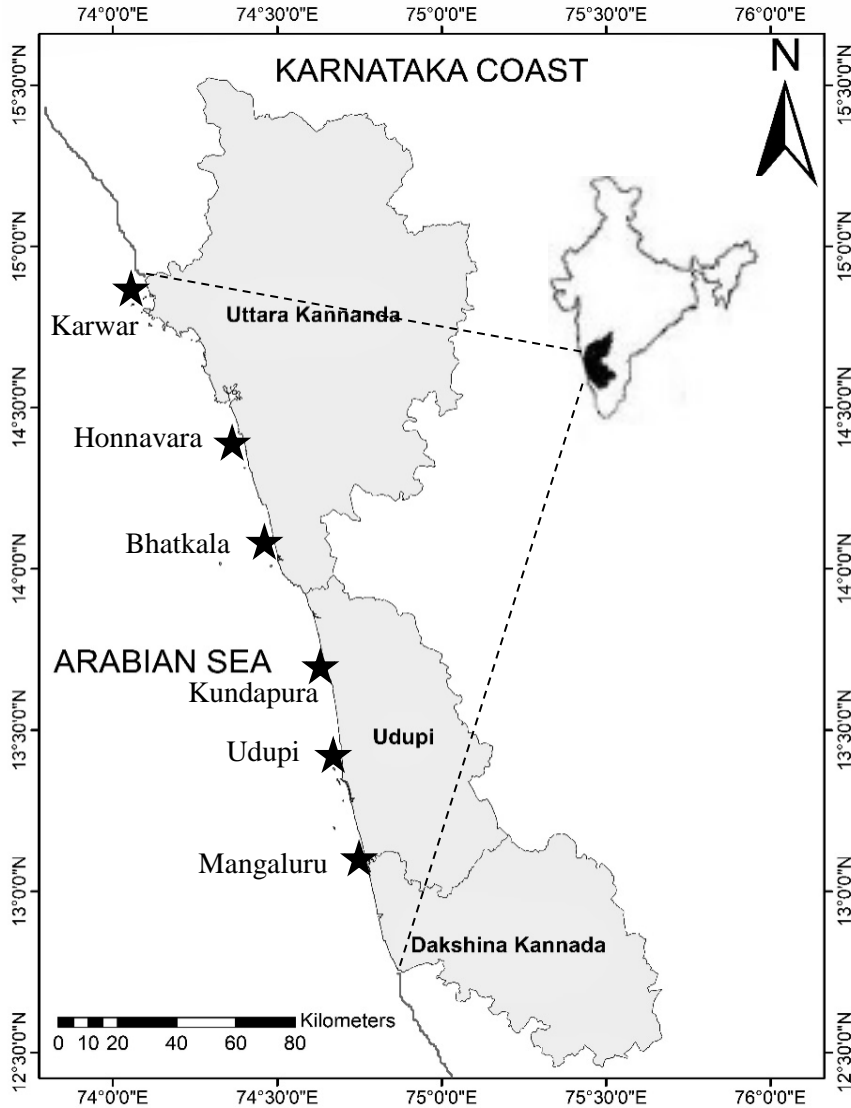
Fig. 6.1 The study area of the Karnataka coast with key locations along the coast

The west coast of India experiences reversing winds seasonally with winds from the south-west direction during the monsoon period of June to September. Followed by a post-monsoon period from October to January where the wind direction is from the north-east (Anoop et al., 2014).

In the present study, the wave climate forecast at six different locations (Table 6.1) along the Karnataka coast are performed for the monsoon period and the wave rose diagrams are plotted for the year 2021. Further, location wise monsoon wave patterns are plotted for the year 2050. The wave parameters at these six locations are simulated up to the year 2070 using the MIKE numerical model driven by CMCC-CM RCP 4.5

wind speeds. The significant wave height and the mean wave period with a 10 and 50 year return period are tabulated.

6.3 NUMERICAL MODELLING

The numerical model is set up using MIKE 21 SW module. The future wave climate prediction is based on CMCC-CM RCP 4.5 up to the year 2070. Euro-Mediterraneo sui Cambiamenti Climatici, Italy is one such CMIP5 climate modelling institute with a GCM model named CMCC-CM. They provide projections for wind speed up to 2100 with a spatial resolution of 0.75º×0.75º. This dataset is selected based on the wind data analysis performed in the present study (Chapter 3). In this study, the wave breaking parameter is set to 0.7. As the measurements correspond to near-shore triad wave interaction is considered. The bottom friction is as per the Nikuradse roughness value of K_n=0.04 m with current friction of 2. White capping is the most sensitive parameter specified as coefficients C_{dis} and δ_{dis} with assigned values of 4.5 and 0.5 respectively. The spectral formulation is as per JONSWAP fetch growth expression. The wave rose diagrams for better visual interpretation of the simulated results are plotted using the plot composer tool in MIKE Zero. The southwest monsoons winds are predominant along the Karnataka coast hence the numerical model is simulated for the monsoon month of June, July, August, and September (JJAS). The wave parameters like significant wave height (H_s), mean wave period (T) and mean wave direction obtained are discussed in the section below.

6.4 RESULTS AND DISCUSSION

Based on the simulated wave climate significant wave height and mean wave period with a 10 year return period are evaluated. The results obtained at six locations are tabulated in Table 6.1. These values will be essential while designing the coastal structures at these locations.

Amongst the six locations studied the southern district Mangaluru showed a higher significant wave height of 5.29 m, 5.59 m and a mean wave period of 10.17 s, 12.59 s for a 10 year, 50 year return period respectively. It is observed that the CMCC-CM RCP 4.5 driven numerical model simulation slightly underestimates the wave climate.

Table 6.1 Simulated wave climate at six locations

Sl. no.	Location details			Wave parameters with 10 year return period		Wave parameters with 50 year return period	
	Location	*Latitude (°N)*	*Longitude (°E)*	*H_s in m*	*T in sec*	*H_s in m*	*T in sec*
1.	Karwar	14.82	74.08	4.73	9.52	4.98	11.49
2.	Honnavara	14.28	74.42	4.45	9.10	4.60	11.29
3.	Bhatkala	14.00	74.50	4.87	9.38	4.95	11.24
4.	Kundapura	13.64	74.61	4.53	9.03	4.68	11.42
5.	Udupi	13.42	74.67	4.54	9.17	4.69	11.76
6.	Mangaluru	12.95	74.79	5.25	10.17	5.59	12.59

6.4.1 Simulated wave climate during the monsoon of 2021

The wave rose diagrams across the monsoon months of 2021 are plotted in Figure 6.2 and Figure 6.3. The wave climate is harsh in July and restores to calm conditions in September. The predominant wave direction is southwest owing to the wind direction during monsoons.
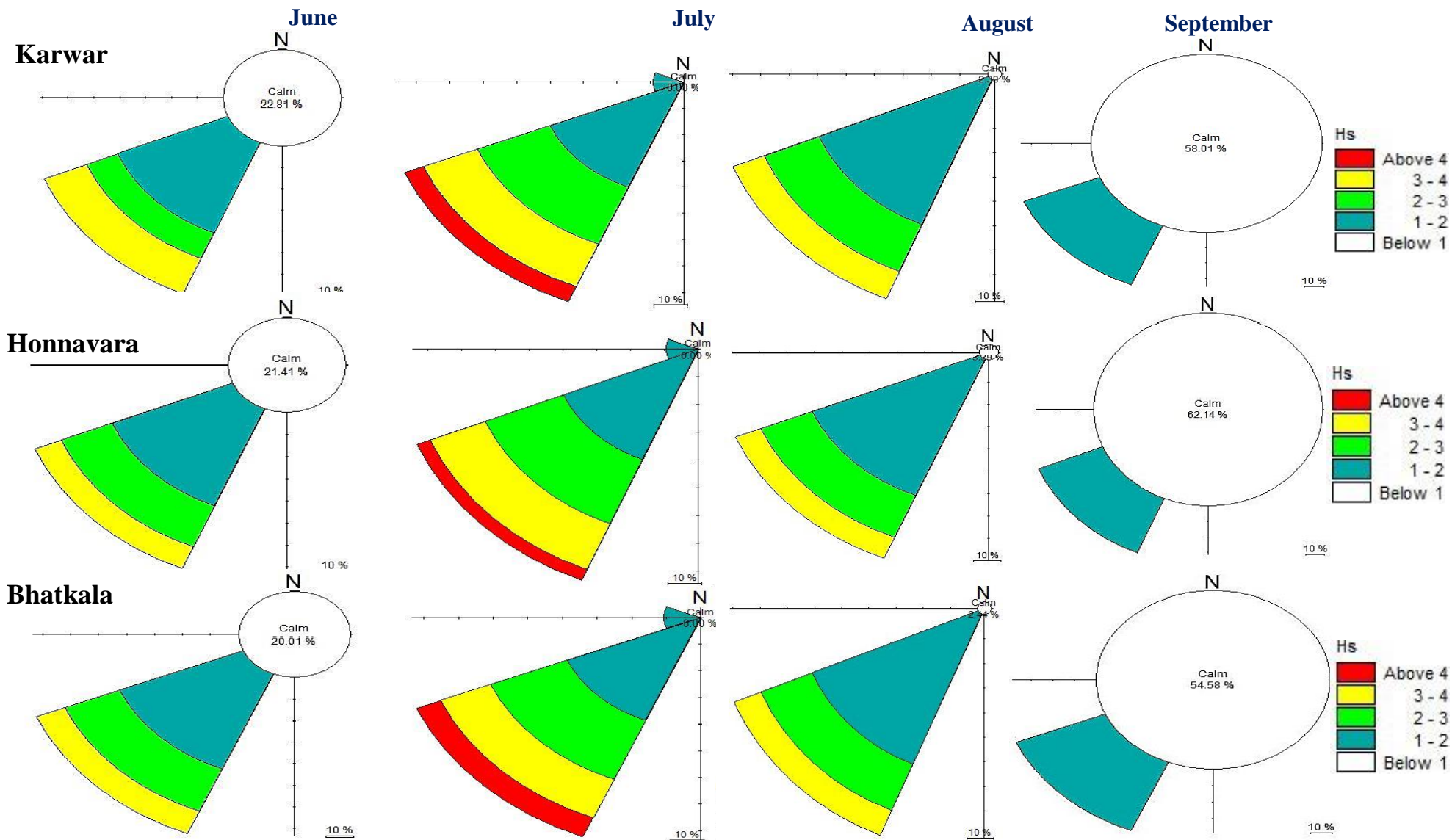
94

Fig. 6.2 The wave rose diagram for the monsoon months at Karwar, Honnavara and Bhatkala for the year 2021
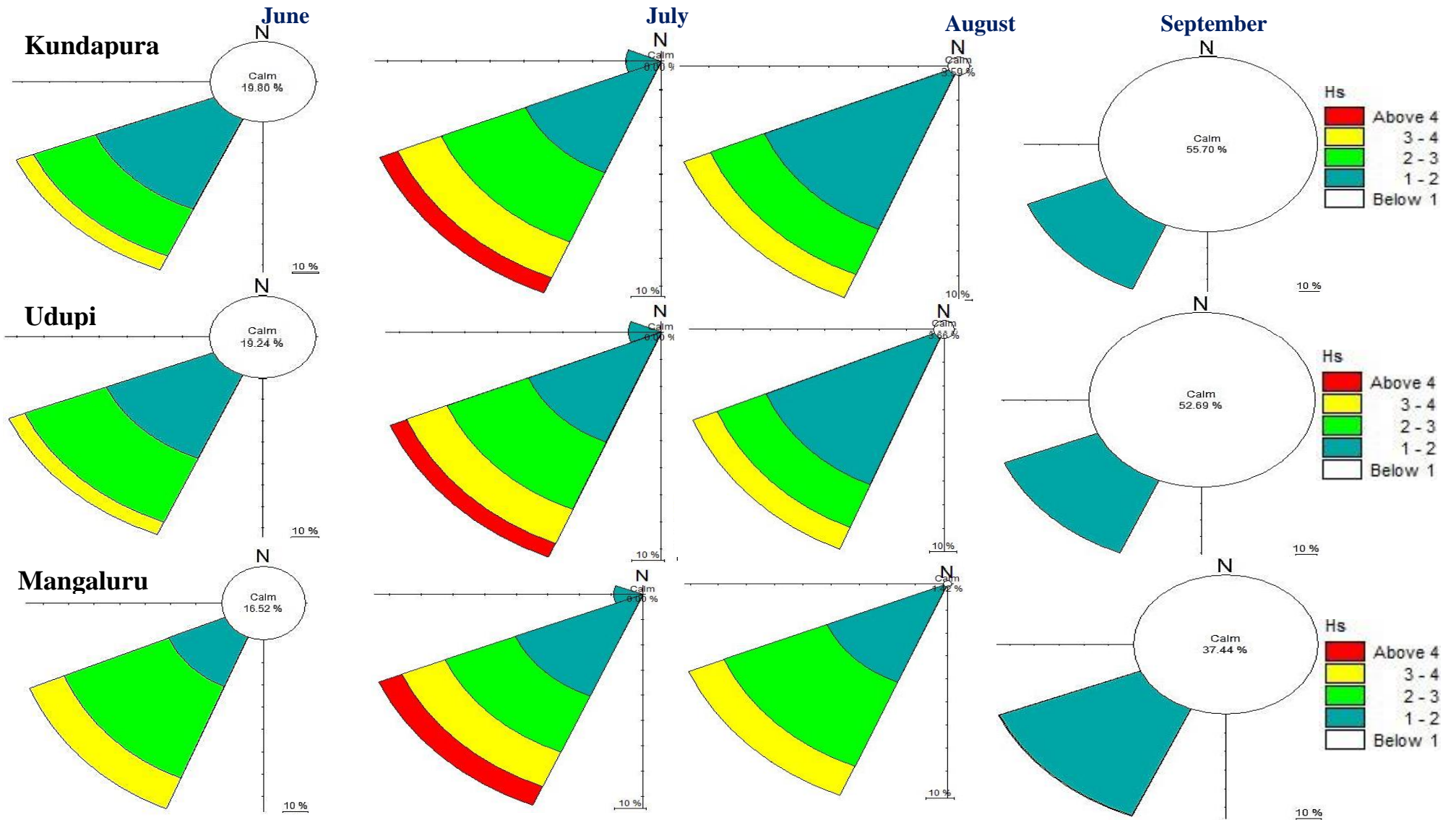
95

Fig. 6.3 The wave rose diagram for the monsoon months at Kundapura, Udupi and Mangaluru for the year 2021

The month of June experiences a calm wave climate with more than 15% of significant wave heights (H_s) below 1m. The figures above clearly indicate that locations such as Mangaluru, Udupi, and Kundapura experienced H_s varying between 2 to 3 m. Overall the H_s above 4 m is not recorded in any of the locations for June.

With the arrival of the monsoon, the month of July experiences a harsh wave climate along the Karnataka coast. The H_s above 1m is observed in all the locations with maximum values of 4.73 m, 4.31 m, 4.66 m, 4.32 m, 4.28 m, and 4.93 m recorded at Karwar, Honnavara, Bhatkala, Kundapura, Udupi, and Mangaluru respectively for the year 2021. The predominant wave direction is southwest with a small per cent of H_s of the range of 1 to 2 m in the west direction. The maximum H_s reaches above 4 m in all the locations during the monsoon period.

In August, the coast is exposed to waves ranging from 1 m to 4 m. Karwar, Honnavara, and Bhatkala experience the majority of H_s in the range of 1 to 2 m. However, the locations further south experiences a higher H_s in the range of 2 to 3 m. The wave climate is the calmest in September with about 50 % of H_s below 1 m in all the locations with an exception of Mangaluru. Overall the wave heights are below 2 m across all locations for September.

6.4.2 Variation of wave parameters during the monsoon of 2050

The wave parameters in terms of significant wave height, mean wave period and wave direction at every 30-minute interval are simulated using MIKE 21 numerical wave model. The wave climate is forecasted for 50 years up to 2070. The typical monsoon wave climate variation is extracted at six locations for the year 2050.

From Figure 6.4 to Figure 6.6 it is clear that the mean wave direction is predominant in the southwest direction during monsoons. The wave direction is expected to reverse by the month of October. These daily forecasts of wave climate can be used for effective coastal management. Locations such as Karwar, Bhatkala and Mangaluru experiences higher waves during monsoons. Overall locations such as Honnavara, Udupi and Kundapur have comparatively lesser intense wave climate.

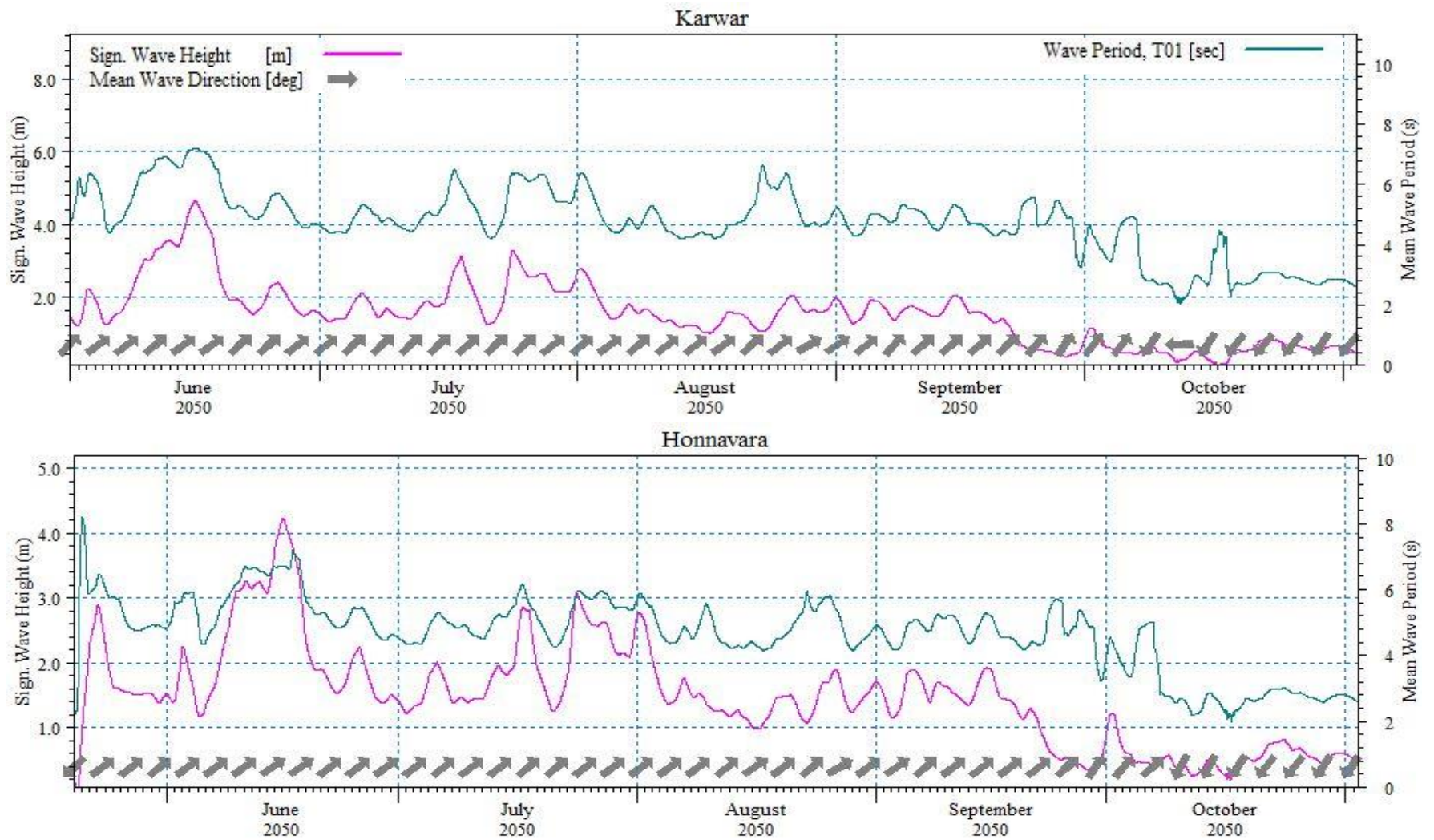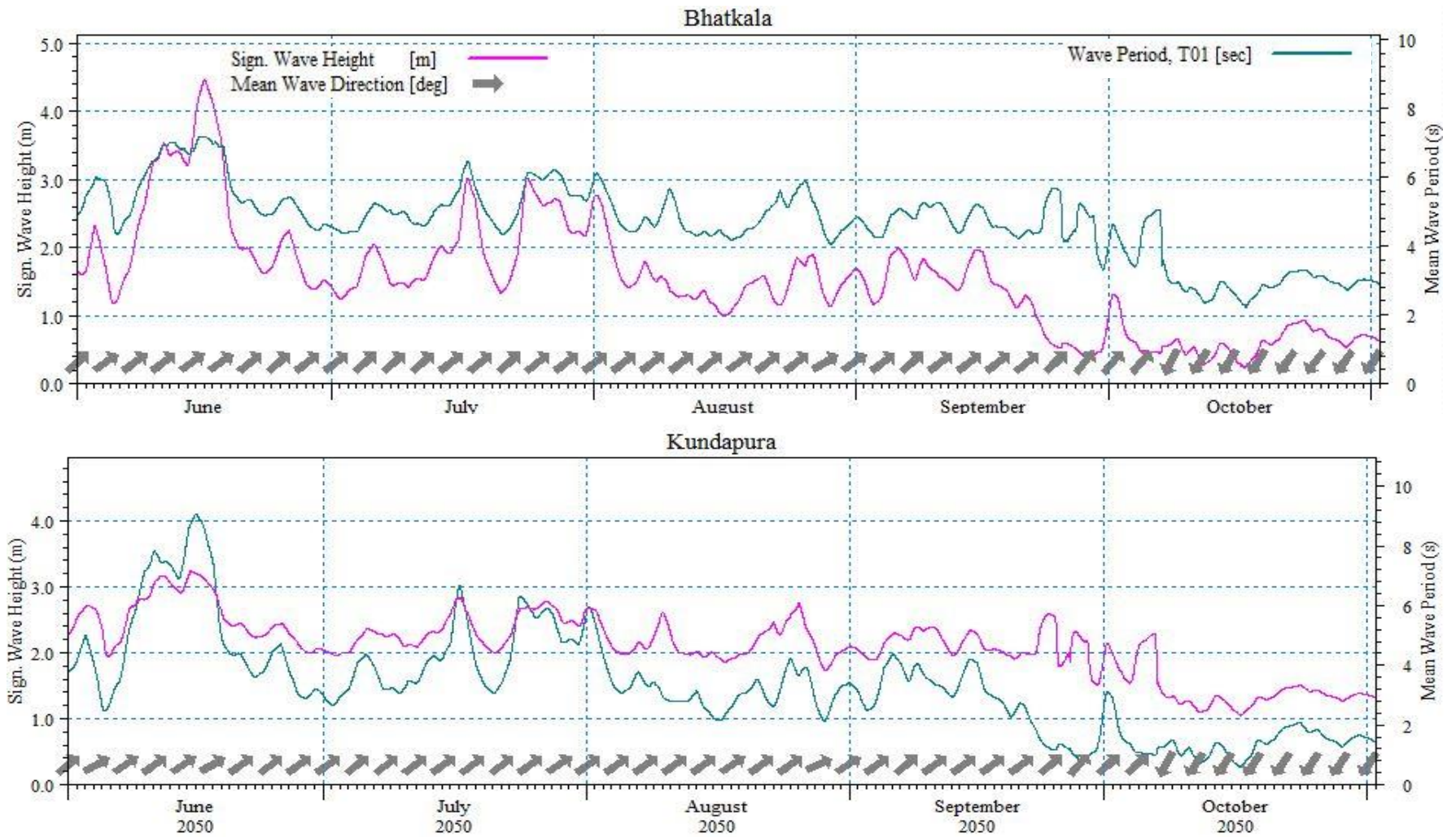**Fig. 6.4 The wave climate at Karwar and Honnavara locations for the year 2050**

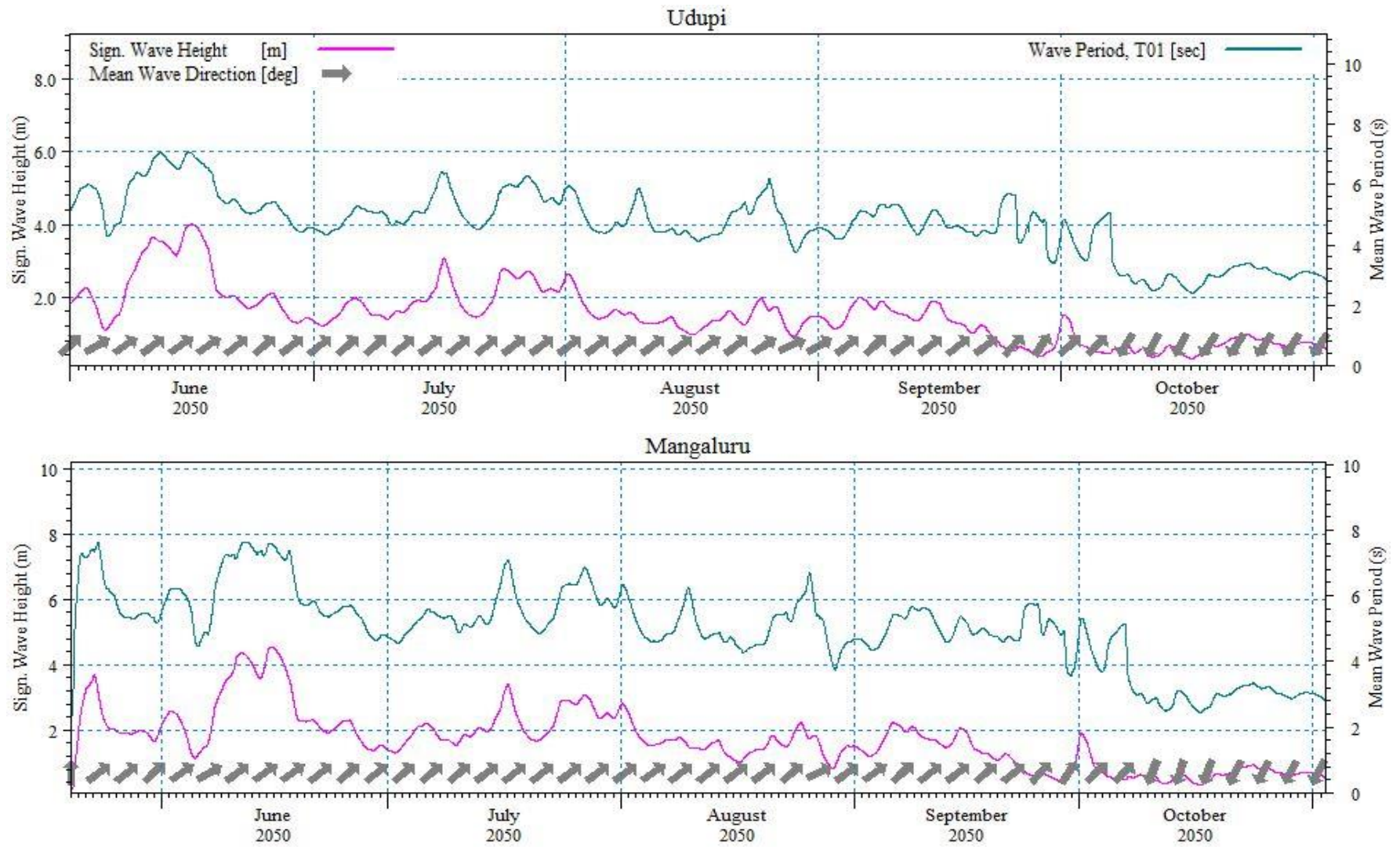**Fig. 6.5 The wave climate at Bhatkala and Kundapura locations for the year 2050**

Fig. 6.6 The wave climate at Udupi and Mangaluru locations for the year 2050

6.5 SUMMARY

The wave climate forecasts at six different locations along the Karnataka coast is simulated using the numerical wave model developed in MIKE 21 SW. The wave climate is projected up to the year 2070 based on CMCC-CM RCP 4.5 wind speed data. From the wave climate analysis performed wave parameters with 10 year and 50 year return period is evaluated.

The wave rose diagrams of significant wave height for the typical year 2021 indicate that the wave height above 4 m in all six locations is expected in the monsoon month of July. In the month of June, up to 20 % of waves are expected to be below 1 m. The month of August has the majority of waves in the range of 1 m to 3 m. A calmer wave climate is expected in the month of September with about 50 % of waves below 1 m in all locations with an exception of Mangaluru.

The projections for the monsoon of 2050 is shown in the time series plot with parameters like significant wave height, mean wave period and mean wave direction. The wave parameters with 10 year return period are higher in locations like Mangaluru, Bhatkala and Karwar region with significant wave heights 5.25 m, 4.87 m and 4.73 m respectively. The locations Honnavara, Kundapura and Udupi have comparatively less intense wave climate. The significant wave height and mean wave period of 5.59 m, 4.95 m, 4.98 m and 12.59 s, 11.24 s and 11.49 s with 50 year return period is expected at locations Mangaluru, Bhatkala and Karwar respectively.

7.1 SUMMARY

In the present study, numerical model studies are performed to assess the wind-wave climate of the Indian domain considering climate change effects. The numerical model of the Indian domain modelled using MIKE 21 SW module is successful in simulating the long-term wave climate. The long-term analysis is performed based on modelled global wind speed datasets spanning across 90 years. The global wind speed dataset from ERA-Interim showed an excellent match with the in-situ measurements taken in the Indian domain. The numerical model outputs generated by these datasets are close to reality. The forecasted wave climate is simulated using GCM from CMIP5. Amongst the 38 different wind speed datasets, CMCC-CM corresponding to RCP 4.5 matched well with the real-time wind speeds modelled by ERA-Interim.

7.2 CONCLUSIONS

Based on the present study the following conclusions are drawn:

1. The ERA-Interim global wind speed dataset values are validated with in-situ measurements taken along the east coast (AD02) and west coast (BD11). The wind speed showed an excellent match for the Indian domain with R-value of 0.93 and 0.84 at buoy location AD02 and BD11 respectively.

2. The wind-wave climate of the Indian domain is simulated using MIKE 21 SW numerical model. The significant wave heights simulated from hindcast of ERA-Interim reanalysed gridded dataset are slightly overestimated when compared with in-situ measurements at Karwar and OB03 locations. The numerical model simulations have an R-value of 0.67 at nearshore location Karwar and 0.66 at offshore location OB03.

3. The design significant wave heights from ERA-Interim simulated hindcast at Mangaluru region are higher by 2.60% and 5.44% for return period 10 years and 50 years respectively when compared with the long-term analysis performed on in-situ

buoy recorded for 5 years. This increase is justified as the hindcast dataset has better temporal coverage and has incorporated climate change effects.

4. The shoreline analysis is performed after the numerical model results were comparable with satellite data with an R-value greater than 0.9. The maximum erosion observed in the year 2015 indicated accretion of about 100 m in the region near the southern breakwater of NMP and the southern profile near Bengre region experienced an erosion of about 100 m. The region near the northern breakwater of NMP showed erosion of about 150 m and erosion of about 75 m at Sasihithlu region.

5. Based on the hindcast study of wind-wave climate, southern coastal states off Goa, Karnataka, Kerala, Tamil Nadu, and Andhra Pradesh have favourable offshore wind speeds (>4m/s) to operate offshore wind turbines. With water depths below 55 m, the effective utilization of renewable energy is always a possibility. However, with mean wave power being on a lower side (<15kW/m) wave energy converter might not produce the required performance.

6. The hindcasted monthly mean wind speeds from multiple CMIP5 datasets are compared with ERA-Interim reanalysed dataset. The analysis of 26 years of data showed CMCC-CM, CSIRO-mk3.6.0, HadGEM-AO, and MIROC5 are effective in capturing the wind speed variations of the Indian domain with a correlation of greater than 0.93.

7. In order to extend the study to wave forecasts considering climate change effects, the RCP projections of the best four CMIP5 datasets are assessed. The projections by CMCC-CM for RCP 4.5 are competent in capturing the current wind speed trends based on the analysis of datasets from 2006 to 2018. The daily comparison showed a Correlation Coefficient is 0.81 and an RMSD of 0.75 m/s with reanalysed ERA-Interim daily wind speeds.

8. The wave parameters with 10 year return period are higher in locations like Mangaluru, Bhatkala and Karwar region with values of 5.25 m, 4.87 m and 4.73 m respectively. The significant wave height of 5.59 m, 4.95 m and 4.98 m for 50 year return period is expected at locations Mangaluru, Bhatkala and Karwar respectively.

7.2 CONTRIBUTIONS FROM THE STUDY

- In the present study, the numerical model is effective for wave hindcast studies, shoreline analysis, assessment of wind-wave climate along the Indian coast and wave forecasting along the Karnataka coast.
- Considering the less volume of numerical model study for wave climate forecasting along the Karnataka coast the study contributes to the body of work.
- The wind-wave climate predictions will help in the analysis and design of coastal structures for the specific return period.

7.3 LIMITATIONS AND FUTURE SCOPE

- The major limitation of this study is restricting the boundary of the Indian Ocean domain up to 4°S this is considered to reduce the computational efforts.
- The forecasts on shoreline changes and wind-wave energy assessment can be performed using the numerical model driven by CMCC-CM RCP 4.5 wind speed dataset.
- The numerical model driven with Regional Climate Models can enhance the model performance and hence can be explored.

REFERENCES

Abdollahzadehmoradi, Y., Erdik, T., Özger, M., & Altunkaynak, A. (2014). Application of MIKE 21 SW for wave hindcasting in Marmara Sea Basin for the year 2012.11th international congress on advances in civil engineering (ACE), 21-25.

Aboobacker, V. M., Vethamony, P., Sudheesh, K., & Rupali, S. P. (2009). Spectral characteristics of the nearshore waves off Paradip, India during monsoon and extreme events. Natural hazards, 49(2), 311-323.

Ackermann, T., & Söder, L. (2002). An overview of wind energy-status 2002. Renewable and sustainable energy reviews, 6(1-2), 67-127.

Aderinto, T., & Li, H. (2019). Review on power performance and efficiency of wave energy converters. Energies, 12(22), 4329.

Alexandru, A., & Sushama, L. (2015). Current climate and climate change over India as simulated by the Canadian Regional Climate Model. Climate Dynamics, 45(3-4), 1059-1084.

Amrutha, M. M., Kumar, V. S., Sandhya, K. G., Nair, T. B., & Rathod, J. L. (2016). Wave hindcast studies using SWAN nested in WAVEWATCH III-comparison with measured nearshore buoy data off Karwar, eastern Arabian Sea. Ocean Engineering, 119, 114-124.

Anoop, T. R., Kumar, V. S., & Shanas, P. R. (2014). Spatial and temporal variation of surface waves in shallow waters along the eastern Arabian Sea. Ocean Engineering, 81, 150-157.

Appendini, C. M., Torres-Freyermuth, A., Salles, P., López-González, J., & Mendoza, E. T. (2014). Wave climate and trends for the Gulf of Mexico: A 30-yr wave hindcast. Journal of Climate, 27(4), 1619-1632.

Arockiaraj, S., Kankara, R. S., Dora, G. U., & Sathish, S. (2018). Estimation of seasonal morpho-sedimentary changes at headland bound and exposed beaches along south Maharashtra, west coast of India. Environmental Earth Sciences, 77(17), 604.

Aydoğan, B., Ayat, B., & Yüksel, Y. (2013). Black Sea wave energy atlas from 13 years hindcasted wave data. Renewable energy, 57, 436-447.

Barbariol, F., Bidlot, J. R., Cavaleri, L., Sclavo, M., Thomson, J., & Benetazzo, A. (2019). Maximum wave heights from global model reanalysis. Progress in oceanography, 175, 139-160.

Bilgili, M., Yasar, A., & Simsek, E. (2011). Offshore wind power development in Europe and its comparison with onshore counterpart. Renewable and Sustainable Energy Reviews, 15(2), 905-915.

Bindoff, N. L., Stammer, D., Le Traon, P. Y., Trenberth, K., Mauritzen, C., Church, J. A., ... & Wilson, S. (2010). Capabilities of Global Ocean Programmes to inform climate services. Procedia Environmental Sciences, 1, 342-353.

Boudia, S. M., & Santos, J. A. (2019). Assessment of large-scale wind resource features in Algeria. Energy, 189, 116299.

Caires, S., & Sterl, A. (2005). 100-year return value estimates for ocean wind speed and significant wave height from the ERA-40 data. Journal of Climate, 18(7), 1032-1048.

Casas-Prat, M., Wang, X. L., & Swart, N. (2018). CMIP5-based global wave climate projections including the entire Arctic Ocean. Ocean Modelling, 123, 66-85.

Census report (2014), Office of the Registrar General & Census Commissioner, India, (http://www.censusindia.gov.in/vital_statistics/SRS_Statistical_Report.html)

Chowdhury, P., & Behera, M. R. (2017). Effect of long-term wave climate variability on longshore sediment transport along regional coastlines. Progress in Oceanography, 156, 145-153.

Chowdhury, P., & Behera, M. R. (2019). Evaluation of CMIP5 and CORDEX derived wave climate in Indian Ocean. Climate Dynamics, 52(7-8), 4463-4482.

Chowdhury, P., Behera, M. R., & Reeve, D. E. (2019). Wave climate projections along the Indian coast. International Journal of Climatology, 39(11), 4531-4542.

Chybowski, L., & Kuźniewski, B. (2015). An overview of methods for wave energy conversion. Scientific Journals of the Maritime University of Szczecin, 41 (113), 17–23.

Clauss G., Lehmann E., Östergaard C. (1992) Features of Offshore Structures. In: Offshore Structures. Springer, London. https://doi.org/10.1007/978-1-4471-3193-9_2

Coastal Zone Management (2003), State of Environment Report, Karnataka.

Collins, M., R. Knutti, J. Arblaster, J.-L. Dufresne, T. Fichefet, P. Friedlingstein, X. Gao, W.J. Gutowski, T. Johns, G. Krinner, M. Shongwe, C. Tebaldi, A.J. Weaver and M. Wehner. (2013). Long-term Climate Change: Projections, Commitments and Irreversibility. In: Climate Change 2013: The Physical Science Basis. Contribution of Working Group I to the Fifth Assessment Report of the Intergovernmental Panel on Climate Change. Cambridge University Press, Cambridge, United Kingdom and New York, NY, USA.

Cucco, A., Quattrocchi, G., & Zecchetto, S. (2019). The role of temporal resolution in modeling the wind induced sea surface transport in coastal seas. Journal of Marine Systems, 193, 46-58.

Curto, D., Franzitta, V., Viola, A., Cirrincione, M., Mohammadi, A., & Kumar, A. (2019). A renewable energy mix to supply small islands. A comparative study applied to Balearic Islands and Fiji. Journal of Cleaner Production, 241, 118356.

Dattatri, J., Raman, H., & Shankar, N. J. (1979). Height and period distributions for waves off Mangalore Harbour-west coast. Journal of Geophysical Research: Oceans, 84(C7), 3767-3772.

Dee, D.P., Uppala, S.M., Simmons, A.J., Berrisford, P., Poli, P., Kobayashi, S., Andrae, U., Balmaseda, M.A., Balsamo, G., Bauer, P., Bechtold, P., Beljaars, A.C.M., van d e Berg, L., Bidlot, J., Bormann, N., Delsol, C., Dragani, R., Fuentes, M., Geer, A.J., Haimberger, L., Healy, S.B., Hersbach, H., Hólm, E.V., Isaksen, L., Kållberg, P., Köhler, M., Matricardi, M., McNally, A.P., Monge-Sanz, B.M., Morcrette, J.-J., Park, B.-K., Peubey, C., de Rosnay, P., Tavolato, C., Thèpaut, J.-N., Vitart, F. (2011). The ERA-Interim reanalysis: configuration and performance of the data assimilation system. Q. J. R. Meteorol. Soc. 137: 553–597. DOI:10.1002/qj.828

Deepthi, R., & Deo, M. C. (2010). Effect of climate change on design wind at the Indian offshore locations. Ocean Engineering, 37(11-12), 1061-1069.

DHI. (2014), LITPACK-An integrated modelling system for littoral processes and coastline kinetics. DHI, Denmark.

DHI, (2015). MIKE 21 wave modelling: MIKE 21 SW-Spectral waves FM. Short

description. DHI, Denmark.

Divinsky, B. V., & Kosyan, R. D. (2017). Spatiotemporal variability of the Black Sea wave climate in the last 37 years. Continental Shelf Research, 136, 1-19.

Divinsky, B., & Kosyan, R. (2018). Parameters of wind seas and swell in the Black Sea based on numerical modelling. Oceanologia, 60(3), 277-287.

Ellabban, O., Abu-Rub, H., & Blaabjerg, F. (2014). Renewable energy resources: Current status, future prospects and their enabling technology. Renewable and Sustainable Energy Reviews, 39, 748-764.

Emori, S., Taylor, K., Hewitson, B., Zermoglio, F., Juckes, M., Lautenschlager, M. and Stockhause, M. (2016). CMIP5 data provided at the IPCC Data Distribution Centre. Fact Sheet of the Task Group on Data and Scenario Support for Impact and Climate Analysis (TGICA) of the Intergovernmental Panel on Climate Change (IPCC), p.8.

Erdik, T., & Beji, S. (2018). Statistical Analyses of Wave Height and Wind Velocity Distributions for the Sea of Marmara. International Journal of Environment and Geoinformatics, 5(1), 76-83.

Erikson, L. H., Hegermiller, C. A., Barnard, P. L., Ruggiero, P., & van Ormondt, M. (2015). Projected wave conditions in the Eastern North Pacific under the influence of two CMIP5 climate scenarios. Ocean Modelling, 96, 171-185.

Eyring, V., Bony, S., Meehl, G. A., Senior, C. A., Stevens, B., Stouffer, R. J., & Taylor, K. E. (2016). Overview of the Coupled Model Intercomparison Project Phase 6 (CMIP6) experimental design and organization. Geoscientific Model Development, 9(5), 1937-1958.

Felix, A., V Hernández-Fontes, J., Lithgow, D., Mendoza, E., Posada, G., Ring, M., & Silva, R. (2019). Wave Energy in Tropical Regions: Deployment Challenges, Environmental and Social Perspectives. Journal of Marine Science and Engineering, 7(7), 219.

Foley, A. M., Leahy, P. G., Marvuglia, A., & McKeogh, E. J. (2012). Current methods and advances in forecasting of wind power generation. Renewable Energy, 37(1), 1-8.

Grabemann, I., & Weisse, R. (2008). Climate change impact on extreme wave

conditions in the North Sea: an ensemble study. Ocean Dynamics, 58(3-4), 199-212.

Guidelines (2010): Improving Wind/Cyclone Resistance of Housing, Building Materials & Technology Promotion, Council Ministry of Housing & Urban Poverty Alleviation Government of India, New Delhi.

Hajira R. (2019). Shoreline changes along new mangalore port, panambur coast using MIKE 21. M.Tech. Thesis, National Institute of Technology Karnataka, Surathkal, Mangaluru, India.

Hemer, M. A., & Trenham, C. E. (2016). Evaluation of a CMIP5 derived dynamical global wind wave climate model ensemble. Ocean Modelling, 103, 190-203.

Hithin, N. K., Kumar, V. S., & Shanas, P. R. (2015). Trends of wave height and period in the Central Arabian Sea from 1996 to 2012: a study based on satellite altimeter data. Ocean Engineering, 108, 416-425.

Holmbom, J. (2011). Modelling of Waves and Currents in the Baltic Sea. Degree Project for the Masters Program in Civil Engineering Hydraulic Engineering, Department of Land and Water Resources Engineering, Royal Institute of Technology (KTH), SE-100 44 STOCKHOLM, Sweden

Ilia, A., & O'Donnell, J. (2018). An Assessment of Two Models of Wave Propagation in an Estuary Protected by Breakwaters. Journal of Marine Science and Engineering, 6(4), 145.

IPCC (2001), Climate Change 2001: The Scientific Basis, Contribution of Working Group I to the Third Assessment Report of the Intergovernmental Panel on Climate Change [Houghton, J.T., Y. Ding, D.J. Griggs, M. Noguer, P.J. van der Linden, X. Dai, K. Maskell, and C.A. Johnson (eds.)]. Cambridge University Press, Cambridge, United Kingdom and New York, NY, USA, p. 881.

IPCC, (2007) Climate Change 2007: Impacts, Adaptation and Vulnerability, Contribution of Working Group-II to the Fourth Assessment Report of the Intergovernmental Panel on Climate Change, Cambridge University Press, Cambridge, UK, p. 976.

IPCC, (2014) Climate Change 2014: Synthesis Report. Contribution of Working Groups I, II and III to the Fifth Assessment Report of the Intergovernmental Panel

on Climate Change. IPCC, Geneva, Switzerland, p. 151.

Jagadeesh H.B. (2018). Physical model studies on wave propagation along approach channel and its effects on harbour tranquility. Ph.D. Thesis, National Institute of Technology Karnataka, Surathkal, Mangaluru, India.

Jadidoleslam, N., Özger, M., & Ağıralioğlu, N. (2016). Wave power potential assessment of Aegean Sea with an integrated 15-year data. Renewable energy, 86, 1045-1059.

Jose, F., & Stone, G. W. (2006). Forecast of nearshore wave parameters using MIKE-21 Spectral wave model, Gulf Coast Association of Geological Societies, 56, 323-327.

Kamphuis, J. W., (2010), Introduction to Coastal Engineering and Management. In: Advanced Series on Ocean Engineering, World scientific Publishing Co. Pte. Ltd., Vol 30, 81-102.

Korde, U. A., & Ringwood, J. (2016). Hydrodynamic control of wave energy devices. Cambridge University Press.

Krishnan, A., & Bhaskaran, P. K. (2019). Performance of CMIP5 wind speed from global climate models for the Bay of Bengal region. International Journal of Climatology. 40(7), 3398-3416.

Krishnan, A., & Bhaskaran, P. K. (2020). Skill assessment of global climate model wind speed from CMIP5 and CMIP6 and evaluation of projections for the Bay of Bengal. Climate Dynamics, 55(9), 2667-2687.

Kulkarni, S., Deo, M. C., & Ghosh, S. (2016). Evaluation of wind extremes and wind potential under changing climate for Indian offshore using ensemble of 10 GCMs. Ocean and Coastal Management, 121, 141-152.

Kulkarni, S., Deo, M. C., & Ghosh, S. (2014). Changes in the design and operational wind due to climate change at the Indian offshore sites. Marine Structures, 37, 33-53.

Kumar, E. D., Sannasiraj, S. A., Sundar, V., & Polnikov, V. G. (2013). Wind-wave characteristics and climate variability in the Indian Ocean region using altimeter data. Marine Geodesy, 36(3), 303-318.

Kumar, V. S., & Deo, M. C. (2004). Design wave estimation considering directional

distribution of waves. Ocean engineering, 31(17-18), 2343-2352.

Kumar, V. Sanil, K. C. Pathak, P. Pednekar, N. S. N. Raju and R. Gowthaman. (2006). Coastal processes along the Indian coastline. Current science, 530-536.

Kumar, V. S., & Philip, C. S. (2010). Variations in long-term wind speed during different decades in Arabian Sea and Bay of Bengal. Journal of Earth System Science, 119(5), 639-653.

Kumar, V. S., Johnson, G., Dora, G. U., Chempalayil, S. P., Singh, J., & Pednekar, P. (2012). Variations in nearshore waves along Karnataka, west coast of India. Journal of earth system science, 121(2), 393-403.

Kumar, V. S., Joseph, J., Amrutha, M. M., Jena, B. K., Sivakholundu, K. M., & Dubhashi, K. K. (2018). Seasonal and interannual changes of significant wave height in shelf seas around India during 1998–2012 based on wave hindcast. Ocean Engineering, 151, 127-140.

Kumaran, V., Nagamani, K., & Mullaivendhan, C. (2015). Wave Climate for the Design of Island Structures Union-Territory (Lakshadweep). Procedia Engineering, 116, 398-405.

Lemos, G., Semedo, A., Dobrynin, M., Behrens, A., Staneva, J., Bidlot, J. R., & Miranda, P. M. (2019). Mid-twenty-first century global wave climate projections: Results from a dynamic CMIP5 based ensemble. Global and planetary change, 172, 69-87.

Li, F., Bicknell, C., Lowry, R., & Li, Y., (2012) A comparison of extreme wave analysis methods with 1994–2010 offshore Perth dataset. Coastal Engineering, 69 1-11.

Liu, M., & Zhao, D. (2019). On the Study of Wave Propagation and Distribution in the Global Ocean. Journal of Ocean University of China, 18(4), 803-811.

Manasseh, R., Sannasiraj, S. A., McInnes, K. L., Sundar, V., & Jalihal, P. (2017). Integration of wave energy and other marine renewable energy sources with the needs of coastal societies. The International Journal of Ocean and Climate Systems, 8(1), 19-36.

ManiMurali, R., Vidya, P. J., Modi, P., & Jayakumar, S. (2014). Site selection for offshore wind farms along the Indian coast. Indian J Geo-Mar Sci. 43(7), 1401-1406.

MIKE (2017), Littoral Processes FM All Modules Scientific Documentation, DHI.

Mishra, P., Mohanty, P. K., Murty, A. S. N., & Sugimoto, T. (2001). Beach profile studies near an artificial open-coast port along south Orissa, east coast of India. Journal of Coastal Research, 164-171.

Mishra, P., Pradhan, U. K., Panda, U. S., Patra, S. K., RamanaMurthy, M. V., Seth, B., & Mohanty, P. K. (2014). Field measurements and numerical modeling of nearshore processes at an open coast port on the east coast of India.Indain journal of Geo-Marine Sciences 43(7), 1272-1280.

Moeini, M. H., & Etemad-Shahidi, A. (2007). Application of two numerical models for wave hindcasting in Lake Erie. Applied Ocean Research, 29(3), 137-145.

Mohan, S., & Bhaskaran, P. K. (2019). Evaluation of CMIP5 climate model projections for surface wind speed over the Indian Ocean region. Climate Dynamics, 1-21.

Morris-Thomas, M. T., Irvin, R. J., & Thiagarajan, K. P. (2007). An investigation into the hydrodynamic efficiency of an oscillating water column. Journal of Offshore Mechanics and Arctic Engineering, 129, 273-278.

Nayak, S., Bhaskaran, P. K., & Venkatesan, R. (2012). Near-shore wave induced setup along Kalpakkam coast during an extreme cyclone event in the Bay of Bengal. Ocean Engineering, 55, 52-61.

Neelamani S, Al-Salem K & Rakha K, (2007). Extreme waves for Kuwaiti territorial waters, Ocean Eng, 34 (10), 1496-1504.

Neelamani S, (2009). Influence of threshold value on Peak Over Threshold Method on the predicted extreme significant wave heights in Kuwaiti territorial waters, J Coastal Res, 564-568.

Nelson, V. C., & Starcher, K. L. (2015). Introduction to renewable energy. CRC press.

Noujas, V., Kankara, R. S., & Selvan, S. C. (2019). Shoreline management plan for embayed beaches: A case study at Vengurla, west coast of India. Ocean & coastal management, 170, 51-59.

Pachauri, R. K., Allen, M. R., Barros, V. R., Broome, J., Cramer, W., Christ, R., ... & Dubash, N. K. (2014). Climate change 2014: synthesis report. Contribution of Working Groups I, II and III to the fifth assessment report of the Intergovernmental Panel on Climate Change, IPCC. p. 151.

Patra, A., & Bhaskaran, P. K. (2016). Trends in wind-wave climate over the head Bay of Bengal region. International Journal of Climatology, 36(13), 4222-4240.

Patra, S. K., Mohanty, P. K., Mishra, P., & Pradhan, U. K. (2015). Estimation and validation of offshore wave characteristics of Bay of Bengal cyclones (2008-2009). Aquatic Procedia, 4, 1522-1528.

Pentapati, S., Deo, M. C., Kerkar, J., & Vethamony, P. (2015). Projected impact of climate change on waves at Mumbai High. In Proceedings of the Institution of Civil Engineers-Maritime Engineering, Thomas Telford Ltd,168 (1), p. 20-29.

Pérez-Collazo, C., Greaves, D., & Iglesias, G. (2015). A review of combined wave and offshore wind energy. Renewable and Sustainable Energy Reviews, 42, 141-153.

Pradhan, S., Mishra, S. K., Baral, R., Samal, R. N., & Mohanty, P. K. (2017). Alongshore sediment transport near tidal inlets of Chilika Lagoon; East coast of India. Marine Geodesy, 40(2-3), 187-203.

Radhika, S., Deo, M. C., & Latha, G. (2013). Evaluation of the wave height used in the design of offshore structures considering the effects of climate change. Proceedings of the Institution of Mechanical Engineers, Part M: Journal of Engineering for the Maritime Environment, 227(3), 233-242.

Rajasree, B. R., Deo, M. C., & Nair, L. S. (2016). Effect of climate change on shoreline shifts at a straight and continuous coast. Estuarine, Coastal and Shelf Science, 183, 221-234.

Rani, N. S., Satyanarayana, A. N. V., & Bhaskaran, P. K. (2015). Coastal vulnerability assessment studies over India: a review. Natural Hazards, 77(1), 405-428.

Rao, S., Shirlal, K. G., & Khan, P. H. (2001). An interpretation of sediment trends along DK coast. ISH Journal of Hydraulic Engineering, 7(1), 33-39.

Rao, S. (2002). Study of coastal erosion along Karnataka Coast. ISH Journal of Hydraulic Engineering, 8(2), 23-33.

Rao, S., Shirlal, K. G., Praveen Suvarna S, Madhu Babu, Subramanian B.R. and Kankara R.S. (2007). Modelling of coastal process around Gurupur-Netravathi river mouth using MIKE 21, Fourth Indian National Conference On Harbour and Ocean Engg., NITK, Surathkal., 392-401

Reistad, M. (2001). Global warming can result in higher waves. Cicerone, 5.

114

Remya, P. G., Kumar, R., Basu, S., & Sarkar, A. (2012). Wave hindcast experiments in the Indian Ocean using MIKE 21 SW model. Journal of earth system science, 121(2), 385-392.

Roshin, E., & Deo, M. C. (2017). Derivation of design waves along the Indian coastline incorporating climate change. Journal of Marine Science and Technology, 22(1), 61-70.

Ruggiero, P., Komar, P. D., & Allan, J. C. (2010). Increasing wave heights and extreme value projections: The wave climate of the US Pacific Northwest. Coastal Engineering, 57(5), 539-552.

Rusu, L., & Onea, F. (2017). The performance of some state-of-the-art wave energy converters in locations with the worldwide highest wave power. Renewable and Sustainable Energy Reviews, 75, 1348-1362.

Sandhya, K. G., Nair, T. B., Bhaskaran, P. K., Sabique, L., Arun, N., & Jeykumar, K. (2014). Wave forecasting system for operational use and its validation at coastal Puducherry, east coast of India. Ocean Engineering, 80, 64-72.

Sanil Kumar, V., & Muhammed Naseef, T. (2015). Performance of ERA-Interim wave data in the nearshore waters around India. Journal of Atmospheric and Oceanic Technology, 32(6), 1257-1269.

Sannasiraj, S. A., & Sundar, V. (2016). Assessment of wave energy potential and its harvesting approach along the Indian coast. Renewable Energy, 99, 398-409.

Sarkar, P. P., Janardhan, P., & Roy, P. (2020). Prediction of sea surface temperatures using deep learning neural networks. SN Applied Sciences, 2(8), 1-14.

Saraçoğlu, K. E., Guner, H. A., Şahin, C., Yuksel, Y., & Çevik, E. (2017). Evaluation of the wave climate over the black sea: field observations and modelling. Coastal Engineering Proceedings, 1(35), 20.

Satyavathi, P., Deo, M. C., Kerkar, J., & Vethamony, P. (2016). Reevaluation of design waves off the western Indian coast considering climate change. Marine Technology Society Journal, 50(1), 88-98.

Satyanand K.(2005). Long-term and spectral analysis of waves off mangalore coast. M.Tech. Thesis, National Institute of Technology Karnataka, Surathkal, Mangaluru, India.

Sawadogo, W., Abiodun, B. J., & Okogbue, E. C. (2019). Projected changes in wind energy potential over West Africa under the global warming of 1.5° C and above. Theoretical and Applied Climatology, 1-13.

Sirisha, P., Sandhya, K. G., Balakrishnan Nair T. M., & Venkateswara Rao B. (2017). Evaluation of wave forecast in the north Indian Ocean during extreme conditions and winter monsoon, Journal of Operational Oceanography, 10(1), 79-92.

Sørensen, O. R., Kofoed-Hansen, H., Rugbjerg, M., & Sørensen, L. S. (2005). A third-generation spectral wave model using an unstructured finite volume technique. In Coastal Engineering 2004: (In 4 Volumes), 894-906.

Sreelakshmi, S., & Bhaskaran, P. K. (2020). Spatio-temporal distribution and variability of high threshold wind speed and significant wave height for the Indian ocean. Pure and Applied Geophysics, 1-17.

Strauss, D., Mirferendesk, H., & Tomlinson, R. (2007). Comparison of two wave models for Gold Coast, Australia. Journal of Coastal Research, 312-316.

Stouffer, R. J., Eyring, V., Meehl, G. A., Bony, S., Senior, C., Stevens, B., & Taylor, K. E. (2017). CMIP5 scientific gaps and recommendations for CMIP6. Bulletin of the American Meteorological Society, 98(1), 95-105.

Subba Rao, Kiran Shirlal G., Radheshyam B., & Satyanand K. (2008). Spectral Analysis of waves off Mangalore Coast. Proceedings of 15th congress of APD-IAHR, IIT Madras, 1003-1013.

Suvire, G. O. (2011). Wind Farm-Technical Regulations, Potential estimation and siting assessment, InTech: Rijeka, Croatia.

Takbash, A., Young, I. R., & Breivik, Ø. (2019). Global Wind Speed and Wave Height Extremes Derived from Long-Duration Satellite Records. Journal of Climate, 32(1), 109-126.

Taylor, K. E. (2001). Summarizing multiple aspects of model performance in a single diagram. Journal of Geophysical Research: Atmospheres, 106(D7), 7183-7192.

Taylor, K. E. (2005). Taylor diagram primer. Work. Paper, 1-4.

Taylor, K. E., Ronald J. Stouffer and Gerald A. Meehl, (2009). A summary of the CMIP5 experiment design. [http://cmippcmdi.llnl.gov/cmip5/docs/Taylor CMIP5 design. pdf, (Dec. 18, 2009)]

Teena, N. V., Kumar, V. S., Sudheesh, K., & Sajeev, R. (2012). Statistical analysis on extreme wave height. Natural hazards, 64(1), 223-236.

Thiagarajan, K. P., & Dagher, H. J. (2012). State-of-the-art review of floating platform concepts for offshore wind energy generation. In International Conference on Offshore Mechanics and Arctic Engineering, American Society of Mechanical Engineers, 44946, 489-495.

The challenged coast of India –A report (2012), BNHS, NCPC, PondyCAN and TISS, COP 11- Convention on Biological Diversity, Hyderabad.

Thomas, T. J., & Dwarakish, G. S. (2015). Numerical wave modelling–A review. Aquatic Procedia, 4, 443-448.

Ulazia, A., Penalba, M., Ibarra-Berastegui, G., Ringwood, J., & Sáenz, J. (2019). Reduction of the capture width of wave energy converters due to long-term seasonal wave energy trends. Renewable and Sustainable Energy Reviews, 113, 109267.

Umesh, P. A., Bhaskaran, P. K., Sandhya, K. G., & Nair, T. B. (2017). An assessment on the impact of wind forcing on simulation and validation of wave spectra at coastal Puducherry, east coast of India. Ocean Engineering, 139, 14-32.

Van Vuuren, D. P., Edmonds, J., Kainuma, M., Riahi, K., Thomson, A., Hibbard, K., ... & Masui, T. (2011). The representative concentration pathways: an overview. Climatic change, 109(1-2), 5.

Venkatesan, R., Lix, J. K., Phanindra Reddy, A., Arul Muthiah, M., & Atmanand, M. A. (2016). Two decades of operating the Indian moored buoy network: significance and impact. Journal of Operational Oceanography, 9(1), 45-54.

Vethamony, P., Sudheesh, K., Rupali, S. P., Babu, M. T., Jayakumar, S., Saran, A. K., ... & Sarkar, A. (2006). Wave modelling for the north Indian Ocean using MSMR analysed winds. International Journal of Remote Sensing, 27(18), 3767-3780.

Vishnu K.(2018). Effect of climate change on wave heights at New Mangalore Port. M.Tech. Thesis, National Institute of Technology Karnataka, Surathkal, Mangaluru, India.

Xu, X., Robertson, B., & Buckham, B. (2020). A techno-economic approach to wave energy resource assessment and development site identification. Applied Energy,

260, 114317.

Young, I. R. (1999). Seasonal variability of the global ocean wind and wave climate. International Journal of Climatology, 19(9), 931-950.

Zhang, R., Zhang, S., Luo, J., Han, Y., & Zhang, J. (2019). Analysis of near-surface wind speed change in China during 1958–2015. Theoretical and Applied Climatology, 1-17.

Zilong, Ti, Zhang, M., Wu, L., Qin, S., Wei, K., & Li, Y. (2018). Estimation of the significant wave height in the nearshore using prediction equations based on the Response Surface Method. Ocean Engineering, 153, 143-153.

ANNEXURE I

Ferret an analysis tool for gridded and non-gridded data can be downloaded from https://ferret.pmel.noaa.gov/Ferret/downloads. This tool is installed as per NOAA/PMEL guidelines. The commands (**in bold**) used for wind speed data processing and their description (*in //*) are mentioned below.

Open the terminal in Ubuntu   *//the terminal should be in same location as that of the work file*

Type **ferret** to open ferret tool.

NOAA/PMEL TMAP
    FERRET v7.2 (optimized)   *//to open .nc file*
    Linux 2.6.32-696.3.2.el6.x86_64 64-bit - 07/11/17
    22-May-18 19:30
                           //details of the ferret tool installed

To import and view .nc file -

yes? **use** file_name   *//to open .nc file*

yes? **sh d**   *//to display file details*

currently SET data sets:
  1> ./file_name.nc (default)   *//1 indicates variable no.*
 name   title   I   J   K   L
 UAS   eastward near-surface wind [m s 1:27   1:24   ...   1:1752

                            //typical file details displayed

yes? **sh grid** variable_name[variable no.]   *//to display values and graphics*

yes? **fill/x=long1:long2/y=lat1:lat2 variable_name[d=variable_no.,t=timestep]**

To compute the resultant wind speed-

yes? **let res_wind=((uas[d=1]*uas[d=1])+(vas[d=2]*vas[d=2]))^0.5**

                      //uas and vas are the variables whose resultant is assigned with a variable name res_wind

yes? **save/file=new_filename.nc res_wind**   *// to save as a new file*

yes? **use** new_filename.nc

yes? **sh d**   *// to display the resultant wind speeds*

To re-grid of the dataset to 0.5ºx0.5º -

yes? **Define axis/x=40:95:0.5 xax**   *// re-gridding for the selected domain*

yes? **Define axis/y=-4:30:0.5 yax**

yes? **let new_wind=res_wind[d=variable_no,gx=xax,gy=yax]**

//assigning the gridded values under the variable name new_wind

yes? **save/file=new_filename2.nc new_wind**

yes? **use new_filename2.nc**

yes? **sh d**

```
currently SET data sets:
  4> ./file_name2.nc  (default)
name          title                                I      J      K      L
new_wind      res_wind[D=3, gx=xax,gy=yax] [m s  1:111   1:69    ...    1:1752
```

//details of data points after re-gridding

To get monthly averages(spatial)-

yes? **list new_wind[d= variable_no,x=40:95@ave,y=-4:30@ave]**

//to obtain monthly average values for the selected domain

yes? **list/file=wind.txt new_wind[d= variable_no,x=40:95@ave,y=-4:30@ave]**

//to save the obtained wind speed values in text format

To Combine/merge files -

Open a terminal (not in ferret)

cdo cat filename1.nc filename2.nc newfilename.nc

//the values in the two files will be merged to the new file

120

Code developed in virtual basic to convert the yearly data (eg: 2012) of wind speeds to MIKE readable ASCII format.

```
Sub main()

Dim i, j, k, l, m, n, P, Q As Integer

Dim count(1), Last(1) As Double

Sheets("2012").Activate

Sheets("2012").Cells.ClearContents

Dim lastRow As Integer

Dim UVal, VVAl As Integer

k = 0

l = 1

m = 0

n = 0

P = 0

Q = 0

j = 3

For i = 1 To 365

With ThisWorkbook.Sheets("U12")

    Sheets("U12").Activate

    lastRow = .Cells(.Rows.count, "A").End(xlUp).Row

    UVal = Application.WorksheetFunction.CountIf(Range("A1:A" & lastRow), i)

    .Range("B" & P + j & ":DI" & 2 + UVal + P).Sort Key1:=Range("B" & P + j & ":B" & 2 + UVal + P), Order1:=xlDescending, Header:=xlNo

    .Range("C" & P + j & ":DI" & 2 + UVal + P).Copy
```

```
Sheets("2012").Activate

    Cells(1 + k + m, 1).Value = Chr(34) & "tstep" & Chr(34)

    Cells(1 + k + m, 2).Value = i - 1

    Cells(1 + k + m, 3).Value = Chr(34) & "item" & Chr(34)

    Cells(1 + k + m, 4).Value = 1

    Cells(1 + k + m, 5).Value = Chr(34) & "layer" & Chr(34) & 0

    "Cells(2, 1).PasteSpecial xlPasteValues

    Cells(l + k + m + 1, 1).PasteSpecial xlPasteValues

    "Worksheets("2019").Range("A2 :DI" & iVal).Select

    "Selection.PasteSpecial xlPasteAll

End With

P = UVal + P

k = UVal + k + 3

With ThisWorkbook.Sheets("V12")

    Sheets("V12").Activate

    lastRow = .Cells(.Rows.count, "A").End(xlUp).Row

    VVAl = Application.WorksheetFunction.CountIf(Range("A1:A" & lastRow), i)

    .Range("B" & Q + j & ":DI" & 2 + UVal + Q).Sort Key1:=Range("B" & Q + j &
":B" & 2 + UVal + Q), Order1:=xlDescending, Header:=xlNo

    .Range("C" & Q + j & ":DI" & 2 + VVAl + Q).Copy

    Sheets("2012").Activate

    Cells(n + k + m, 1).Value = Chr(34) & "tstep" & Chr(34)

    Cells(n + k + m, 2).Value = i - 1

    Cells(n + k + m, 3).Value = Chr(34) & "item" & Chr(34)

    Cells(n + k + m, 4).Value = 2

    Cells(n + k + m, 5).Value = Chr(34) & "layer" & Chr(34) & 0
```
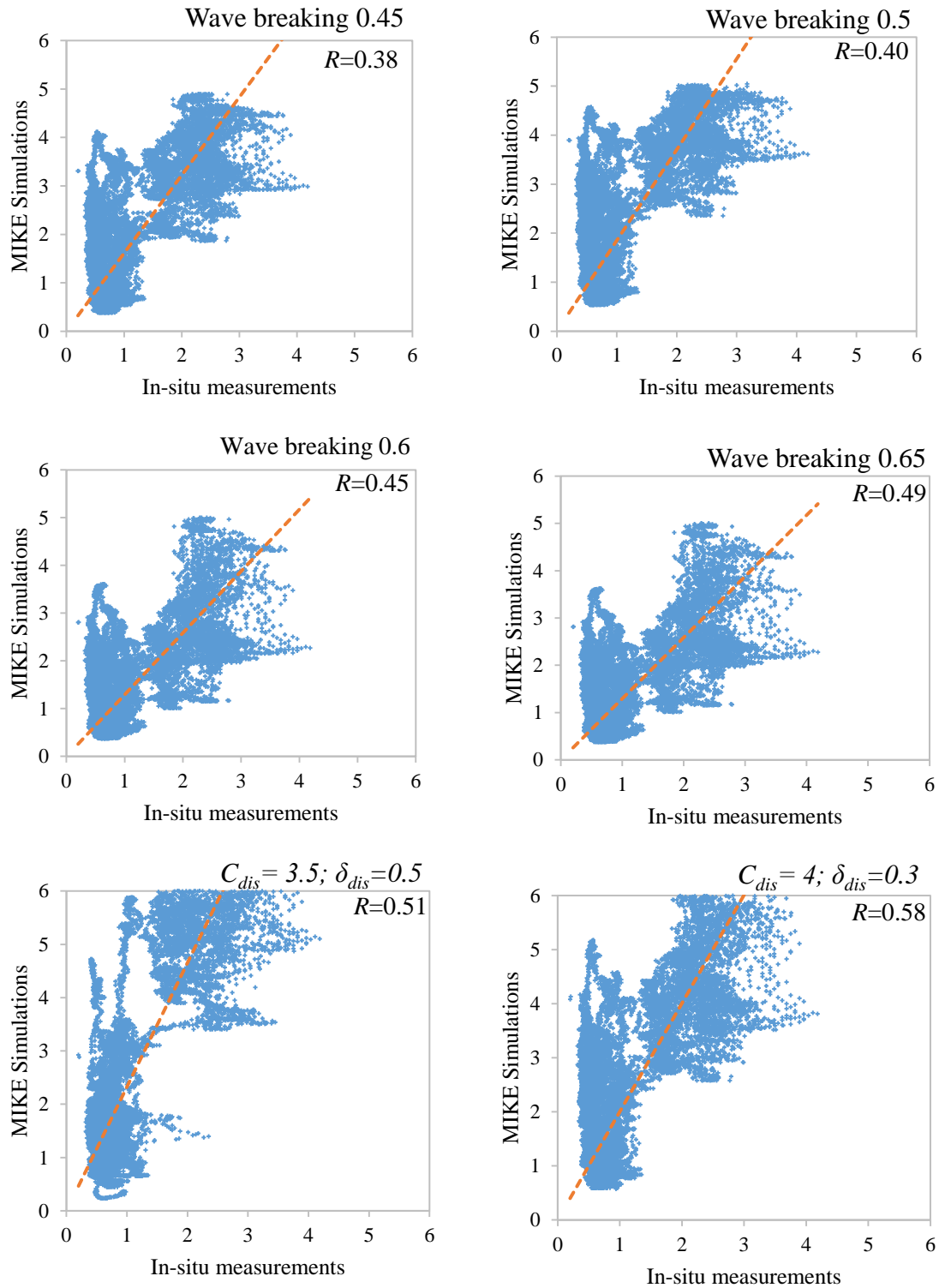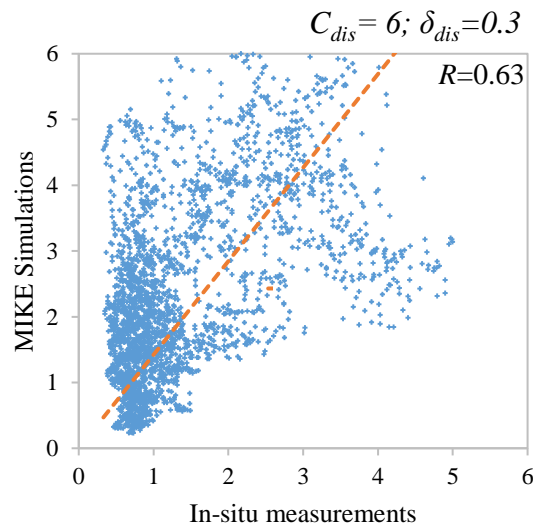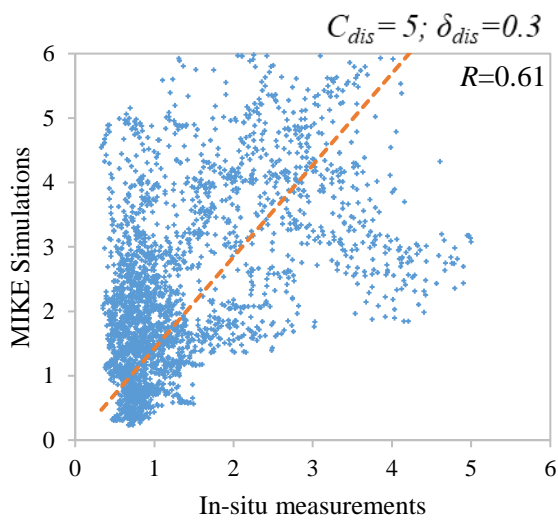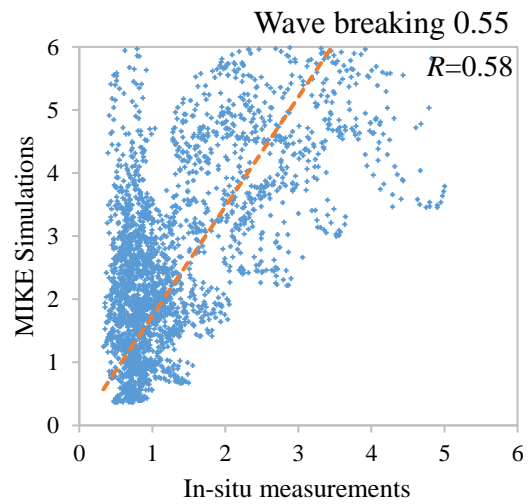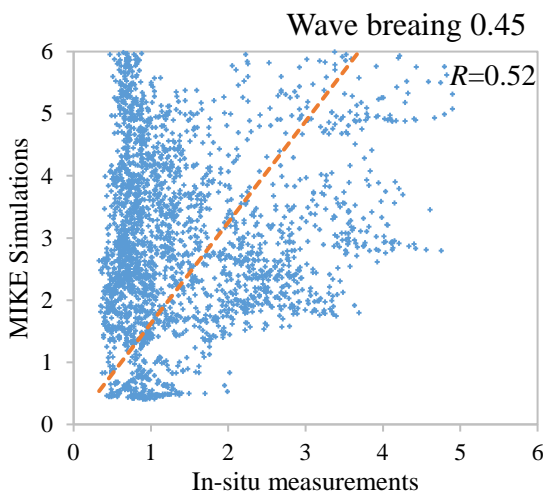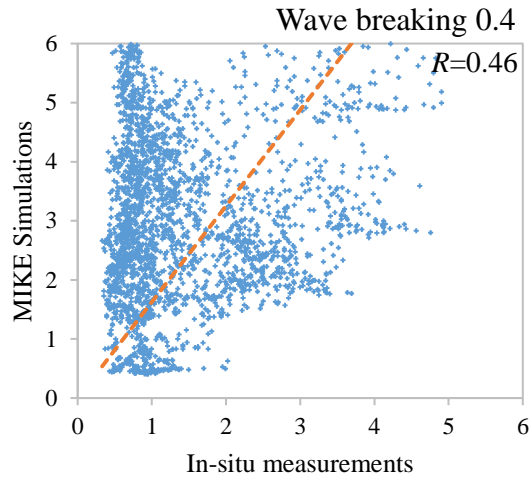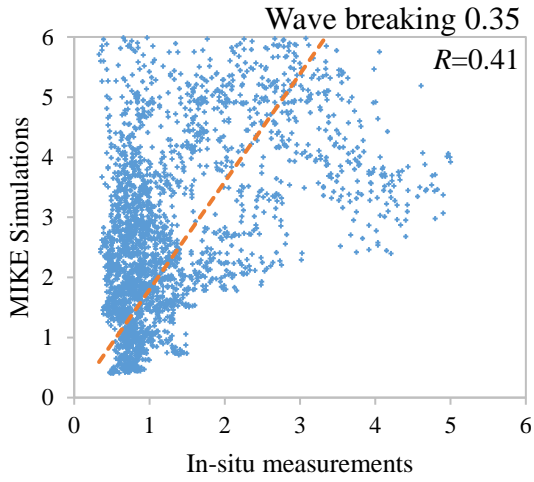
```
"Cells(2, 1).PasteSpecial xlPasteValues

Cells(n + k + m + 1, 1).PasteSpecial xlPasteValues

 "Worksheets("2019").Range("A2 :DI" & iVal).Select

 "Selection.PasteSpecial xlPasteAll

End With

Q = VVAl + Q

m = VVAl + m + 1

Next

End Sub
```

Scatter plots of some trail model setup for Karwar region in MIKE 21

125

Scatter plots of some trail model setup for OB03 region in MIKE 21

INTERNATIONAL JOURNAL PUBLICATIONS:

1. Sandesh Upadhyaya K., Subba Rao, and Manu, (2020), Long-term analysis of waves off Mangaluru coast, Indian Journal of Geo-Marine Sciences (IJMS), ISSN: 0379-5136, e-ISSN:0975-1033, Vol. 49 (05), 717-723.

2. Sandesh Upadhyaya K., Subba Rao, and Manu. Prediction of wind-wave climate along Karnataka Coast, Journal of Earth System Sciences [Accepted]

CONFERENCES

1. Sandesh Upadhyaya K., Subba Rao, and Manu, (2020), Assessment of wind and wave energy potential along the Indian coast, International conference on Recent Advancements in Renewable Energy [RARE-2020], NITK Surathkal, India. Proc. of RARE 2020, Bluerose Publishers, pp 130-135 (ISBN: 978-1-64826-759-8).

2. Sandesh Upadhyaya K., Subba Rao, and Manu, (2019), Evaluating Wind Speed Datasets for Indian Domain, 24th HYDRO-2019 International conference, Osmania University, Hyderabad, India. Proc. of HYDRO-2019, Vol II, pp. 3220 – 3227 (ISBN- 978-93-8935-484-3).

3. Sandesh Upadhyaya, Subba Rao and Manu, (2019), Simulation of Design Wave Height along Karnataka Coast Using Mike 21 Numerical Model, International symposium on Advances in Coastal Research with special reference to Indo Pacific [AdCoRe IP-2019], National Centre for Coastal Research (NCCR), Chennai, India. Book of abstracts AdCoRe IP-2019, p. 90.

4. Sandesh Upadhyaya K., Subba Rao, and Manu. (2019). Historical data analysis of wind speeds from ERA-interim dataset and CMIP5 models for Arabian Sea, Proc. of CCIVA 19, International Conference on Climate Change Impacts, Vulnerabilities, and Adaptation: Emphasis on India and Neighbourhood-CCIVA, Centre for Ocean, Rivers, Atmosphere and Land Sciences (CORAL), IIT, Kharagpur, W.B., 38. **(The paper was awarded third prize for oral presentation).**

5. Sandesh Upadhyaya K., Subba Rao, and Manu. (2018). A review of computational studies on Indian coast considering climate change effects, Proc. of HYDRO-2018, HYDRO-2018 International, NIT Patna, Bihar, India, 263.

BIO-DATA

Mr. SANDESH UPADHYAYA K.

#F009, Block II
"Sri Krishnadhama", SR Yashodhama,
Bailakere, Kunjibettu
Udupi– 576102
Karnataka, India
Mobile: +91 7829868110
E-mail: sandeshupadhyaya@gmail.com / sandesh.uk@manipal.edu
ORCID ID: https://orcid.org/0000-0001-7776-9545

Working as Assistant Professor in the Department of Civil Engineering Manipal Institute of Technology, Manipal since June 2014. Has published 04 journal papers and 13 conference papers. Has guided 01 PG and 07 UG student projects. Have handled courses like Coastal Engineering, Engineering Statics and Dynamics, Mechanics of Solids, Strength of Materials, Analysis of Indeterminate Structures etc.

EDUCATION & CREDENTIALS

M.Tech. (Structural Engineering), Manipal Institute of Technology, Manipal, 2014
(Manipal Academy of Higher Education, Manipal)

B.E. (Civil Engineering), Malnad College of Engineering, 2012
(autonomous under VTU, Belgaum)

PERSONAL DETAILS

Date of Birth: 27-Nov-1990

Languages known: Samskrita, English, Hindi, Kannada and Tulu.

Computing Skills: MIKE 21, ArcGIS, MATLAB, R, AutoCAD, Microsoft Office.